

APPLICATION OF FTIR SPECTROSCOPY FOR MONITORING WATER QUALITY IN A HYPERTROPHIC AQUATIC ECOSYSTEM (LAKE AUENSEE, LEIPZIG)

Der Fakultät für Lebenswissenschaften

der Universität Leipzig

eingereichte

DISSERTATION

zur Erlangung des akademischen Grades

Doctor rerum naturalium

(Dr. rer. nat.)

vorgelegt von

Diplom-Biologin Zhixin Liu

geboren am 05.02.1981 in Liaoning, VR China

Verteidigung: 25.10.2019

Leipzig, den 12.11.2019

My family

Bibliographische Darstellung

Zhixin Liu

Application of FTIR spectroscopy for monitoring water quality in a hypertrophic aquatic ecosystem (Lake Auensee, Leipzig)

Fakultät für Lebenswissenschaften

Universität Leipzig

Dissertation

147 Seiten, 368 Literaturangaben, 29 Abbildungen, 13 Tabellen

FTIR spectroscopy as molecular fingerprint has been used to assess macromolecular and elemental stoichiometry as well as growth rates of phytoplankton cells. Chemometric models have been developed to extract quantitative information from FTIR spectra to reveal macromolecular composition (of proteins, carbohydrates and lipids), C:N ratio, and growth potential. In this study, we tested these chemometric models based on lab-cultured algal species in monitoring changes of phytoplankton community structure in a hypertrophic lake (Lake Auensee, Leipzig, Germany), where a seasonal succession of spring green algal bloom followed by cyanobacterial dominance in summer can be commonly observed. Our results demonstrated that green algae reacted to environmental changes such as nitrogen limitation (due to imbalanced nitrogen and phosphorus supply) with restricted growth by changing carbon allocation from protein synthesis to storage carbohydrates and/or lipids, and increased C:N ratio. By contrast, cyanobacteria proliferated under nitrogen limiting conditions. Furthermore, the FTIR-based growth potential of green alga matched well with the population biomass determined by the Chl-*a* concentration. However, the predicted growth potential based on FTIR spectroscopy cannot describe the realistic growth development of cyanobacteria in this lake. These results revealed that green algae and cyanobacteria have different strategies of C-allocation stoichiometry and growth patterns in response to environmental changes. These taxon-specific responses may explain at a molecular level why green algae bloomed in the spring under conditions with sufficient nutrient, lower pH and lower water temperature; while cyanobacteria overgrew green algae and dominated in the summer under conditions with limited nutrient availability, higher pH and higher water temperature. In addition, the applicability of these chemometric models for predicting field cyanobacterial growth is of limited value. This may be attributed to other special adaptation properties of cyanobacterial species under stress growth conditions. We used flow cytometry to isolate functional algal groups from the water samples. Despite some drawbacks of the flow cytometry combined FTIR spectroscopy technique, this method provides prospects of monitoring water quality and early warning of harmful algal blooms.

Table of contents

I List of abbreviations	5
II Summary	11
III Zusammenfassung	15
1 Introduction	21
1.1 Water quality monitoring	22
1.2 Environmental parameters for monitoring water quality	23
1.2.1 Light conditions	23
1.2.2 Temperature	25
1.2.3 Dissolved oxygen	28
1.2.4 pH value	29
1.2.5 Electric conductivity	30
1.2.6 Nutrients	31
1.3 Algae as biological indicators of water quality	36
1.3.1 Primary production	37
1.3.2 Phytoplankton composition and Chl- <i>a</i> concentration	40
1.4 <i>In situ</i> growth prediction models	41
1.4.1 Growth prediction models based on the efficiency of light utilization	42
1.4.2 Growth prediction models based on C-allocation	43
1.5 FTIR spectroscopy	47
1.6 Aims of this study	49

2 Materials and methods	51
2.1 Information about the measurement period and Lake Auensee	51
2.2 Measurement of ecological factors and nutrients	51
2.3 Determination of Chl- <i>a</i> concentration	52
2.4 Flow cytometry and electrostatic cell sorting	54
2.4.1 Flow cytometer	54
2.4.2 Principle of algal cell isolation	55
2.4.3 Laser configuration	57
2.4.4 Preparation of freshwater samples	57
2.5 FTIR spectroscopy analysis	58
2.5.1 Construction and function of FTIR spectrometer	58
2.5.2 Physical basis of FTIR spectroscopy	58
2.5.3 Samples preparation and FTIR-spectrum measurements	60
2.5.4 FTIR-based quantification models	61
2.6 Statistic analysis	62
3 Results	65
3.1 Determination of seasonal environmental changes	65
3.1.1 Light conditions	65
3.1.2 Water temperature	66
3.1.3 Dissolved oxygen	68
3.1.4 pH value	69

3.1.5 Electric conductivity -----	70
3.1.6 Nutrient conditions -----	71
3.2 Determination of phytoplankton community structure -----	74
3.2.1 Phytoplankton species in Lake Auensee -----	74
3.2.2 HPLC-based analysis of seasonal phytoplankton dynamics -----	75
3.3 Isolation of functional algal groups by flow cytometry -----	77
3.3.1 Identification and separation of phytoplankton groups -----	77
3.3.2 FCM-based analysis of seasonal phytoplankton dynamics -----	80
3.4 FTIR spectroscopy analysis -----	82
3.4.1 FTIR-spectra of field phytoplankton samples -----	82
3.4.2 Determination of cellular macromolecular composition -----	83
3.4.3 Determination of cellular elemental C:N ratios -----	86
3.4.4 Prediction of algal growth potential -----	89
3.5 Statistical correlation analysis -----	91
4 Discussion -----	95
4.1 Effects of seasonal environmental changes on phytoplankton group succession -----	95
4.1.1 Nutrient conditions -----	95
4.1.2 Light conditions -----	99
4.1.3 Water temperature -----	101
4.1.4 Dissolved oxygen -----	102
4.1.5 pH values -----	104
4.1.6 Electric conductivity -----	104

4.1.7 Regulation of seasonal phytoplankton succession by environmental factors -	105
4.2 Effects of seasonal environmental changes on C-allocation in algal cells -----	107
4.2.1 Macromolecular composition dynamics in response to nutrient limitation ----	107
4.2.2 Cellular C:N ratio as an indicator of algal growth under N-limitations -----	111
4.3 Prediction of phytoplankton growth using FTIR spectroscopy -----	113
4.4 Technique advantages and limitations -----	116
4.4.1 Flow cytometry-coupled FTIR spectroscopy for phytoplankton monitoring --	116
4.4.2 FTIR spectroscopy for freshwater phytoplankton monitoring -----	118
5 References -----	121
6 Acknowledgements -----	144
7 Curriculum vitae -----	145
8 Declaration of authorship -----	147

I List of abbreviations

$(\text{CH}_2\text{O})_n$	carbohydrate
μ	algal growth potential
A_k	coefficient of alloxanthin
All	alloxanthin
ATP	adenosine triphosphate
C	carbon
C:N	molar carbon-to-nitrogen ratio
Ca^{2+}	calcium ion
CaCO_3	calcium carbonate
CAH	carbon allocation hypothesis
CCMs	CO_2 -concentrating mechanisms
CH_2	methylene group
CH_3	methyl group
Chl- <i>a/b</i>	chlorophyll a/b
C_k	coefficient of chlorophyll b
CO_2	carbon dioxide
COO^-	carboxyl group
CR	community respiration
DIN	dissolved inorganic nitrogen
DIN:TP	mass ratio of dissolved inorganic nitrogen to total phosphorus

DNA	deoxyribonucleic acid
DO	dissolved oxygen
EC	electric conductivity
E_d	radiation intensity
eMP	entire macromolecular pool
FACS	fluorescence-activated cell sorting
FCM	flow cytometry
F_k	coefficient of fucoxanthin
FSC	forward-scattered light
FTIR spectroscopy	Fourier transformed infrared spectroscopy
Fuc	fucoxanthin
GAP	glyceraldehydes-3-phosphate
GPP	gross primary production
GRH	growth rate hypothesis
H ₂ O	water
H ₂ S	hydrogen sulfide
HABs	harmful algal blooms
HCO ₃ ⁻	bicarbonate
HPLC	high performance liquid chromatography
I	light saturation parameter
IR	infrared
k	vertical extinction coefficient
L _g	global radiation

L_k	coefficient of lutein
L_m	intensity of photosynthetically available radiation
LP	long pass filter
Lut	lutein
MP	marker pigment
N	nitrogen
n	number of samples
$N(CH_3)_3$	trimethylamine
NaCl	sodium chloride
NADPH	nicotinamide adenine dinucleotide phosphate
NEP	net ecosystem production
NPP	net primary production
NPQ	non-photochemical chlorophyll fluorescence quenching
Num	total cell number
O_2	oxygen
OP	ortho-phosphorus
P	phosphorus
P	photosynthetic rate
p	statistical significance of evidence
PAR	photosynthetically available radiation
PBP	phycobilinprotein
PBS	phycobilisome
PC	phycocyanin

PE	phycoerythrin
Per	peridinin
P_k	coefficient of peridinin
PLSR	partial least square regression
PMT	photomultiplier tube
Pro:Sto	mass protein-to-storage ratio
Q_{phar}	absorbed photosynthetic energy
r	Pearson's r correlation coefficient
R^2	coefficient of determination
RNA	ribonucleic acid
rRNA	ribosomal ribonucleic acid
RubisCo	ribulose-1-5-bisphosphate-carboxylase-oxygenase
RuBP	ribulose bisphosphate
SD	Secchi-depth
Si	silicon
SSC	side-scattered light
T	water temperature
TN	total nitrogen
T_{opt}	optimal growth temperature
TP	total phosphorus
UNEP	United Nation Environmental Programme
z	water depth
Zea	zeaxanthin

Z_k	coefficient of zeaxanthin
α	light utilization efficiency
Φ_{ALT}	energy invested in alternative electron pathways
Φ_C	quantum efficiency of C production
$\Phi_{f,D}$	non-regulated energy dissipation
Φ_{GECG}	gross energy invested in growth processes
Φ_{NPQ}	energy dissipation in the form of heat

II Summary

Phytoplankton algae are sensitive to environmental changes in their habitat, and thus, their growth patterns and many algal species are used as indicators of water quality. They have been accepted as a major indicator of eutrophication in freshwater as their blooms are common in waters affected by nutrient over-enrichment. Eutrophication in reservoirs and lakes may lead to decline of phytoplankton diversity and eventually to cyanobacterial dominance and toxin production. Therefore, monitoring the growth development and composition of phytoplankton communities is important for water quality control and early warning of harmful algal blooms (HABs).

Recent studies established growth models based on cellular traits such as carbon (C) allocation related macromolecular and elemental ratios. The specific energetic and macromolecular stoichiometry exists as a function that can be used to predict growth rates of microalgae under a given growth condition regulated by e.g. nutrient supply or temperature. Fourier transform infrared (FTIR) spectroscopy has been widely used in chemometric analysis of phytoplankton cells because it is a rapid, nondestructive, time saving method that can detect a range of functional groups and is highly sensitive to changes in molecular structure. Recent studies developed chemometric models to extract quantitative information from FTIR spectra to reveal growth rates (Jebsen et al., 2012), as well as C-allocation related traits e.g. macromolecular composition of proteins, carbohydrates and lipids (Wagner et al., 2010) and elemental carbon to nitrogen (C:N) ratios (Wagner et al., 2019). The development of these chemometric models was based on different methods including PLSR (Partial least square regression), spectral reconstruction or band peak ratios. In this study, we tested the applicability of these models for the first time in determining the C-allocation traits and predicting growth potential of phytoplankton communities in a natural aquatic ecosystem (Lake Auensee, Leipzig, Germany).

In the hypertrophic Lake Auensee, there are two annual blooms, the spring bloom forms majorly by cryptophytes and green algae, and cyanobacteria commonly bloom in summer. In the observation term of the study, we focused on the succession process from the green algal abundance to the cyanobacterial blooms. Here the cellular C-allocation stoichiometry changed simultaneously in response to seasonal environmental changes such as nutrient supply, light condition, water temperature, pH, dissolved oxygen concentration and electric conductivity.

The green algal bloom was associated with sufficient nutrient supply in water due to the spring turnover. The complete lake mixing allowed the nutrients fluxes from the bottom water into the upper water layers that promoted high growth rates of primary producers and other organisms. Rapid phytoplankton growth in spring consumed nutrients in a great amount within the surface waters. In turn, the reduction of nutrient availability may also restrict the growth development of phytoplankton. The dependence of green algal growth on N availability can be confirmed by the cellular C-allocation traits determined using FTIR spectroscopy. Under N-limitation conditions, green algae showed a decrease in protein contents, as well as increases in carbohydrate contents and C:N ratios. The results evidenced the C-allocation hypothesis (CAH) that nutrient limitation may induce the reallocation of photosynthetic energy/carbon switching from N-rich protein synthesis for maintaining growth to energy storage in forms of carbohydrates and/or lipids. Furthermore, the FTIR-predicted growth potential can reflect the seasonal biomass development of this algal group. The analysis demonstrated that the chemometric models based on FTIR-spectra can be used in monitoring the growth potential and to explain the C-allocation strategies in response to environmental changes, not only for algal lab-cultures, but also for field green algal subcommunity. Beside the nutrient stresses, decreased water transparency, increased pH values and water temperatures, as well as grazing pressure of zooplankton may also directly or indirectly influence the cellular C-allocation stoichiometry and restrict the growth rate of green algae. The reduce of the spring bloomers resulted in the formation of a clear-water phase during the late-spring and early-summer in Lake Auensee.

After the onset of the clear-water phase, cyanobacteria (mainly colonial and filamentous species) became abundant in the epilimnion and formed harmful blooms in the summer, likely due to combination of favorable nutrient stoichiometry, i.e. imbalanced N and P supply determined as low DIN:TP (dissolved inorganic nitrogen to total phosphorus) ratios, elevated pH and water temperature in this long-term stratified lake. In this situation, the macromolecular stoichiometry responded to environmental changes by decreased protein content, as well as increased carbohydrate and lipid contents and C:N ratios. These C-allocation responses of cyanobacterial cells were similar as that of green algae. Nevertheless, the growth rate of cyanobacteria was not limited by these environmental stresses, intense bloomed even under N-limiting conditions. This specific growth response can be attributed to the specific energy allocation under diazotrophic conditions. Since high energy requirement for N₂-fixation processes may influence the allocation of photosynthetic energy towards growth maintenance,

the metabolic strategies of cyanobacteria to N-limitations are more complicate and different from those of the green algae. Thus, the specific C-allocation and growth responses cannot be solely explained by the CAH.

The predicted growth potential of cyanobacteria based on FTIR-model was not consistent with the real variation tendency of population biomass, which indicated that the growth model is not always suitable for the prediction of cyanobacterial growth under natural conditions. The possible reasons are as follows. The N₂-fixing and non-N₂-fixing genera have different sensitivity and growth response to N-deficiency. Diazotrophic species can maintain growth under N-limitation conditions, and their growth rates become decreased when N is depleted; whereas, non-N₂-fixing cyanobacteria decrease growth rate in response to N-limitations. Furthermore, the coexistence of N₂-fixing and non-N₂-fixing cyanobacteria can lead to dramatic enhancement of taxonomic growth rates. These species-specific responses to environmental stresses and interactions between cyanobacterial species may shift the nature of the predicted relationship between growth patterns and nutrient supply (as well as other environmental factors) and increase the difficulty of establishing a taxon-specific growth model for field studies. Furthermore, the filtration of samples in the preparation process led to losses of large amounts of filamentous and large colonial cyanobacteria, probably accounting for the deviation of the predicted growth potential from the actual growth rates. In addition, cyanobacterial growth can benefit from their other physiological traits, such as buoyancy control and grazing resistance, the relationships of which to C-allocation traits are still unclear. Therefore, as a next step, the use of a species-specific growth model for some major bloom-forming species (e.g., *Microcystis* and *Anabaena*) may be more applicable for monitoring water quality and early warning the occurrence of cyanobacteria dominated HABs.

In this study, we used flow cytometry (FCM) to isolate green algal and cyanobacterial cells from water samples of Lake Auensee. The FCM in combination with FTIR spectroscopy allowed rapid experimental processes (within several hours) from water sampling to cell selection to FTIR-spectra measurements. The fast implementation prevented possible interference due to long-term storage. Considering natural water samples commonly having high species diversity and low cell number, this combined method stands for its rapid speed, simple operation, and saving cell materials that is ideal applicable for long-term studies of field phytoplankton.

Because FTIR spectra as fingerprint mirror the biochemical changes in response to envi-

ronmental factors, they can be used on a molecular level to explain the growth mechanisms why green algae prefer conditions with higher nutrient and light availability, and lower temperature and pH; while cyanobacteria benefit from environments with low N supply, higher temperature and pH. The spectral properties further provide a better understanding of how environmental dynamics driving the seasonal variations of phytoplankton community structure in an ecological niche.

FTIR spectroscopy links one hand the cellular macromolecular biomass, on the other hand, it links the environmental conditions. If the cellular biochemical stoichiometry in response to abiotic or biotic conditions is known, the FTIR spectrum can mirror this environment. For example, the Redfield C:N ratio of 6.6 may serve as a cellular critical ratio to determine N-limitation in water. Since external N-depletion may have effects on decrease in cellular N-pool and enhancement of C:N ratio, it provided evidence that green algae and cyanobacteria decreased their standing crop of biomass, or restricted their growth to a low level, when the cellular C:N ratio was far above the Redfield ratio. Interestingly, the cyanobacteria often proliferated when the C:N ratio was in the range between 4.5 and 6.0, slightly lower than the Redfield C:N ratio. This phenomenon provides a possibility that the non-N₂-fixing cyanobacteria benefit from fixed nitrogen supplied by diazotrophic cyanobacteria in this situation, and the facilitation between cyanobacteria genera eventually cause outbreak of cyanobacterial blooms. The cellular biochemical composition serving as indicators of the environment is particularly important for providing guiding direction in future studies of eutrophication control, water quality management and early warning of HABs. Despite the fact that at present the method of FCM combined with FTIR spectrometry has some limitations, it provides the prospects of monitoring physiological changes in target phytoplankton groups/species, as well as studying or predicting the processes controlling changes in phytoplankton growth and community composition in response to environmental changes.

III Zusammenfassung

Phytoplanktonalgen reagieren empfindlich auf Umweltveränderungen in ihrem Lebensraum. Daher werden ihre Wachstumsmuster und viele Algenarten als Indikatoren für die Wasserqualität verwendet. Sie sind als Hauptindikator für die Eutrophierung im Süßwasser anerkannt, da ihre Blüten häufig in Gewässern auftreten, die von einer Überanreicherung mit Nährstoffen betroffen sind. Die Eutrophierung in Stauseen und Seen kann zur Abnahme der Phytoplankton-Diversität und schließlich zur Dominanz der Cyanobakterien und zur Toxin-Produktion führen. Daher ist die Überwachung der Wachstumsentwicklung und der Zusammensetzung von Phytoplanktongemeinschaften wichtig für die Wasserqualitätskontrolle und die Frühwarnung vor schädlichen Algenblüten (HABs).

In den letzten Jahren wurden die Wachstumsmodelle entwickelt, die auf zellulären Merkmalen wie der Allokation von Kohlenstoff (C) zu makromolekularen und elementaren Verhältnissen basieren. Die spezifische energetische und makromolekulare Stöchiometrie existiert als eine Funktion, die verwendet werden kann, um Wachstumsraten von Mikroalgen unter einer gegebenen Wachstumsbedingung vorherzusagen, die z.B. Nährstoffversorgung oder Temperatur. Die Fourier-Transformations-Infrarot-Spektroskopie (FTIR-Spektroskopie) wird häufig für die chemometrische Analyse von Phytoplanktonzellen verwendet. Die Methode ist schnell, zerstörungsfrei und zeitsparend, kann eine Reihe von funktionellen Gruppen identifizieren und ist sehr empfindlich gegenüber Änderungen der Molekülstruktur. Aktuelle Studien entwickelten chemometrische Modelle, um quantitative Informationen aus FTIR-Spektren zu extrahieren und Wachstumsraten aufzudecken (Jebsen et al., 2012) sowie C-Allokations-bezogene Eigenschaften, z.B. makromolekulare Zusammensetzung von Proteinen, Kohlenhydraten und Lipiden (Wagner et al., 2010) und Verhältnis von elementarem Kohlenstoff zu Stickstoff (C:N) (Wagner et al., 2019). Die Entwicklung dieser chemometrischen Modelle ist auf verschiedenen Methoden basieren, z.B. PLSR (Partial Least Square Regression), spektraler Rekonstruktion oder Absorptionsband-Verhältnissen. In diesem Projekt haben wir die Anwendbarkeit dieser Modelle zum ersten Mal getestet, um die C-Allokationsmerkmale zu bestimmen und das Wachstumspotenzial von Phytoplankton-Gemeinschaften in einem natürlichen aquatischen Ökosystem (Auensee, Leipzig, Deutschland) vorherzusagen.

Im hypertrophen Auensee gibt es zwei jährliche Blüten, die Frühlingsblüte, die hauptsächlich aus Cryptophyten und Grünalgen besteht, und die Sommerblüte aus Cyanobakterien.

Im Beobachtungszeitraum, fokussieren wir uns auf den Folgeprozess der Dominanz von Cyanobakterien gegenüber der Abundanz von Grünalgen, bei dem sich die Stöchiometrie der zellulären C-Allokation gleichzeitig als Reaktion auf saisonale Umwelt-veränderungen wie Nährstoffversorgung, Lichtbedingungen, Wassertemperatur, pH-Wert, Konzentration des gelösten Sauerstoffs und elektrische Leitfähigkeit.

Die Grünalgenblüte war aufgrund der Frühjahrszirkulation mit einer ausreichenden Nährstoffversorgung im Wasser verbunden. Die vollständige Vermischung des Sees ermöglichte den Nährstoffflüssen vom Grundwasser in die oberen Wasserschichten, was das explosive Wachstum von Primärproduzenten und anderen Organismen förderte. Das schnelle Wachstum des Phytoplanktons im Frühjahr verbrauchte in großen Mengen Nährstoffe in den Oberflächengewässern. Die Verringerung der Nährstoffverfügbarkeit kann wiederum die Wachstumsentwicklung von Phytoplankton einschränken. Die Abhängigkeit des Grünalgenwachstums von der Stickstoff-Verfügbarkeit kann durch die mithilfe der FTIR-Spektroskopie bestimmten zellulären C-Allokationsmerkmale bestätigt werden. Unter N-limitierenden Bedingungen zeigten die Grünalgen einen Abstieg des Proteingehalts sowie einen Anstieg des Kohlenhydratgehalts und des C:N-Verhältnisses. Die Ergebnisse bestätigten die C-Allokationshypothese (CAH), dass eine Nährstoffmangel den Übergang der photosynthetischen Energie-/Kohlenstoffverteilung von der stickstoffreichen Proteinsynthese zum Wachstum in die Energiespeicherung in Form von Kohlenhydraten und/oder Lipiden bewirken könnte. Darüber hinaus kann das von FTIR vorhergesagte Wachstumspotenzial die saisonale Biomasseentwicklung dieser Algengruppe widerspiegeln. Die Analyse zeigte, dass die auf FTIR-Spektren basierenden chemometrischen Modelle zur Überwachung des Wachstumspotenzials und zur Erklärung der C-Allokationsstrategien in Reaktion auf Umweltveränderungen nicht nur für Algenlaborkulturen, sondern auch für Feldgrünalgen verwendet werden können. Neben den Nährstoffbelastungen können auch eine verminderte Wassertransparenz, erhöhte pH-Werte und Wassertemperaturen sowie der Weidedruck des Zooplanktons die zelluläre C-Allokationsstöchiometrie direkt oder indirekt beeinflussen und die Wachstumsrate von Grünalgen einschränken. Durch die Reduzierung der Frühjahrsblüher bildete sich im Spätfrihling und Frühsommer am Auensee eine Klarwasserphase.

Nach dem Einsetzen der Klarwasserphase traten im Epilimnion häufig Cyanobakterien (hauptsächlich in Kolonien und Filamenten) auf und bildeten im Sommer schädliche Blüten, wahrscheinlich aufgrund der Kombination einer günstigen Nährstoffstöchiometrie, d.h. einer

unausgewogenen N- und P-Ernährung, die als niedrige DIN:TP (gelöster anorganischer Stickstoff zu Gesamtphosphor)-Verhältnisse bestimmt wurde und erhöhter pH-Wert und Wassertemperatur in diesem langfristig geschichteten bzw. stratifizierten See. In solchen Situationen reagierte die makromolekulare Stöchiometrie auf Umweltveränderungen mit verringertem Proteingehalt sowie erhöhten Kohlenhydrat- und Lipidgehalten und C:N-Verhältnissen. Diese C-Allokation von Cyanobakterienzellen beantwortete ähnlich wie die von Grünalgen. Die Wachstumsrate von Cyanobakterien war nicht durch diese Umweltbelastungen begrenzt, und diese Algengruppe blühte intensiv trotz N-limitation auf. Diese spezifische Wachstumsreaktion kann auf die spezifische Energieverteilung unter diazotrophen Bedingungen zurückgeführt werden. Da ein hoher Energiebedarf für N₂-Fixierungsprozesse die Allokation der photosynthetischen Energie beeinflussen kann, sind die Stoffwechselstrategien von Cyanobakterien komplizierter und unterscheiden sich von denen der Grünalgen. Somit können die spezifischen C-Allokations- und Wachstumsstrategien nicht allein von der CAH interpretiert werden.

Das FTIR-Modell vorhergesagte Wachstumspotenzial von Cyanobakterien stimmte nicht mit der tatsächlichen Variationstendenz der Populationsbiomasse überein, was darauf hindeutete, dass das Wachstumsmodell nicht für die Vorhersage des Wachstums von Cyanobakterien unter natürlichen Bedingungen geeignet ist. Die möglichen Gründe sind wie folgt. Die N₂-fixierenden und Nicht-N₂-fixierenden Gattungen weisen eine unterschiedliche Empfindlichkeit und Wachstumsreaktion auf N-Mangel auf. Zusätzlich können diazotrophe Spezies unter N-Limitation Bedingungen das Wachstum aufrechterhalten, während die Wachstumsrate verringert wird, wenn N in Wasser erschöpft wird. Im Vergleich dazu verringern die Nicht-N₂-fixierenden Cyanobakterien die Wachstumsrate unter N-Limitation. Darüber hinaus kann die Koexistenz von den N₂-fixierenden und Nicht-N₂-fixierenden Cyanobakterien zu einer dramatischen Steigerung der taxonomischen Wachstumsraten führen. Diese artspezifischen Reaktionen auf Umweltbelastungen und die Interaktion zwischen cyanobakteriellen Spezies können die Abhängigkeit-Vorhersage der Wachstumsrate von der Nährstoffversorgung (sowie anderen Umweltfaktoren) verändern, und die Schwierigkeit erhöhen, ein taxon-spezifisches Wachstumsmodell für Phytoplankton in Freilandforschungen zu etablieren. Außerdem führte die Filtration der Proben während des Aufbereitungsprozesses zu Verlusten großer Mengen von den fadenförmigen und kolonialen Cyanobakterien, was die Abweichung des vorhergesagten Wachstumspotenzials von den tatsächlichen Wachstumsraten verursachen könnte. Zusätzlich kann das Wachstum von anderen physiologischen Merkmalen wie Auftriebskontrolle und Fraßen-Resistenz profitieren, aber der Zusammenhang dieser To-

lerante mit den Mechanismen der C-Allokation ist noch unklar. Daher kann als nächster Schritt die Verwendung eines speziesspezifischen Wachstumsmodells für einige Hauptalgenblüten Spezies (z. B. *Microcystis* und *Anabaena*) für Monitoring der Wachstum-Development und Frühwarnung der Cyanobakterien-dominierten HABs geeigneter sein.

In dieser Studie verwendeten wir die Durchflusszytometrie (FCM), um Grünalgen- und Cyanobakterienzellen aus Wasserproben von Auensee zu isolieren. Das FCM in Kombination mit der FTIR-Spektroskopie ermöglichte schnelle experimentelle Prozesse (innerhalb weniger Stunden) von der Wasserentnahme, über die Zellektion bis hin zu den Messungen der FTIR-Spektren. Die schnelle Durchführung verhinderte mögliche Interferenzen durch Langzeitlagerung. Freilandwasserproben weisen üblicherweise eine hohe Artenvielfalt und eine niedrige Zellzahl. Diese kombinierte Methode steht für schnelle Geschwindigkeit, einfache Bedienung und Einsparung von Zellmaterialien, welche hervorragend für die langfristige Beobachtung des Feldphytoplanktons verwendbar sind.

Da FTIR-Spektren als Fingerabdruck die biochemischen Veränderungen in Abhängigkeit von Umweltfaktoren widerspiegeln, ermöglichen die FTIR-Spektren auf molekularer Ebene die Wachstumsmechanismen zu erklären, warum Grünalgen unter Bedingungen mit höherer Nährstoff- und Lichtverfügbarkeit sowie niedrigerer Temperatur und niedrigerem pH-Wert bevorzugen; während Cyanobakterien von Umgebungen mit N-Limitierung, höherer Temperatur und höherem pH-Wert profitieren. Die spektralen Eigenschaften bieten darüber hinaus ein besseres Verständnis dafür, wie die Umweltdynamik die jahreszeitlichen Schwankungen der Phytoplankton-Gemeinschaftsstruktur in einer ökologischen Nische beeinflusst.

Die FTIR-Spektroskopie verknüpft einerseits die zelluläre makromolekulare Biomasse und andererseits die Umgebungsbedingungen. Wenn die zelluläre biochemische Stöchiometrie als Reaktion auf abiotische oder biotische Bedingungen bekannt ist, kann das FTIR-Spektrum diese Umgebung vorhersagen. Beispielsweise kann das Redfield-C:N-Verhältnis von 6,6 als zelluläres kritisches Verhältnis zur Bestimmung der N-Limitierung in Wasser dienen. Eine externe N-Depletion kann auf die Abnahme des zellulären N-Pools und die Erhöhung des C:N-Verhältnisses auswirken. Dies ergab Hinweise darauf, dass Grünalgen und Cyanobakterien ihre Populationsbiomasse verringerten oder ihr Wachstum auf ein niedriges Niveau beschränkten, wenn das zelluläre C:N-Verhältnis lag weit über dem Redfield-Verhältnis. Interessanterweise vermehrten sich die Cyanobakterien häufig, wenn das C:N-Verhältnis im Bereich zwischen 4,5 und 6,0 lag, etwas niedriger als das Redfield-C:

N-Verhältnis. Dieses Phänomen in dieser Situation bietet die Möglichkeit, dass das von diazotrophen Cyanoabacterium fixierte N als N-Quelle für die nicht-N₂-fixierenden Cyanobakterien diene. Schließlich verursachte die Erleichterung zwischen den Cyanobakterien-Gattungen den Ausbruch von Cyanobakterienblüten. Die zelluläre biochemische Zusammensetzung als Indikatoren für die Umwelt sind besonders wichtig, um Leitlinien für die künftige Forschung zur Eutrophierungskontrolle, zum Wasserqualitätsmanagement und zur Frühwarnung von HAB bereitzustellen. Trotz der Tatsache, dass die Methode der FCM in Kombination mit der FTIR-Spektrometrie derzeit einige Einschränkungen aufweist, bietet sie eine Aussicht auf das Monitoring physiologischer Veränderungen der Ziel-Phytoplanktongruppen/-spezies, sowie die Untersuchung/Vorhersage der Abhängigkeit des Phytoplanktums und der Population-Zusammensetzung von den Umweltveränderungen.

1 Introduction

Water is essential for life. It is the major constituent (70–90%) of all living cells. Freshwater is an essential resource not only for the existence of plants and animals, but also for humans and their commercial activities such as agriculture and industry. However, the high demand for freshwater resource because of increasing population, industrial growth, and intensification of agricultural production has resulted in reckless overconsumption, misuse, pollution, and eutrophication. Eutrophication (or hypertrophication) is defined as the enrichment of a water body with an excessive amount of nutrients for phototrophs. This process may cause negative ecological consequences on aquatic ecosystem structures, processes, and functions, leading to an extensive growth of phytoplankton that can deteriorate water quality (Western, 2001; Beeton, 2002). For a long time now, eutrophication and its effects on algal blooms have been recognized as a water pollution problem (Rodhe, 1969). This problem has become increasingly critical over the past 50 years (Mainston and Parr, 2002). Recently, the increasing severity of water eutrophication has been brought to the attention of governments and the public. The investigation from the United Nation Environmental Programme (UNEP) indicates that about 30–40% of the lakes and reservoirs around the world have been more or less affected by water eutrophication.

The excessive eutrophication nutrients resulting from nutrient inflow disturb the intrinsic equilibrium of an aquatic ecosystem, thus leading to the damage of this ecosystem with a gradual degeneration of its functions. As a result, dense algae blooms—mainly of Cyanophyta and Chlorophyta—are induced often forming a thick layer of “green scum” on the water surface, which reduces water clarity and quality. Algal blooms limit light penetration thus weakening or stopping photosynthesis of plants under the water (Lehtiniemi et al., 2005). These dense algal blooms die when the nutrients have been consumed and the consequent, microbial decomposition severely depletes dissolved oxygen and increases the concentrations of ammonium and hydrogen sulphid in water, which is toxic for aquatic animals and will cause their die-offs. Furthermore, some cyanobacteria release toxins (cyanotoxins) and form harmful algal blooms (HABs), which degrade the quality of drinking water sources and poison fish and shellfish.

Although HABs are known to be formed by a combination of physical, chemical, and biological factors of aquatic ecosystems, how these factors combine to create a 'bloom' of algae

is not well understood. The monitoring of these factors may provide us information on the development of algal blooms and water quality that may be used for bloom assessment and advanced warning of HABs.

1.1 Water quality monitoring

Water quality refers to: 1) a set of concentrations, speciation, and physical partitions of inorganic or organic substances; 2) composition and state of aquatic biota; 3) temporal and spatial variations resulting from factors internal and external to a water body (Chapman, 1996). The monitoring of water quality provides a collection of information at set locations and at regular intervals in order to provide data that may be used to define current conditions, establish trends, etc., supporting decision making on health and environmental issues. Water monitoring is mainly performed through the measurement of two types of water quality parameters: physic-chemical basic parameters (temperature, pH, dissolved oxygen, dissolved organic matter, and nutrients) and biological parameters of microorganisms and phytoplankton. These abiotic and biotic parameters can be used to identify certain conditions regarding the ecology of living organisms and suggest appropriate conservation and management strategies (Thirupathaiah et al., 2013).

Waters with different trophic conditions differ in their natural or anthropogenic-altered developmental history and in their associated chemical and biological parameters. The trophic classification of lakes is based on its primary productivity, which in turn reflects nutrient richness. Water clarity (Secchi disk depth), chlorophyll content, and the concentration of nitrogen and phosphorus are key parameters used to define the trophic state of a water body (Table 1).

Table 1 Classification of waters based on trophic criteria (Gunkel, 1994)

	Secchi-depth [m]	Chlorophyll <i>a</i> [$\mu\text{g l}^{-1}$]	Ortho-phosphate [mg l^{-1}] *	Total phosphate [mg l^{-1}] *	Nitrogen [mg l^{-1}] *
Oligotrophic	≥ 6	≤ 3	≤ 0.002	≤ 0.015	≤ 0.01
Mesotrophic	≥ 4	≤ 10	0–0.005	≤ 0.04	≤ 0.03
Eutrophic	≥ 1	10–40	0–0.1	0.04–0.3	≤ 0.1
Hypertrophic	< 0.5	> 60	> 0.5	> 0.5	> 0.5

*Mean value for epilimnion during summer stagnation

1.2 Environmental parameters for monitoring water quality

1.2.1 Light conditions

Light is one of the most important factors that affect the fundamental properties of water bodies. The absorption and attenuation of light by the water column are major factors controlling temperature and potential photosynthesis of organisms. Photosynthesis provides the organic carbon that forms the base of food chains and delivers most of the dissolved oxygen in the water which allows higher life forms in the aquatic environment. Solar radiation is not only the energy source for photosynthesis but also the major source of heat for the water column driving water turbulence in the basin in combination with wind energy. The solar radiation that reaches the horizontal surface of the earth is called global radiation, and it consists of direct solar radiation and diffuse radiation resulting from reflected or scattered sunlight, respectively. The sun as a light source emits electromagnetic waves. Wave lengths range from energetic short-waves (UV light, 280–380 nm) and visible light (350–700 nm) to lower-energy infrared light (700–3,000 nm). Photosynthetically available radiation (PAR) is restricted to the visible light spectrum.

The intensity of PAR varies seasonally and with cloud cover, and it decreases with increasing depth of the water column. A small part of the direct sunlight impinging on the water surface is lost by reflection, whereas most part of the radiation penetrates the water column and exponentially decreases with water depths, as described mathematically by Lambert-Beer's law:

$$E_d(z) = E_d(0) * e^{-k_d * z} \quad (\text{Eq. 1}),$$

where $E_d(z)$ indicates radiation intensity [$\mu\text{Em}^{-2}\text{s}^{-1}$] in the water depth z [m], $E_d(0)$ is radiation intensity [$\mu\text{Em}^{-2}\text{s}^{-1}$] at the water surface, and k_d is the vertical attenuation coefficient [m^{-1}]. Equation 1 shows that the attenuation is strongly wavelength dependent.

The rate at which the PAR intensity decreases with water depth also depends on the amount of light-absorbing dissolved substances (mostly organic carbon compounds washed in from decomposing vegetation in the watershed) and the amount of absorption and scattering caused by suspended materials (soil particles from the watershed, algae, and detritus). The depth in which 1% of the solar radiation at water surface $E_d(0)$ is measured is generally defined as the euphotic layer; almost all of the photosynthesis occurs within this layer, thus the depth of

the eutrophic zone is generally proportional to the level of primary production. The percentage of surface light absorbed or scattered in a 1 m-long vertical column of water is called the vertical extinction coefficient (k). In lakes with low k -values, light penetrates deeper than in those with high k -values.

Algal growth increases almost linearly at low irradiance, saturates at an optimal irradiance level for growth, and then declines because of photoinhibition (Langdon, 1988; Talmy et al., 2013; Edwards et al., 2016). The optimal irradiance for phytoplankton commonly varies between 33–400 $\mu\text{mol m}^{-2} \text{s}^{-1}$ (Singh and Singh, 2015). In natural environments, light intensity at a lake surface is often high above the saturation level that may induce photoinhibition and inhibit phytoplankton growth. The increase of light intensity may induce a higher incorporation of carbon into carbohydrates (Cook, 1963; Ross and Geider, 2009) and storage lipids in phytoplankton cells (Gordillo et al., 1998), whereas light limitation may decrease these storage pools (Jebsen et al., 2012). If eutrophication progresses, phytoplankton overgrowth and subsequent death result in a greenish slime layer over the water body surface. This slime layer reduces light penetration and restricts reoxygenation of water through air currents. The decline of macrophytes and phytoplankton in many shallow water bodies probably occurs because of light limitation due to algal blooming. Furthermore, phytoplankton in aquatic ecosystems is often subjected to light fluctuation with short timescales, ranging from seconds to hours or days (Litchman and Klausmeier, 2001), and the vertical mixing of the water column changes underwater light intensity from complete darkness to full sunlight (MacIntyre et al., 2000). Fluctuating light conditions exert a great influence on phytoplankton photosynthesis, growth rates, and species composition (Marra, 1978; Litchman, 2000; Wagner et al., 2006).

Besides measuring radiation intensity, Secchi-depth is used to measure water transparency, which is also an indicator of lake trophic status. Water transparency directly affects the amount of light penetrating a lake, and it influences photosynthesis and oxygen production. Algae and suspended particles from erosion make the water turbid or coloured, thus decreasing the transparency of a lake. Therefore, low Secchi-depth readings indicate water column either with high algal concentration or high concentration of suspended particles or inorganic nature. A general rule of thumb is that the eutrophic depth is $\sim 2\text{--}3$ times the Secchi-depth.

Clear-water phases have been observed in many eutrophic lakes in late spring (Sommer et al., 1986; Deneke and Nixdorf, 1999). Intense grazing of filter-feeding zooplankton (i.e.,

cladocerans) because of increasing temperature has been proved to be the main mechanism behind the fast decline in algal biomass (Lampert et al., 1986; Deneke and Nixdorf, 1999). Moreover, other factors such as nutrient limitation may also reduce phytoplankton growth at the end of the spring maximum (Reynolds, 1984). During a clear-water phase, zooplankton grazing may lead to changes in standing crop of biomass, distribution, and community composition (Sommer et al., 1986; Stock and Dunne, 2010; Mitra et al., 2014; Stock et al., 2014).

1.2.2 Temperature

Temperature is a key parameter in water quality monitoring as it likely plays a critical role in driving a lake's circulation and stratification (**Figure 1**). Solar radiation is absorbed by the surface water of a lake, which increases the temperature of the water and therefore changes its density. As the surface water temperature increases from 0°C to 4°C, it becomes denser and sinks. When the temperature and density of the surface water become equal to those of the bottom water, the spring/autumn turnover begins. The warming of the surface waters eventually leads to a boundary between surface water and deep water. The temperature profile is then called stratified, and the water body is formed by the upper warm epilimnion and the lower cold hypolimnion. Between these layers is the metalimnion (thermocline), which is a temperature jumping layer and has the greatest relative temperature changes (Hutchinson, 1957). The occurrence of stratification depends on characteristics like depth, shape, and size of a lake. In some small and shallow lakes, seasonal thermal stratification may not occur because the wind mixes water of the entire water body. In other lakes, such as Lake Auensee (in Leipzig, Germany), thermal stratification commonly occurs because of the combination between geographic location and lake depth. Stratification has important impacts on phytoplankton populations, fisheries management, and water supply quality, such as: 1) it may result in lack of dissolved oxygen in the hypolimnion; 2) in anoxic conditions, phosphorus and ammonia release from the sediments and transfer to the hypolimnion, repelling fish that are sensitive to ammonia; 3) the loss of oxygen by the hypolimnion may induce denitrification and N-depletion in the bottom waters. It is suggested that long-term stratification together with temperature and salinity are major factors inducing cyanobacterial blooms (Paerl and Otten, 2013).

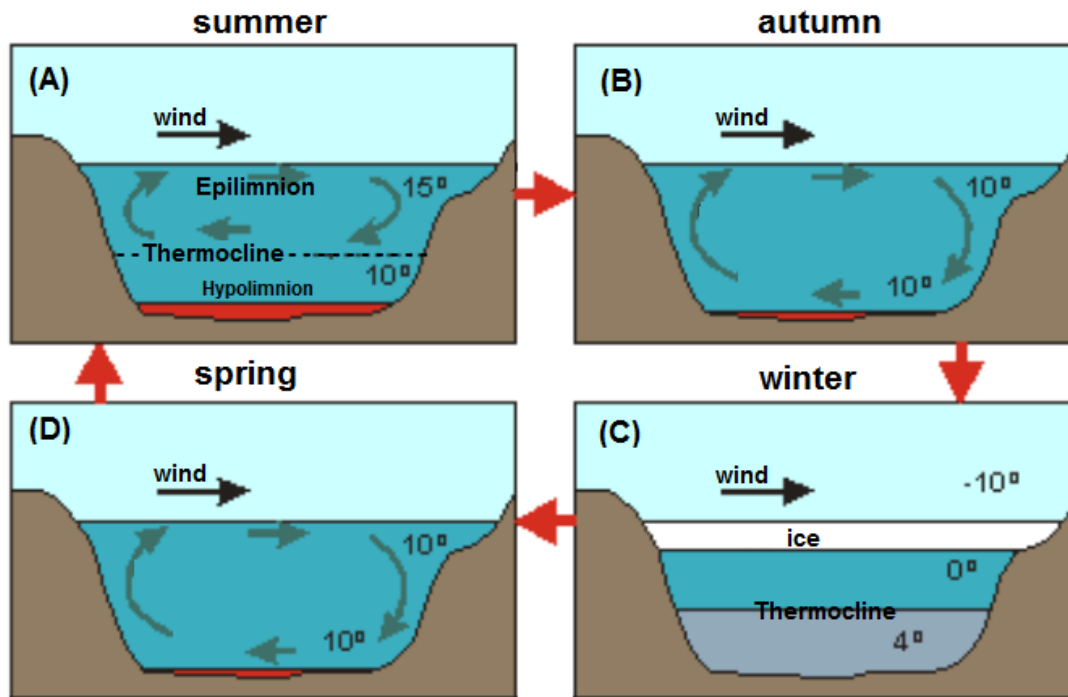


Figure 1 Circulation in a freshwater lake. The diagram shows a cross section through a typical freshwater lake. In summer (A), the temperature of the surface water is increased, and the surface water becomes lighter than the bottom water. Although wind-induced surface currents stir the water around, if the lake is deep, they are not strong enough to mix the entire lake, and a thermocline is developed. Without a cooler autumn, water temperature in the entire lake eventually becomes similar because of the downward conduction of heat. Organisms living above the thermocline consume all available nutrients there and then their deceased bodies sink to the bottom layer. The bottom layer may become anoxic (i.e., lacking oxygen) because oxygen is used in the decomposition of dead organisms. In autumn (B), the temperature of surface water decreases until no thermocline remains, enabling surface currents to lift nutrient-rich bottom water to the surface. In winter (C), an ice sheet forms, and surface water becomes colder than the bottom water as a result of the unique property of water of being heaviest at 4°C. With this, another thermocline develops. Fish hibernate in the layer under the thermocline. In spring (D), the winter layering disappears and the whole lake is mixed, enabling spring blooms of phytoplankton and other organisms (Anthoni, 2000).

Temperature as well as temperature-related environmental processes may significantly influence phytoplankton growth rates, nutrient stoichiometry, and spatial and temporal species distribution in freshwater systems. The growth rate of phytoplankton has been demonstrated to increase slowly (frequently nonlinearly) with increasing temperature up to a species-specific optimal growth temperature (T_{opt}), followed by a fast decrease in growth rate at temperatures above the optimum one (Ahlgren, 1987; Renaud et al., 2002; Briand et al., 2004; Jöhnk et al., 2008; Montagnes et al., 2008). For example, diatoms tend to have relatively low T_{opt} , ranging between 15–25°C (Ignatiades and Smayda, 1970; Foy and Gibson, 1993; But-

terwick et al., 2005), which is similar to that of cryptophytes (19–24°C; Ojala, 1993). The T_{opt} of dinoflagellates is between 21–26°C (Kim et al., 2004). Cyanobacteria and chlorophytes appear to have the highest T_{opt} levels between 25–35°C (Robarts and Zohary, 1987; Sosik and Mitchell, 1994; Bouterfas et al., 2002; Zargar et al., 2006; Cho et al., 2007). Together with factors such as nutrient availability, light, and grazing pressure, temperature affects the primary productivity and seasonal dynamics of phytoplankton communities (Karentz and Smayda, 1984), i.e., in dimictic lakes in temperate regions, spring blooms of diatoms and cryptophytes, early-summer blooms of green algae, summer booms of cyanobacteria, and autumn blooms of diatoms and/or dinofytes (Lewis, 1978).

From the physiological point of view, temperature does not influence the primary reactions in photosynthesis but exerts a strong effect on the activity of enzymes that play key roles in metabolism by regulating metabolic pathways and reaction rates that control algal growth and physiology (Konopka and Brock, 1978; Béchet et al., 2013). Temperature has been reported to affect the biochemical composition of cells. For example, as temperature increases beyond the optimum value, the level of unsaturated fatty acids in cell membrane gradually decrease and lipid synthesis is inhibited (Kalacheva et al., 2002; Converti et al., 2009), leading to the accumulation of polysaccharides. Furthermore, several studies have demonstrated that, when organisms are grown at higher temperatures, higher cellular nitrogen-to-phosphorus and carbon-to-phosphorus ratios can be observed because fewer phosphorus-rich ribosomes relative to nitrogen-rich proteins are required to sustain growth and maintenance (Toseland et al., 2013; Yvon-Durocher et al., 2015).

Global warming is one of the main features of climate change, and strongly interacts with higher efflux of nutrients stimulating eutrophication of water systems (Li and Liao, 2002). Global average surface temperatures have been predicted to increase 1.1–6.4°C within the next 100 years (IPCC, 2007), and this may increase water temperatures, alter the thermal regime of many freshwater habitats (Webb and Nobilis, 2007), and change phytoplankton community structure and distribution in especially sensitive aquatic ecosystems such as small and shallow eutrophic lakes. For example, many authors have suggested that climate warming may cause the decrease of phytoplankton diversity and promote HABs (Paerl and Huisman, 2009; Paerl et al., 2011). Therefore, a better understanding of the relationship between temperature and phytoplankton growth potential will improve our ability to predict species turnover and productivity and will allow early warning systems for HABs.

1.2.3 Dissolved oxygen

Dissolved oxygen is the amount of oxygen dissolved in lake water. Oxygen is necessary for the survival of all living organisms except some bacteria, and it is an important indicator of pollution or eutrophication in aquatic ecosystems.

Dissolved oxygen is supplied to a lake from two main sources: diffusion from the atmosphere and photosynthesis. Oxygen diffuses into the surface of a lake from the atmosphere because of wave action and turbulence. Alternatively, oxygen is supplied in well-illuminated eutrophic zones with active photosynthetic aquatic organisms (i.e., plants and phytoplankton). In the photosynthesis process, plants and phytoplankton use chlorophyll and sunlight energy to convert carbon dioxide (CO₂) and water into sugar (glucose, C₆H₁₂O₆) and release oxygen into the water. Dissolved oxygen is consumed mainly by respiration, decomposition and various chemical reactions. Respiration is when animals breathe in oxygen and use it to produce energy, releasing CO₂ and water as by-products. Decomposition is the natural process of metabolic degradation of organic matter (e.g., animal tissues, plant residues and microbial material) into simple organic and inorganic compounds by invertebrates, bacteria and fungi.

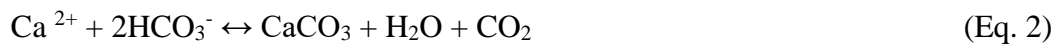
In a stratified water body, the epilimnion is often oxygen-saturated or oversaturated during the day because of oxygen production by photosynthesis, while at night aquatic organisms respire and consume oxygen. Moreover, temperature changes oxygen solubility in water, so cold waters contain more oxygen than warm waters (Wetzel, 1975). Therefore, variations in dissolved oxygen may occur seasonally or even over 24-hour periods depending on temperature, salinity, turbulence, atmospheric pressure, and biological activity.

Oxygen stratification often occurs in water bodies with strong thermal stratification. Especially in eutrophic waters, oxygen concentration greatly decreases with depth (heterograde distribution). In the darker hypolimnion, dissolved oxygen is often depleted because of the absence of photosynthesis and the high activity of microbial decomposition processes of dead plant and animal tissues that come from the upper water layers. These processes are highly promoted during HABs (Chen et al., 2012). Massive algal blooms last from a few days to many months and lead to anoxic dead zones in the hypolimnion, where neither fish nor plants are able to survive (Diaz and Rosenberg, 2008). Anoxic waters are defined by having dissolved oxygen concentration below 0.5 mg/L (US Geological Survey, 2013).

1.2.4 pH value

Among the physical factors, pH is a very important factor that influences phytoplankton distribution, diversity, and productivity (Chen and Durbin, 1994; Locke and Sprules, 2000; Hansen, 2002). It reflects the acid-base condition of waters. Mathematically, the pH value is the negative logarithm of the proton concentration ($\text{pH} = -\log c(\text{H}^+)$). Values in the range of $0 > \text{pH} > 7$ indicate acidic conditions, $7 < \text{pH} < 14$ indicate alkaline conditions, and $\text{pH} = 7$ indicates neutral conditions.

The consumption of CO_2 during photosynthesis changes the lime-carbonic acid balance in the lake water, as follows:



When CO_2 is consumed (i.e., by photosynthesis), this equilibrium shifts to the right to supply CO_2 and insoluble calcium carbonate (CaCO_3), and pH values are above 8.3. At $\text{pH} > 8.3$ almost no free CO_2 is available. At $\text{pH} > 10$, there is more carbonate than bicarbonate; the carbonates of calcium is much less soluble than their bicarbonate forms. In freshwater systems, photosynthesis and respiration affect pH values and their temporal (i.e., diurnal) and vertical gradients. More alkaline conditions occur at the end of the day, whereas at night pH is recovered by the release of CO_2 from respiration.

Daily and seasonal fluctuations in pH are commonly minor compared to those of temperature and biological interactions; however, pH variations of 1–2 units implicate in 10- to 100-fold changes in free hydrogen ion activity (Weisse and Stadler, 2006). Changes in pH also have strong impacts on the solubility, bioavailability, and toxicity of nutrients such as phosphate, ammonium/ammonia, iron, aluminium, and other heavy metals (Anderson, 1988; Wetzel, 2001), especially in increased temperatures and anaerobic conditions (Redshaw et al., 1990; De-Montigny and Prairie, 1993; Wang et al., 2008; Hou et al., 2013). Furthermore, hydrogen ion concentration changes increase the energy demand to regulate intracellular pH, membrane potential, energy partitioning, photosynthetic electron transport, and activity of intra- and extracellular enzymes (Stumm and Morgan, 1981; Walsby, 1982; Beardall and Raven, 2004, Riebesell, 2004, Giordano et al., 2005). Extreme pH values are stressful and harmful to aquatic organisms. High pH levels may increase dissociation of toxic ammonia (at $\text{pH} > 10.5$), which can kill fish and other organisms, whereas low pH levels mobilize heavy metals in the sediment more mobile. It has also been indicated that $\text{pH} < 6.5$ may be harmful

to many species of fish (US. EPA, 1980). A pH value between 6.5–9.0 would be suitable for the protection of aquatic habitats. Optimum growth of cyanobacteria is generally reported to occur in neutral to alkaline pH as these organisms are alkalophiles (Ritchie, 1991; Kaushik, 1994).

1.2.5 Electric conductivity

Electric conductivity is a measure of the ability of water to conduct an electric current. It is widely used as a quick indicator of salinity. Salinity is the total concentration of all dissolved salts in water (Wetzel, 2001), approximating the overall concentration of total dissolved solids present in their ionic form, such as sodium, potassium, chloride, carbonate, sulphate, calcium, magnesium, etc. The rise of electric conductivity in freshwater is commonly dependent on increases in water salinity and temperature (Talley, 2000). Micro siemens per centimetre ($\mu\text{S cm}^{-1}$) is the standard and commonly used unit for the electric conductivity freshwater measurements. The electric conductivity between 200–1000 $\mu\text{S cm}^{-1}$ is the normal value for most major rivers; water with electric conductivity out of this range is unsuitable for certain species of fish or insects. Studies have suggested that salinity and nutrient availability have often been considered the most important variables determining changes in the phytoplankton growth and species composition (Comín and Valiela, 1993; Romo and Miracle, 1995; López-Flores et al., 2006; Reyes et al., 2007; Specchiulli et al., 2008; Redden and Rukminasari, 2008; Flöder et al., 2010; Larson and Belovsky, 2013; Dalu et al., 2014; López-Flores, 2014).

Electric conductivity is an important indicator not only for water quality monitoring, but also for monitoring a water body's surrounding environments (Pal et al., 2015). Significant changes in conductivity may be attributed to natural flooding, evaporation or man-made pollution; any of these factors can be detrimental to water quality, so a sudden increase or decrease in conductivity in a water body may indicate pollution. Agricultural runoff and sewage leakage may be primary causes of increased conductivity because of the additional chloride, phosphate, and nitrate ions.

1.2.6 Nutrients

Nutrients consist of a variety of chemical elements and compounds that are essential for growth and survival of living organisms. In aquatic ecosystems, carbon (C), nitrogen (N), phosphorus (P), and silicate (Si, for diatoms) are the most important macroelements for phytoplankton growth. Micronutrients (such as iron, manganese, copper, and molybdenum) and organic compounds (polypeptides, amino acids, vitamin B12-cobalamin, B1-thiamine, and B7-biotin) also affect algal growth. In aquatic ecosystems, chemical elements are found in the following forms: 1) organic particulate nutrients, i.e., living and dead organic matter such as bacteria, plants, and animals; 2) inorganic particulate nutrients, i.e., minerals and nutrients attracted to the surface of suspended inorganic sediment particles; 3) dissolved inorganic forms. Most nutrients in lakes and reservoirs are derived from the bedrock, atmospheric deposition, vegetation and animal life in and around the water body, and input from human activities.

Even though the mechanisms of water eutrophication are not fully understood, excessive total nitrogen (TN) and total phosphorus (TP) in water are considered to be the major factors that induce water eutrophication and algal blooms (Tong et al., 2003; Fang et al., 2004; Yang et al., 2008). Generally, the influencing factors of water eutrophication include: 1) excessive TN and TP; 2) slow current velocity; 3) adequate temperature and other favourable environmental factors; and 4) microbial activity and biodiversity (Li and Liao, 2002). Water eutrophication may occur rapidly when all of these conditions are favourable.

Phosphorus

The most common form of phosphorus used by biological organisms is ortho-phosphate (PO_4^{3-}), which plays a key role in the formation of cell membranes, adenosine triphosphate (ATP), and nucleic acids (DNA and RNA) (Harris, 1986). ATP is important for energy storage and use and a key molecule in the Krebs's cycle; moreover, the backbones of DNA and RNA are formed by sugar-phosphate groups. Thus, P availability usually limits the primary production of a water system.

The P cycle in an aquatic ecosystem is connected to the food chains. Faecal waste and dead organisms with P sink to the bottom of a water body, where the element becomes part of the sediments. Rooted plants then absorb P from the sediments and transform it into organic

compounds. Once these plants are consumed by herbivores, P is either incorporated into the herbivores' tissues or excreted. When the animal or plant decays, P is returned to the water (Horne and Goldman, 1994). P levels in water samples collected from lakes are usually determined by measuring ortho-phosphorus (OP; in the form of $\text{PO}_4^{3-}\text{-P}$) and TP. TP includes OP, dissolved organic P, and stored P (Wetzel, 2001).

In eutrophic lakes, large amounts of P are usually released during summer stratification and accumulate in the form of soluble reactive phosphate in the hypolimnion (Nürnberg, 1987). The mechanisms behind sediment P-release are, for instance, effects of temperature, mineralisation, redox conditions, and microbial processes. When water P level is enhanced, a dramatic drop in nitrogen-to-phosphorus (N:P) ratio leads to nutrient imbalance in the system (Rhee, 1974, 1978; Goldman et al., 1979; Burkhardt et al., 1999; Geider and La Roche, 2002). Eutrophication and imbalance of nitrogen and phosphorus are considered to be main causes of HABs (Schindler, 1977; Smith, 1983; Havens et al., 2003; Huisman and Hulot, 2005). HABs can negatively impacts other organisms' (e.g., submerged macrophytes) growth and species diversity because of enhanced shading and toxin stress on plant metabolism (Barker et al., 2008; Olsen et al., 2015; Yu et al., 2015).

According to the “experienced molecular formula”— $\text{C}_{106}\text{H}_{263}\text{O}_{110}\text{N}_{16}\text{P}$ —of algae, N and P are the two elements that least contribute to alga biomass. Some studies have suggested that P is the ultimate limiting nutrient that controls phytoplankton biomass and production (Mainstone and Parr, 2002), based on the elemental stoichiometry and strong relationships between TP and chlorophyll (Sakamoto, 1966; Dillon and Rigler, 1974; Schindler, 1977). This means that the available quantity of this nutrient controls the pace at which algae biomass is produced. Studies have suggested that P limitation is a problem in lakes, where the ratio of N:P has been enhanced by increased anthropogenic input of N (Bergström and Jansson, 2006; Camarero and Catalan, 2012; Moss et al., 2013). It was reported that reported that 80% of lake and reservoir eutrophication is restricted by P (Zhao, 2004).

Nitrogen

Nitrogen is essential for the growth and reproduction of living organisms. It is primarily found in proteins, nucleic acids, and many other organic and inorganic compounds. Proteins comprise not only structural components but also enzymes essential for the functioning of all living

organisms. N is also an important component of chlorophyll, which is essential for primary production. N exists either in an oxidized form dissolved in water, usually as nitrate (NO_3^-) and nitrite (NO_2^-), or in a reduced form, mainly as ammonium (NH_4^+) and ammonia (NH_3). Both inorganic forms are used by algae and other primary producers (Smith, 1986). The dissolved inorganic nitrogen (DIN) levels in water samples collected from lakes are usually determined by measuring nitrate and ammonium in $[\text{mg l}^{-1}]$. Atmospheric dinitrogen gas (N_2) is also directly used as a nutrient source by some species of cyanobacteria (i.e., N_2 -fixing/diazotrophic cyanobacteria).

Organic N, as an N compound originated from living materials (such as excreta and tissues), are converted by bacteria into inorganic forms of N (eventually to ammonium or ammonia) and become available for primary producers (Wetzel, 2001). The decomposition processes are called ammonification/mineralisation. The conversion of ammonium/ammonia to nitrite followed by the oxidation of nitrite to nitrate is performed by different types of bacteria in aerobic conditions and is called nitrification. Nitrification removes ammonia from the water column, which is important as ammonia gas is toxic to plants and animals. Other bacterial species reduce nitrates into nitrogen gas through a process of internal loss of N called denitrification. Denitrification is a microbial-facilitated reduction of nitrate- or nitrite-N to a gaseous form, either nitric oxide (NO), nitrous oxide (N_2O) and/or N_2 . The main consequence is the conversion of biologically available N to biologically unavailable N, leading to N-limitation in aquatic ecosystems. Denitrification is an anaerobic process, which occurs when no oxygen or extremely low concentrations of oxygen are available. The simplified cycle of N in aquatic ecosystems is shown in **Figure 2**.

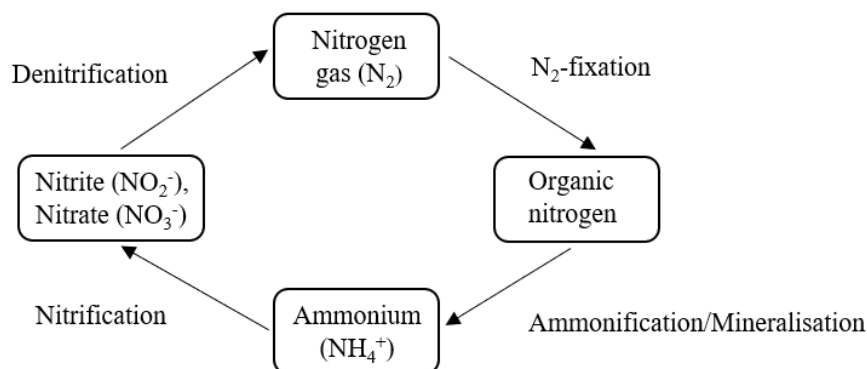


Figure 2 Simplified nitrogen cycle in aquatic ecosystems, which involves different forms of nitrogen and transformation processes.

Although it is generally believed that P limitation often occurs in freshwater phytoplankton and N-limited growth is more common in marine phytoplankton (Cloern, 2001; Philips, 2002), limnological experiments have shown that N is at least as likely as P to limit phytoplankton growth (Elser et al., 1990, 2007). N limitation or co-limitation of N and P can occur when the N supply to the system is outpaced by the P supply. Several studies have reported that N limitations commonly occur short-termly in freshwater systems even when nutrient conditions do not indicate N-limitation (Barica, 1990; Hyenstrand et al., 1998; Matthews et al., 2002).

Determination of nutrient limitation based on TN:TP mass ratios

The nutrient status of a lake may be inferred by the observation of TN:TP mass ratio in relation to the phytoplankton nutritional requirements; this can be used to infer whether a lake is likely to be limited by N or P or both nutrients. The Redfield N:P mass ratio of 7:1 (Redfield, 1958) is broadly used as a benchmark of balanced growth requirements to determine the limiting nutrient. A significantly low ratio suggests that the lake water is N-limited, while a significantly high ratio indicates P-limitations.

However, the TN:TP ratio for determining nutrient limitation should be used with caution. On one hand, the critical TN:TP mass ratio, which indicates nutrient-limited growth of cells in ecosystems, is very plastic. Moss et al. (2013) reported that a TN:TP value of 3.6–13.5 should be used to separate P-limitation from N-limitation. Abell et al. (2010) identified a potential N-limitation at $TN:TP < 7$. Moreover, based on studies on a broad range of lakes and ocean sites, Guildford and Hecky (2000) concluded that N-deficient growth was noticeable at $TN:TP < 9$, whereas P-deficient growth consistently occurred when $TN:TP > 22.6$. Therefore, the determination of limiting nutrient must consider the available N and P concentrations in the water. On the other hand, the environmental TN and TP availability in ecosystems is not always responsible for the cellular nutrient stoichiometry (Hall et al., 2005). For example, diazotrophic cyanobacteria are likely to enhance the cellular N:P ratio by N_2 -fixation when N is less available in water systems. Moreover, in shallow lakes, some benthic algae appear to take up nutrients directly from sediments, thus their cellular N:P ratio may differ from that measured in the water column. Therefore, TN:TP ratios should be used with caution in the prediction of nutrient limitation in individual systems because they do not al-

ways identify the limiting nutrient as nutrient bioassays do (Nikolai and Dzialowski, 2014). Alternatively, cellular nutrient ratios (see **Section 1.4.4**) may provide more accurate information about the nutritional status of microalgae.

As aforementioned, the use of external N:P ratio to monitor phytoplankton nutrient limitation should be considered in combination with other criteria such as absolute N and P concentrations (**Table 2**). Some studies have suggested that the DIN:TP ratio is the best predictor for limiting nutrient in freshwater ecosystems (Morris and Lewis, 1988; Bergström, 2010; Ptacnik et al., 2010). Bergström (2010) indicated the existence of a shift from N-limited to P-limited growth of phytoplankton with increases in DIN:TP mass ratios. Moreover, nutrient uptake (**Table 3**) is also an important indicator of phytoplankton species-specific nutrient status. Species' nutrient uptakes are characterized by nutrient-specific Michaelis-Menton constants, which result from genetic differences. In this study, the aforementioned criteria such as absolute N and P concentrations, DIN:TP ratio and species' nutrient uptakes have been used to determine N/P-limitation of phytoplankton in Lake Auensee.

Table 2 Criteria of nutrient sources influencing algal mass and species composition based on references from the literature. DIN, dissolved inorganic nitrogen; TP, total phosphorus; OP, ortho-phosphorus.

Ratio or level	Significance	Reference
N:P = 7:1 (mass ratio)	"Redfield ratio"	Redfield, 1958
DIN:TP < 1.5 (mass ratio)	Indicator of N limitation	Bergström, 2010
DIN:TP > 3.4 (mass ratio)	Indicator of P limitation	Bergström, 2010
Inorganic N < 0.1 mg l ⁻¹	Indicator of N limitation	Gophen et al. 1999
OP < 0.002 mg l ⁻¹	Indicator of P limitation	Lee and Jones-Lee, 1998
Ortho-phosphate > 0.01mg l ⁻¹	Dominance of cyanobacteria	Smith et al., 1995
TP > 0.1 mg l ⁻¹	Risk of cyanobacterial dominance ~80%	Downing et al. 2001

Table 3 Half-saturation constants (k_m) for phosphate and nitrate uptake of different algal species: ¹⁾ green algae, ²⁾ cyanobacteria). References: ^{a)} Gotham and Rhee (1981), ^{b)} summarized by Kohl and Nicklisch (1988)

Species	Phosphorus uptake [mg l ⁻¹]	Nitrate uptake [mg l ⁻¹]
<i>Scenedesmus</i> sp. ¹⁾	0.06 ^{a)}	0.2–0.3 ^{a)}
<i>Ankistrodesmus</i> sp. ¹⁾	0.4 ^{a)}	0.08–0.6 ^{a)}
<i>Anabaena</i> sp. ²⁾	0.1 ^{b)}	4 ^{b)}
<i>Microcystis</i> sp. ²⁾	0.15 ^{a)}	

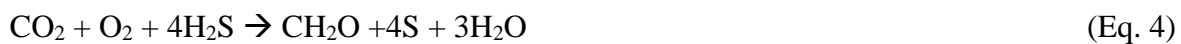
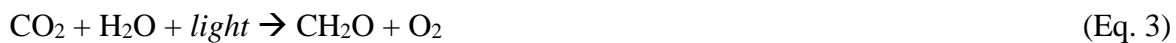
1.3 Algae as biological indicators of water quality

Algae provide interpretable indications of specific changes in water quality because they have high species numbers and each species is differentially sensitive to a broad range of environmental conditions (e.g., diatoms; Kwandrans et al., 1998). The advantages of using algae as biological indicators for lake monitoring were summarized by Murphy et al. (2002) as follows: 1) algae usually have rapid reproduction rates and very short life cycles, making them a valuable indicator of short-term (day-to-week) effects; 2) algae are valuable indicators of ecosystem conditions because they respond quickly to physical and chemical factors; 3) algae are sensitive to certain contaminants that may not significantly affect other aquatic organisms or may only affect other organisms at higher concentrations; 4) changes in community composition may provide a finer-scale assessment of changes resulting from ecological impacts; 5) easy sampling, low price, the least impact on the residents of biota; 6) algae provide a good indication of the nutritional status of the lake such as P and N.

While physical and chemical parameters can indicate the level of water eutrophication, these measurements represent only a snapshot of the current conditions in aquatic ecosystems by giving only a transient picture of prevailing environmental conditions. In comparison, the abundance and composition patterns of phytoplankton *in situ* reflect precisely the water quality at any point. Phytoplankton can also be used to compare relative variations in water quality in terms habitat variability or time (Karacaoğlu et al., 2006; Demir, 2007; Gokce and Ozhan, 2011). In phytoplankton-related assessments, primary production, total biomass of algae, distribution, and taxonomic composition are usually used as indicators of water quality (European environmental agency, 2001; Gharib et al., 2011).

1.3.1 Primary production

In aquatic ecosystems, phytoplankton is the basis of the aquatic food web (Reynolds, 1984). Primary production is the process of organic carbon formation that sustains food webs and fuels microbially-mediated carbon, nutrient (N, P, trace metals) and oxygen (O₂) cycling in the aquatic environment. Primary production is driven by the process of photosynthesis, which uses sunlight as its source of energy; however, a minute fraction of primary production also occurs through chemosynthesis, which uses the oxidation or reduction of inorganic chemical compounds as its source of energy. Regardless of its source, this energy is used to synthesize complex organic molecules from simpler inorganic compounds such as carbon dioxide (CO₂) and water (H₂O). The following equations are simplified representations of photosynthesis (Eq. 1.3) and a form of chemosynthesis (Eq. 1.4):



In both cases, the end point is a polymer of reduced carbohydrate, (CH₂O)_n, which is typically found in molecules such as glucose or other sugars. The photochemical reaction occurs in the chloroplasts, where photosynthetically active pigments bound to proteins are present in the thylakoid membranes. Photosynthesis is divided into a light-dependent and an enzymatic light-independent Calvin cycle. Light quanta are absorbed by pigment molecules and are supplied as exactions to the reaction centres. H₂O acts as an electron donor for photosystem II and O₂ is formed. The hydrogen released by the splitting of water is used to form two further compounds that act as immediate energy storage means: reduced nicotinamide adenine dinucleotide phosphate (NADPH) and the photophosphorylation energy equivalent created in the form of ATP. In plants, algae, and cyanobacteria, long-term energy storage in the form of sugars is produced by a subsequent sequence of light-independent reactions called the Calvin cycle. In the Calvin cycle, atmospheric CO₂ is incorporated into already existing organic C compounds, such as ribulose biphosphate (RuBP), through a process called carbon fixation. Using the ATP and NADPH produced by the light-dependent reactions, the resulting compounds are then reduced and removed to form further carbohydrates, such as glucose or other sugars. These relatively simple molecules may be then used to further synthesize more complicated molecules, including proteins, complex carbohydrates, lipids, and nucleic acids, or be used for cellular respiration and maintenance of existing tissues (i.e., growth respiration and

maintenance respiration) (Amthor and Baldocchi, 2001; Sigman and Hain, 2012).

Gross primary production (GPP) is the total number of electron equivalents originating from the photolysis of water (Fogg, 1980; Falkowski and Raven, 1997). Photosynthesis is defined as the conversion of light into metabolic energy (Fogg, 1980). Net primary production (NPP) is estimated as GPP corrected for algal respiration. Respiration is the conversion of metabolic energy into ATP. Net ecosystem production (NEP) is GPP corrected for the metabolism of the entire autotrophic and heterotrophic community (i.e., community respiration, CR) and is defined as GPP minus CR (Williams, 1993). The aforementioned variables are based on C units, but parallel terms that express phytoplankton production in units of N also exist (Dugdale and Goering, 1967; Minas and Codispoti, 1993).

Primary production is widely used to assess water quality. In aquatic systems, primary production is typically measured using one of four methods:

- 1) Variations in oxygen concentration within a sealed bottle. This dynamic system was first achieved using the Winkler technique for estimating dissolved oxygen concentrations, introduced by Gaarder and Gran (1927). Nowadays the light-dark bottle oxygen technique is considered insufficiently sensitive, and its resulting rates have poor accuracy and precision (Marra, 2002).
- 2) Incorporation of inorganic carbon-14 (^{14}C , in the form of sodium bicarbonate) into organic matter (Steeman-Nielsen, 1951, 1952; Marra, 2002). This is currently the most commonly used method to infer primary production because it is sensitive and relatively simple. ^{14}C estimates approximate GPP, NPP or some value in between GPP and NPP; if respiration is low (i.e., a low amount of CO_2 from respiration is available for photosynthesis), the ^{14}C estimate is $\sim\text{GPP}$; the ^{14}C estimate is $\sim\text{NPP}$ under all other conditions (Williams, 1993; Marra, 2002). However, use of radioisotopes requires special procedures for handling and disposal that can greatly complicate or preclude some field operation. Also, there are filtration effect safety concerns due to radioactive hazards. Therefore, this method is commonly used in ocean environments.
- 3) Stable isotope methods. A modulator of the isotope ratio of particulate organic C (^{13}C) is the isotopic composition of dissolved inorganic C available for the growth of the organisms (Quay et al., 1986; Herczeg and Fairbanks, 1987). The isotopic ratio of dissolved inorganic C in surface waters is determined by a balance between photosynthetic uptake and respiratory production. The oxygen (^{18}O) method (Bender et al., 1987) directly measures

the GPP using the stable isotope ^{18}O as a tracer of molecular oxygen production through photosynthesis. One disadvantage of this method is that gross oxygen production determined by the ^{18}O method evaluates total oxygen production and it is unclear if this is directly linked to C assimilation (Bender et al., 1999; Robinson et al., 2009).

- 4) Fluorescence methods. These indirect, non-invasive methods measure phytoplanktonic productions from active chlorophyll fluorescence (Kolber and Falkowski, 1993), which has the potential to evaluate the instantaneous depth and time-dependent value of primary production and quantify rapid changes in productivity. These methods also have the advantage of providing higher temporal sampling rates closely matched to sampling rates for physical variables (e.g., temperature, salinity, oxygen, etc.), which allows a better coupling between environmental and production measurements. Moreover, it resolves primary production at spatial (< 1 m) and temporal (~ 1 s) resolutions that cannot be achieved by *in vitro* approaches (Robinson et al., 2009). Furthermore, this method also provides a better signal-to-noise ratio and allows more robust measurements in oligotrophic ecosystems (Regaudie-de-Gioux et al., 2014). Fluorescence is the emission of visible light by specific molecules at longer (or less energetic) wavelengths than the wavelengths absorbed. In the case of photosynthesis, the energy in the blue region of the sunlight spectrum (430–440 nm) is absorbed by chlorophyll *a* (Chl-*a*) and the emitted light is in the red region (680–685 nm), corresponding to the absorption maxima of Chl-*a* (Jeffrey et al., 1997). After photon absorption by Chl-*a*, the energy can be used for photochemistry, lost as heat, or emitted as light through fluorescence. The fluorescence is approximately inversely proportional to photosynthesis. However, the relationship is not strong, because fluorescence is highly dependent on intensity and quality of the incident light. Low irradiance levels of incident light induce fluorescence positively correlated with Chl-*a* concentration in the cell, while high irradiance levels of incident light quench chlorophyll fluorescence in a nonphotochemical process. Nevertheless, there are some assumptions and uncertainties in the fluorescence method. For example, the conversion of fluorescence data into carbon fixation rate is still an unsolved problem (Gilbert et al., 2000). Absolute electron transport rates calculated from fluorescence data tend to overestimate primary production because of the decoupling of the electron transport rate by the cyclic electron flow around photosystem II (Falkowski et al., 1986; Prášil et al., 1996), photorespiration (Raven and Johnston, 1991), and the Mehler reaction (Kana, 1992).

1.3.2 Phytoplankton composition and Chl-*a* concentration

Phytoplankton demonstrates water quality through changes in its community composition, distribution, and proportion of sensitive species (Gharib et al., 2011). A dominant phytoplankton group can be defined for each sampling event by the highest relative proportion of total biomass (Dunker et al., 2016). In eutrophic lakes, the dominant algal group/species usually shows mass growth (with high density of cells), which is known as algal bloom; these events, such as harmful cyanobacterial blooms, may compromise water quality and have serious consequences to the health of humans and animals (Bouvy et al., 2003).

Phytoplankton abundance and composition patterns are sensitive to alterations in the habitats, and thereby phytoplankton total biomass and many phytoplankton species can be used as *in situ* indicators of aquatic habitat quality (Reynolds, 1984; Chellappa et al., 2009). Desmids, Chrysophyceae, and diatoms (from the genera *Tabellaria* and *Cyclotella*), for example, are found in oligotrophic lakes. Cyanobacteria (*Anabaena*, *Aphanizomenon*, and *Microcystis*) and diatoms (*Asterionella*, *Aulacoseira*, *Fragilaria*, and *Stephanodiscus*) frequently appear in eutrophic lakes (Reynolds, 1998). Diatoms, chlorophytes, and cyanobacteria are found in water systems with wide trophic ranges, from ultra-oligotrophy to hypertrophy. Cyanobacteria have been recognized as key indicators of eutrophication in freshwater because their blooms are common in waters affected by excessive nutrient supply.

Chl-*a* has been largely used as an indicator of autotrophic biomass associated with primary productivity in freshwaters, estuaries, coastal, and marine waters (Steele, 1962; Cullen, 1982). Chl-*a* concentration reflects the net result (standing stock) of both growth and loss processes in pelagic waters, and it is the main easily measured variable used as a nutritional status indicator. Chl-*a* concentration is commonly determined using biochemical (i.e., DIN 38412-L16, 1985), spectrophotometric, fluorometric, or high performance liquid chromatography (HPLC) method. HPLC is a modern technique to determine the composition of phytoplankton communities that allows a simple and fast inventory of the pigments in waters (Becker et al., 2002; Millie et al., 2002). The major taxonomic groups of freshwater ecosystems include green algae, cyanobacteria, cryptophytes, dinoflagellates, and diatoms. Each of these groups contains (besides Chl-*a*) one specific xanthophyll indicative for its presence; the ratio of each group's specific xanthophyll per Chl-*a* is used to determine the percentage contribution of this group to total Chl-*a* (Wilhelm et al., 1991). HPLC allows the quantitative determination of xanthophylls and chlorophylls. The distribution pattern of the pigments is therefore used as a chemotaxonomic-photophysiological feature for the analysis of phyto-

plankton communities.

1.4 *In situ* growth prediction models

Previous methods for the determination of phytoplankton growth rate were commonly modelled based on physiological traits (mostly external to cells) such as cell chlorophyll content, biovolume, carbon to chlorophyll ratio, photon demand per assimilated carbon, and nutrient uptake rates (Walsby, 1997; Schöl et al., 1999; Litchman et al., 2010). However, the high diversity of physiological features such as species morphology and pigmentation may complicate growth determination in the real environment. For example, a main weakness of the use of Chl-*a* is the great variability of cellular chlorophyll content (0.1–9.7% of fresh algal weight) depending on the algal species (Boyer et al., 2009). A great variability (seasonal or on an annual basis) in individual cases is expected as a result of species composition, light conditions, and nutrient availability. Another problem of determining the Chl-*a* concentration of field phytoplankton communities regards physical parameters such as water body turbidity and circulation (MacIntyre et al., 2000). Sudden increases of cell density during sampling may occur because of algae transport by water currents or movement by swimming; for example, some algae in a water layer sink during the morning and float at night (Wilhelm et al., 1995).

The growth-dependent environmental conditions of field phytoplankton are also difficult to determine. For example, real light absorption cannot be accurately measured in natural conditions. Light conditions—i.e., fluctuating light (because of day-night period) and light intensity gradient—should also be considered, together with factors such as turbidity and circulation (MacIntyre et al., 2000). Moreover, to determine nutrient availability, besides ionic concentration, diversity of sources, forms, and fluxes of nutrients must also be taken into account, as well as the interaction between the growth of algal species and other members of the food web (Glibert et al., 2010). Therefore, the growth rates of algae cannot be predicted directly by the dependence on local environmental parameters (Escalera et al., 2010). A higher predictability of algal growth in the field and of phytoplankton dynamics could be attained by using intracellular parameters. The use of the biochemical composition (internal trait of the cell) in growth models may allow more accurate predictions of *in situ* growth rates and simplify the monitoring process. Recent studies have used two specific levels of metabolism in

growth models: the efficiency of light use (e.g., the different metabolic pathways of the absorbed energy, see **Section 1.4.1**), and the carbon or energy allocation to cellular constituents (e.g., C fixed in primary macromolecules, see **Section 1.4.2**).

1.4.1 Growth prediction models based on the efficiency of light utilization

Phytoplankton growth rate is dependent on the amount of absorbed light energy invested in growth processes, the dissipation of excessive energy, and the channelling of electrons into pathways other than C-fixation (Cardol et al., 2011; Fanesi et al., 2016). The most efficient pathway of energy dissipation is measured as non-photochemical chlorophyll fluorescence quenching (NPQ), which includes constitutive heat dissipation, fluorescence, and regulated heat dissipation at light harvesting pigment-protein complexes (Müller et al., 2001; Fanesi, 2016). Another prominent mechanism is to partition excessive energy through different alternative electron pathways such as cyclic electron transport around both photosystems, pseudo-cyclic electron transport via the water-water cycle, photorespiration, and excretion (Wagner et al., 2006; Wilhelm and Selmar, 2011). The contribution of each of these metabolic processes defines the ratio between the fraction of energy used for growth and the fractions of energy actively and passively lost by different energy dissipation pathways, which vary according to different environmental conditions (Fanesi et al., 2016). Fanesi et al. (2016) developed a linear least square regression model to predict algal growth rate in response to temperature gradient based on physiological traits that characterize cell composition—i.e., Chl-*a* content and C:Chl-*a* ratio—, photosynthesis performance—i.e., photosynthetic rate (P), light saturation parameter (I), light utilization efficiency (α), and quantum efficiency of C production (Φ_C)—, light absorption, and energy dissipation—i.e., absorbed photosynthetic energy (Q_{phar}), non-regulated energy dissipation in the form of fluorescence and heat ($\Phi_{f,D}$), regulated energy dissipation in the form of heat (Φ_{NPQ}), energy invested in alternative electron pathways (Φ_{ALT}), and gross energy invested in growth processes (Φ_{GECG}). Fanesi et al. (2016) demonstrated that the growth model can be used to compare the strategies of temperature-dependent absorbed energy partitioning among phytoplankton groups. They further found that cyanobacteria and green algae had relatively low C-fixation capacity at low temperatures; thus, the excessive energy was dissipated by, for example, non-photochemical quenching and alternative electron pathways. In contrast, they found that diatoms could maintain stable C-fixation capacities over the temperature gradient, which prevented the cells from experiencing exces-

sive excitation pressure. Nevertheless, they found taxon-specific growth rates to be positively correlated with increased temperatures as the absorbed energy was mostly invested in growth at high temperatures.

This temperature-dependent growth model has been developed in the later study by using PLSR (partial least square regression) (Fanesi et al., 2017). The PLSR model further confirmed the physiological parameters, which can be identified as the most important descriptors of cell growth rate, included the Φ_C , Φ_{NPQ} , Φ_{GECG} , temperature, the C:Chl-*a* and the Chl-*a* content. Φ_C described the amount of C fixed through the activity of light reaction. Growth rate was positively correlated with the fraction of Φ_{GECG} , but it was negatively correlated with the fraction actively dissipated as heat (Φ_{NPQ}). Φ_{GECG} and Φ_{NPQ} represented opposite pathways of energy partitioning and defined the rate of energy allocated to growth processes. The C:Chl-*a* ratio is a key factor for phytoplankton growth that incorporates two major metabolic processes: light harvesting and C biomass formation (Geider, 1987; Halsey and Jones, 2015; Fanesi et al., 2017). The C:Chl-*a* ratio is correlated with Chl-*a* content, and it exponentially decreases with increasing temperature at constant light levels (Geider, 1987). In the model of Fanesi et al. (2017), Chl-*a* and the C:Chl-*a* ratio were negatively correlated with growth rate. The set of variables relate to most of the cellular functions connected to growth processes (Halsey and Jones, 2015; Wilhelm and Jakob, 2011). This PLSR model successfully identified acclimation strategies of different taxonomic groups in response to temperature changes. Fanesi et al. (2017) suggested that the PLSR model may optimize the modelling for primary production and water quality monitoring.

1.4.2 Growth prediction models based on C-allocation

The second level for growth modelling is based on the cellular C-allocation stoichiometry such as the macromolecular composition/stoichiometry of proteins, carbohydrates, and lipids. Through the Calvin-Benson cycle, CO₂ is fixed by the enzyme Ribulose-1-5-bisphosphate-carboxylase-oxygenase (RubisCo) into organic C and converted into a three-carbon sugar, glyceraldehydes-3-phosphate (GAP). GAP is allocated based on cellular demand to several primary macromolecules, mainly proteins, structural and storage carbohydrates, and lipids, in response to environmental conditions. Proteins are among the most abundant macromolecules in cells, constituting approximately 30–60% of the dry mass under nutrient replete conditions (Geider and La Roche, 2002). Proteins contain the largest portion

of organic N in phytoplankton cells. Carbohydrates and lipids are important macromolecular components, which usually accumulate under nutrient limitation conditions. Both carbohydrates and lipids constitute 10–50% of the cell mass (Geider and La Roche, 2002). Carbohydrates are divided into structural components and storage components. Structural carbohydrates constitute a large fraction of dry weight of algal biomass (e.g., high cellulose contents in cell walls of some species). Carbohydrates are also common energy and carbon storage products in algae that allow an imbalance between the rate of reduced C production in photosynthesis and the rate of reduced C consumption in growth (Raven and Beardall, 2003). Lipids are divided in neutral lipids (e.g., acylglycerols, sterols, etc.) and polar lipids (i.e., phospholipids) according to their structure. Neutral lipids serve as energy storage pools of microalgae, whereas polar lipids are important structural components of all cell membranes. Under optimal growth conditions, high growth rates are balanced with optimal C-allocation for maintaining maximal growth rate; meanwhile, the amounts of all cellular components increase exponentially at the same rate (Montecchiario et al., 2006). When in stressful conditions such as N-limitation, the balance between alga optimal growth rate and C-allocation is interrupted. This occurs because cells react to stress by changing their metabolic pathways and redistributing resources to minimize the effects of environmental perturbation on their reproductive and growth rates (Geider and Osborne, 1989; Montecchiario and Giordano, 2010; Giordano and Ratti, 2013).

Macromolecular composition as a C-allocation trait for growth model

The growth prediction model of Shuter (1979) demonstrated that environmental factors that affect the growth rate of phytoplankton cells also change the C-allocation strategies of four primary compartments: photosynthetic, structural, storage, and biosynthetic pools. A later study added elemental and energetic stoichiometries in this growth model (Kroon and Thoms, 2006). In response to environmental changes, microalgae redistribute energy in parallel with the reallocation of cellular C to form or breakdown macromolecular constituents such as proteins, carbohydrates, lipids, and nucleic acids, which are required for growth (Halsey and Jones, 2015). Many studies have demonstrated that nutrient deficiencies (such as N and P) can decrease growth rates and induce the accumulation of carbohydrates and lipids in Chlorophyceae, Bacillariophyceae, and Cyanobacteria (Goldman et al., 1979; Rhee and Gotham, 1981; Shifrin and Chisholm, 1981; Lohrenz and Taylor, 1987; Geider et al., 1996; Lynn et al.,

2000; Giordano et al., 2001; Bertilsson et al., 2003; Stehfest et al., 2005; Sigee et al., 2007; Dean et al., 2008 a, b). N or P limitations may delay the biosynthesis of N-rich compounds e.g. protein for algal growth, and result in reallocation of C generated in photosynthesis processes towards N-poor storage compounds e.g. carbohydrates and lipids (Palmucci et al., 2011). Here, if the C-allocation hypothesis (CAH) is true, microalgae are expected to restrict growth rate and change C-allocation stoichiometry (e.g. decreases in protein contents, and decreases in biomass ratios of protein-to-carbohydrate or protein-to-lipid), when N or P supply is limiting in environments.

Considering the vast diversity of phytoplankton in natural freshwater ecosystems, it is not surprising that the C-allocation strategies are quite different among phytoplankton taxa/species (Goldman et al., 1979; Lohrenz and Taylor, 1987; Giordano et al., 2001; Montecchiario and Giordano, 2010). Two major physiological responses of C-allocation under changing growth conditions are commonly considered: either cells maintain a very stable homeostatic C partitioning strategy (Montecchiario et al., 2006; Palmucci et al., 2011; Wagner, 2014) or they react to environmental variations with significant changes of macromolecular ratios (Palmucci et al., 2011; Jungandreas et al., 2012; Jebsen et al., 2012). Different taxonomic algal groups react to nutrient stress by having specific C-allocation strategies primarily depending on genetic characters and stress degree. Therefore, the determination of algal growth is hypothesized to be achieved using a taxon-specific prediction model.

C:N:P stoichiometry as a C-allocation trait for growth model

Since organism growth is tightly linked to its macromolecular and elemental composition (Vrede et al., 2004), C:N:P stoichiometry is the basis of growth modelling as it connects phytoplankton energy/C-allocation mechanisms with major environmental factors such as light, temperature, and nutrients (Rhee, 1978; Laws and Bannister, 1980; Urabe et al., 2002; Finkel et al., 2006; Toseland et al., 2013; Garcia et al., 2016; Lopez et al., 2016). The stoichiometric theory suggests that, the average C:N:P molar ratio for optimally growing in nutrient-replete cultures is close to the Redfield ratio ($C_{106}N_{16}P_1$) (Redfield, 1934; Geider and La Roche, 2002), whereas the ratio may widely change under nutrient limitation (Falkowski, 2000; Geider and La Roche, 2002; Vrede et al., 2004).

The used of cellular N:P ratio in growth model is based on the growth rate hypothesis

(GRH). According to the GRH, growth rate is positively correlated with P content (Sterner and Elser, 2002) because growth depends on the P-rich ribosomal RNA (rRNA) concentration. Ribosomal RNA is the major structural component of a ribosome. Ribosome is the structure in which proteins are synthesized in eukaryotes and prokaryotes. Since proteins are key structural components and may act as enzymes in living cells, ribosomes constitute the core of the biosynthesis machinery in all cells. Thus, the N:P stoichiometry reflects the ratio between proteins and the number of ribosomes. Algal growth rate can be found negatively related with the cellular N:P stoichiometry in many studies (Sterner and Elser, 2002; Vrede et al., 2004; Flynn et al., 2010). The cellular C:N stoichiometry is based on allocation patterns between carbohydrates and RubisCo. RubisCo represents a dominant pool of N in autotroph biomass that composes a great proportion of protein in cells. Thus, the C:N stoichiometry reflects how allocations to carbohydrates and to RubisCo jointly affect potential growth of autotroph biomass (Vrede et al., 2004). Therefore, like macromolecular stoichiometry, the C:N:P elemental stoichiometry can also be used for growth modelling of algal species (Rhee, 1978; Poorter et al., 1990; Fujimoto et al., 1997; Pramanik and Keasling, 1997; Jebsen et al., 2012; Halsey and Jones, 2015).

However, the predictive power of the GRH for phytoplankton growth in nature appears to be severely limited. Flynn et al. (2010) suggested that the growth model based on elemental stoichiometry required careful consideration, because the variation ranges are species-specific (Rhee and Gotham, 1981; Lynn et al., 2000; Liu et al., 2001; Bertilsson et al., 2003). Another possible limitation of this growth model is that different phytoplankton stoichiometry strategies are differentially constrained during exponential growth and stationary equilibrium (Klausmeier et al., 2004). Some studies demonstrated that high growth rate and phytoplankton C:N and N:P are highly constrained to a narrow range of values (Klausmeier and Litchman, 2004; Vrede et al., 2004). When cells rapidly grow, nutrient levels are high. In this context, phytoplankton stoichiometry approaches the optimal growth ratio under the optimal uptake assumption; therefore, along a gradient of growth rates, phytoplankton stoichiometry converges on a species-specific optimal ratio at high growth rates (Hillebrand et al., 2013). In contrast, slowly growing autotroph biomass can have highly variable C:N:P values (Vrede et al., 2004). At low growth rates, available nutrients are quite scarce and phytoplankton consume almost all nutrients; therefore, biochemical stoichiometry matches the nutrient ratio supplied in the system (Klausmeier and Litchman, 2004). The relative lack of homeostasis in phytoplankton chemical composition is suggested to be restricted to low growth rates, where-

as fast-growing phytoplankton requires a more constrained stoichiometry (Hillebrand, 2013). Thus, the predicted relationship between growth rate and phytoplankton C:N:P stoichiometry is often not linear (Klausmeier and Litchman, 2004).

1.5 FTIR spectroscopy

FTIR spectroscopy is a novel technique that has been widely used in phytoplankton research, such as taxonomic identification and discrimination of phytoplankton species (Kansiz et al., 1999; Sigee et al., 2002; Duygu et al., 2012; Kenne and Merwe, 2013), biofuel analysis (O'Donnell et al., 2013), nutrient-status analysis of phytoplankton (Beardall et al., 2001 b; Giordano et al., 2001; Heraud et al., 2005; Stehfest et al., 2005; Dean and Sigee, 2006; Jakob et al., 2007; Sigee et al., 2007; Dean et al., 2008a,b; Palmucci et al., 2011) etc. A FTIR spectrum of mid-infrared regions is complex and shows overlapping contributions from all cellular macromolecules, such as proteins, carbohydrates, lipids, and nucleic acids. Thus, it provides a molecular fingerprint that can be used to determine the changes in the relative abundance of cellular organic pools based on their characteristic infrared absorption bands.

FTIR spectra quantification models for determining cellular biochemical traits have been developed for semi-quantitative to absolute-quantitative methods. For semi-quantitative analyses, biochemical composition can be determined by comparing peak ratios of absorption bands or integrating characteristic organic bands of interest. These semi-quantitative methods provide relative contents or variation trends of macromolecules in response to environmental changes but not absolute values of the macromolecules of interest, e.g. the determination of species-specific changes in macromolecular composition (e.g. lipid-to-protein and carbohydrate-to-protein ratios) under nutrient stress by comparing absorbance peak ratios (Giordano et al., 2001; Stehfest et al., 2005; Dean et al., 2010), and monitoring relative contents of macromolecules (e.g. lipids) via band integration (Miglio et al., 2013). The absolute quantitative determination provides more precise information on biomass of cellular macromolecules and their absolute concentrations. There are two main methodical approaches. The first approach is based on band integral calibrated by a single external standard substance used for the quantitative analysis of biomass composition (Pistorius et al., 2009; Laurens and Wolfrum, 2011; Mayers et al., 2013). The second approach is based on a multiple linear regression protocol for fitting single reference spectra into the original cell spectra to calculate the absolute

amount of proteins, carbohydrates and lipids in picogram per cell (Wagner et al., 2010).

Recent studies used a partial least square regression (PLSR) of the whole region of phytoplankton FTIR-spectra to predict growth rates and determine C-allocation stoichiometry. For example, Jebsen et al. (2012) have developed a species-specific PLS model using the entire FTIR spectrum and demonstrated that the cyanobacterium *Microcystis aeruginosa* showed significantly different growth regimes in response to environmental changes when compared to the dinoflagellate *Protoceratium reticulatum*. Fanesi et al. (2017) have modelled the growth rate of phytoplankton cells grown at different temperatures using FTIR spectroscopy. They demonstrated that at low temperature, the low growth rate of phytoplankton was associated with the accumulation of lipids, phosphorylated compounds, and carbohydrates, whereas a preferential allocation of C to protein was observed at a relatively high growth rate at high temperature. In addition, PLSR models have been used to quantitatively determine macromolecular compositions in single cells of green algae, diatom, and cyanobacteria species (Fanesi et al., 2019), and elemental C:N ratio of phytoplankton (Wagner et al. 2019).

Most FTIR studies are focused on laboratory-cultured material; only few analyses have been conducted on field phytoplankton communities. Freshwater microalga communities are commonly complex, being highly species-diverse but with low abundances for each species. To optimize the measurement, FTIR spectroscopy usually combines other techniques to achieve measuring few cells, single cells or even cell components. For example, the use of a synchrotron radiation source, which has a ~100 times higher light intensity than normal light source, can greatly enhanced the resolution of FTIR spectroscopy for the determination of C-allocation stoichiometry (Heraud et al., 2005; Dean and Sigee, 2006; Hirschmugl et al., 2006). The combination of FTIR spectroscopy with a microscope allows the selective analysis of functional microalgae cells from field samples (Stehfest et al., 2005; Dean et al., 2012). The main advantage of this method is that the FTIR spectra can be measured at single-cell level, allowing the characterisation of algal cells directly by their spectra as they occur in the aquatic ecosystem. Wagner et al. (2013) reported a methode of FTIR spectroscopy coupled with flow cytometry (FCM) to determine taxon-specific C-allocation response of different phytoplankton groups in a freshwater system (flow chart of this approach simplified in **Figure 3**). FCM is a powerful tool that provides a fast overview of community heterogeneity and structure at the single-cell level (Toepel et al., 2004; Müller and Nebe-von-Caron, 2010; Picot et al., 2012). It is a laser- or impedance-based, biophysical technology that simultaneously

measures and analyses multiple physical characteristics of single particles, usually cells, which are suspended in a stream of fluid passing through an electronic detection apparatus. FCM provides fast, objective, and quantitative recordings of fluorescent signals from individual cells besides physically separating cells of particular interest. The properties that can be measured include cell size, relative granularity, relative autofluorescence intensity, DNA content, membrane integrity, membrane potential, enzyme activity, and stress response (da Silva et al., 2012).

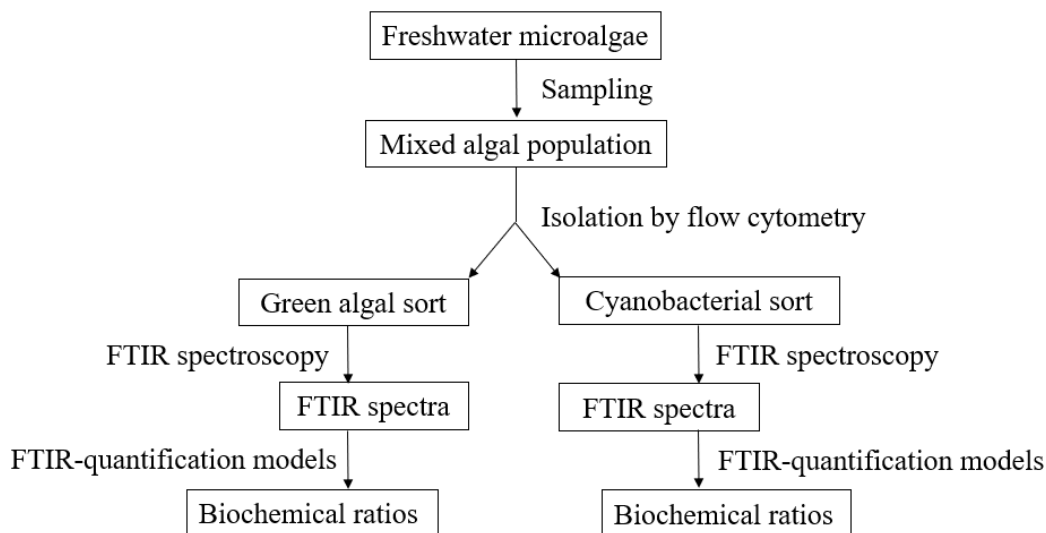


Figure 3 Flow chart of the experiment according to Wagner et al. (2013).

1.6 Aims of this study

The main aim of this study was to test the applicability of FTIR spectroscopy coupled with FCM in a long-term monitoring of phytoplankton growth in Lake Auensee. The functional algal groups (e.g., green algae and cyanobacteria) were isolated from the water samples and their taxon-specific FTIR spectra were measured, according to the approach developed by Wagner et al. (2013) (see **Figure 3**). Based on the FTIR spectra of each algal group, C-allocation-associated biochemical traits and growth potentials were determined using the chemometric models developed in previous studies (Wagner et al., 2010, 2019; Jebsen et al., 2012). These data should be correlated with the measurements of the seasonal variations of a set of environmental factors, including light conditions, water temperature, pH values, dissolved oxygen concentration, and electric conductivity, which may influence the seasonal

succession of phytoplankton in the lake. Finally, a correlation analysis among FTIR-predicted C-allocation traits, population biomass, and environmental factors were performed to test the feasibility of the FTIR-based prediction model and the following hypotheses:

- (1) The content of structure heterogeneity in nature phytoplankton populations varies with seasonal changes of environments.
- (2) Effects of environmental changes on phytoplankton populations can be explained by C-allocation-related traits, such as macromolecular and elemental composition.
- (3) Seasonal variation of phytoplankton growth in response to environmental stresses (e.g., nutrients) can be predicted using FTIR spectroscopy.
- (4) The C-allocation hypothesis, which was confirmed by laboratory experiments, is also suitable for phytoplankton communities in natural conditions.

2. Materials and methods

2.1 Information about the measurement period and Lake Auensee

Auensee (Leipzig, Germany 51.369°, 12.319°) is a hypertrophic shallow lake fed by groundwater (Langner et al. 2004). The lake was formed initially due to gravel mining for the construction of Leipzig's main railway station at the beginning of the 20th century. Two smaller rivers, the White Elster in the north and the Luppe in the south, framed the lake. The average depth is 3–4 m, with a minimum of 3 m in the east and a maximum of 7 m in the west. The lake has a total area of $120 \times 10^3 \text{ m}^2$ (about 12 ha) and a volume of about $526 \times 10^3 \text{ m}^3$.

A single station with maximal depth of 7 m near the southwest strand of Lake Auensee (see **Figure 4**) was chosen as a fixed observation point for the whole observation period between April and early-October 2011. Water samples were collected from the 0–1 m surface layer using a Ruttner-Schöpfer bottle (1 litre capacity, Dangelat, Berlin, Germany), and sieved over a 210- μm mesh filter shipboard to remove zooplankton. Samples were ice cooled, kept in dark and immediately transferred to the laboratory within a few hours for FCM sorting and FTIR spectroscopy analysis.

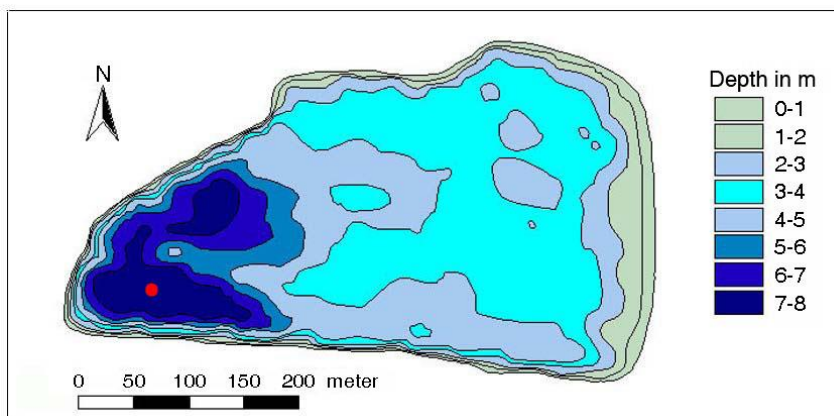


Figure 4 Isobathic map of Lake Auensee 1995 (1:2500) from Institut für angewandte Gewässerökologie Brandenburg, Potsdam. The red pointed on the western side marks the location for water sampling.

2.2 Measurement of ecological factors and nutrients

The global radiation referred to the online data measured by Saechsisches Landesamt fuer Umwelt, Landwirtschaft und Geologie (<http://www.landwirtschaft.sachsen.de/Wetter09/asp/inhalt.asp?seite=uebersicht>). The meas-

urements have been performed daily at 2 m height above the ground (Weather station Leipzig-Möckern (L01), Latitude: 51.37° north of the equator, Longitude: 12.34° east of Greenwich, Geographical height: 100 m). The data describe the number of photosynthetically active photons (PAR: $\lambda = 400\text{--}700$ nm) that are delivered to a specific area over a 24-hour period. The global radiation data were averaged weekly. The light intensity at 0m and 1m depths was estimated from PAR determination using a spherical sensor (Zemoko, Kouderkerke, The Netherlands) in combination with a data-display (LI-250, LICOR, Lincoln, USA, measurement range: 199-19999 $\mu\text{mol s}^{-1} \text{m}^{-2}$). The Secchi-depth was measured to determine the clarity of the water column. The Secchi-disk is a circular plate (20 cm in diameter), and it was attached to a rope and lowered into the water on the shady side of the boat. The disk was kept lowering slowly until it was no longer visible. The depth would be noted.

The dissolved oxygen concentration, pH and water temperature were determined *in situ* with a multiparameter sensor (U-51-10; Horiba, Oberursel, Germany) at 0 m, 0.5 m, 1 m, 1.5 m, 2 m, 3 m, 4 m, 5 m, and 7 m depths.

The phosphorus and nitrogen availabilities in 0m-1m water samples were analysed using the procedure of DIN EN ISO 6878 (D 11) for ortho-phosphate, DIN EN ISO 11885 (E 22) for total-phosphate, DIN EN ISO 10304 2 for nitrate and DIN 38 406 E 5 for ammonium.

2.3 Determination of Chl-*a* concentration

The HPLC-aided pigment analysis of freshwater phytoplankton was performed to determine the structure of phytoplankton communities. The reconstruction of phytoplankton composition is based on the relationship between Chl-*a* and taxon-specific photosynthesis-active pigments (i.e. xanthophylls). These pigments can be used as marker pigments for qualitative and quantitative prediction of Chl-*a* concentration. The corresponding marker pigments of the five major microalgal groups present in Lake Auensee are summarized in **Table 4**.

Table 4 Marker pigments for phytoplankton population analysis via HPLC

Groups	Chlorophyta	Diatoms (incl. Chrysophyceae)	Dinophyta	Cryptophyta	Cyanophyta
Marker pigments	Chl- <i>a</i>	Chl- <i>a</i>	Chl- <i>a</i>	Chl- <i>a</i>	Chl- <i>a</i>
	Lutein, Chlorophyll b	Fucoxanthin	Peridinin	Alloxanthin	Zeaxanthin (Myxoxanthophyll)

The water samples (200–600 ml) from Lake Auensee was vacuum-filtered on a glass fibre filter (50 mm diameter), frozen in liquid nitrogen, freeze-dried and stored at -80°C . For HPLC analysis, the filters were homogenized (20s) by a cell homogenizer (Braun, Melsungen, Germany) in 1.5 ml HPLC-extraction media (90% methanol/0.2 M ammonium acetate (90/10), 10% ethyl acetate [v:v]). The resulting homogenate was centrifuged at 20 800 g for 2 min, and the supernatant was used for injection into the HPLC system. The HPLC-aided pigment analysis of freshwater phytoplankton was described in the previous study by Wilhelm et al. (1995).

The quantification was based on the chromatogram by area/pigment factors developed by Becker, (2000). The quantitative analysis of phytoplankton population and composition of the water samples was carried out by using taxon-specific marker pigments (MPs). Based on defined molar ratios of Chl-*a* to MP (**Table 5**), the predicted Chl-*a* concentration of individual algal group and its percentage in the total population can be calculated, according to the form:

$$\text{Chl-}a = \text{const} + Z_k * \text{Zea} + (\text{L}_k * \text{Lut} + \text{C}_k * \text{Chl-}b) + \text{A}_k * \text{All} + \text{F}_k * \text{Fuc} + \text{P}_k * \text{Per} \quad (\text{Eq. 5})$$

Chl-*a*: calculated total chlorophyll a concentration [$\mu\text{g l}^{-1}$]

const: correlation constant

$Z_k/\text{L}_k/\text{C}_k/\text{A}_k/\text{F}_k/\text{P}_k$: coefficients of zeaxanthin, lutein, chlorophyll b, alloxanthin, fucoxanthin and peridinin, respectively

Zea/Lut/Chl-*b*/All/Fuc/Per: determined pigment concentrations [$\mu\text{g l}^{-1}$] of zeaxanthin, lutein, chlorophyll b, alloxanthin, fucoxanthin and peridinin, respectively

Table 5 Ratio of Chl-*a* to marker pigment (Chl-*a*:MP) used for Auensee in 2011.

Algal group	Marker pigment	Chl-<i>a</i>:MP
Dinophyta	Peridinin	2.433
Bacillariophyceae	Fucoxanthin	2.225
Cryptophyta	Alloxanthin	3.153
Chlorophyta	Lutein/Chl- <i>b</i>	1.539
Cyanobacteria	Zeaxanthin	6.34

2.4 Flow cytometry and electrostatic cell sorting

2.4.1 Flow cytometer

A flow cytometer (BD FaCSAria II) is made up of three main systems: fluidics, optics and electronics. The fluidics system transports particles in a stream to the laser beam for interrogation. The sample is injected into a stream of sheath fluid with the flow chamber (nozzle tip). The flow of sheath fluid accelerates the particles and restricts them to the center of the sample core (known as hydrodynamic focusing), where the laser-beam will then interact with the particles. The movement of particles can be controlled by stream transporting, so that only one cell or particles should move through the laser-beam at a given moment. The optics system consists of lasers to illuminate the particles in the sample stream and optical filters to direct the resulting light signals to the appropriate detectors. When particles pass through the laser intercept, they scatter laser light. Any fluorescent molecules present on the particle fluoresce. The scattered and fluorescent light is collected by appropriately positioned lenses. A combination of beam splitters and filters steers the scattered and fluorescent light to the appropriate detectors. There are two main types of photo detectors used in FCM: one is the photodiode, which is used for strong signals, when saturation is a potential problem; another is the photomultiplier tube (PMT), which is more sensitive than a photodiode. A PMT is used for detecting small amounts of fluorescence emitted from fluorochromes. The detectors produce electronic signals proportional to the optical signals striking them. The electronics system converts the detected light signals into electronic signals that can be processed by the computer. During FACS (fluorescence-activated cell sorting) (**Figure 5**), a vibrating mechanism causes the stream of cells to break into individual droplets after passing through the scattering or fluorescence measuring station.

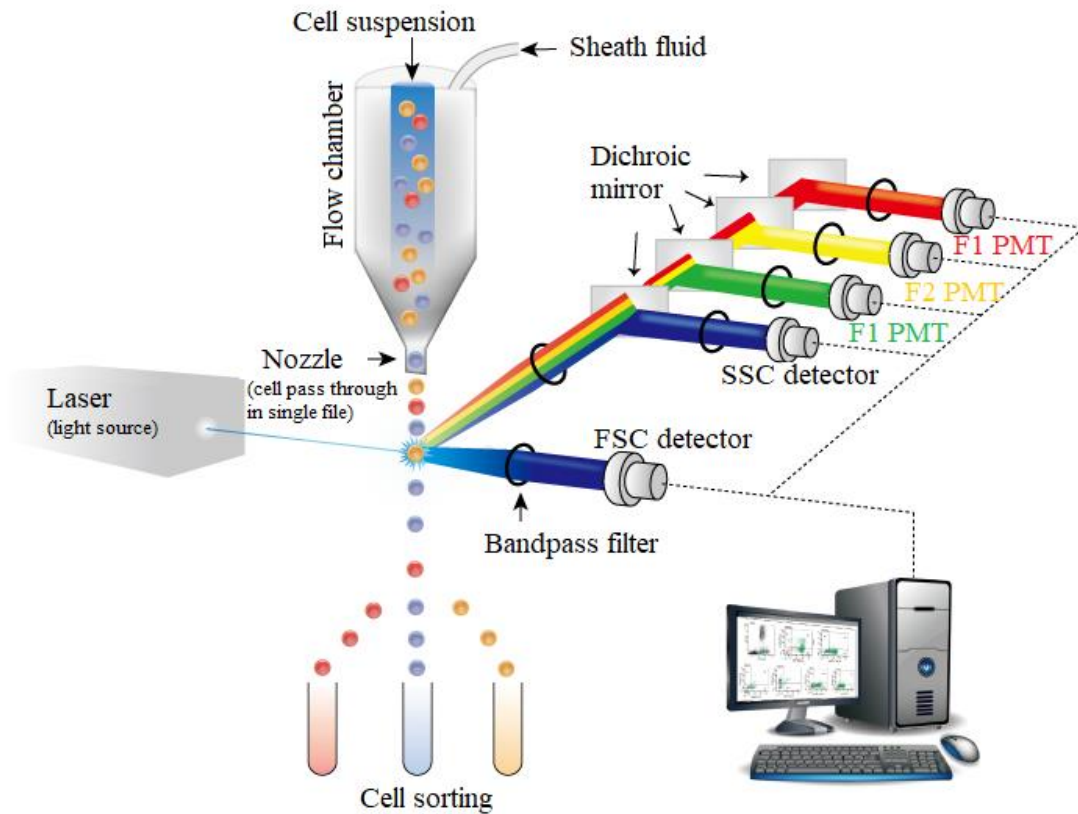


Figure 5 Schematic representations of a Fluorescence-activated cell sorting (FACS), including the flow cell, sheath stream, laser beam, sensing system computer, and droplet collection (<https://www.creative-diagnostics.com/flow-cytometry-guide.htm>).

2.4.2 Principle of algal cell isolation

The basic principle of flow cytometry is that cells/particles pass in single file through a laser beam, so they can be detected, counted and sorted. The amount and type of cells/particles in a sample can be determined in this passage process. The determination is based on the combination of two types of signals detected by FCM: light scatter signals and fluorescence signals.

Light Scatter.

Light scattering occurs when a particle deflects incident laser light. The light scattering signals depend on the physical properties of a particle, such as size and internal complexity. Factors, which affect the signal strength, include cell's membrane, nucleus, and any granular material inside the cell. Cell shape and surface topography also contribute to the total light

scatter. There are two types of signals to determine by FCM (see **Figure 6**). Forward-scattered light (FSC) signals can be used to differ particles in cell-surface area or size. Side-scattered light (SSC) signals are proportional to cell granularity or internal complexity. SSC is a measurement of mostly refracted and reflected light that occurs at any interface within the cell where there is a change in refractive index. SSC is collected at approximately 90 degrees to the laser beam by a collection lens and then redirected by a beam splitter to the appropriate detector.

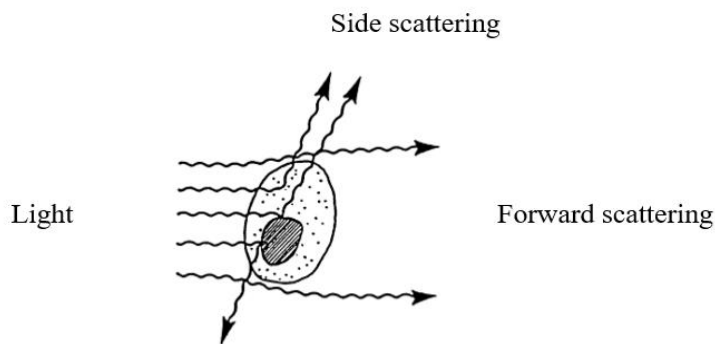


Figure 6 Light-scattering properties of a cell

Fluorescence

When cells/particles sheathed by fluid pass through the laser beam in single file, cell components such as pigments of phytoplankton are fluorescently labelled and excited by the laser to emit light at varying wavelengths. The light emission is known as fluorescence. The fluorescence can be measured to determine the amount and type of cells present in a sample. The range over which a fluorescent cellular compound can be excited is termed its absorption spectrum. As more energy is consumed in absorption transitions than is emitted in fluorescent transitions, emitted wavelengths will be longer than those absorbed. The range of emitted wavelengths for a particular compound is termed its emission spectrum. The fluorescence signals of specific pigments are characteristic for different phytoplankton groups (**Table 6**).

Table 6 Absorption maxima of algal pigments summarized by Braun (1974).

Pigment	Maximal absorbance [nm]	Maximal emission [nm]	Occurrence
Chlorophyll a	435, 670–680	673, 726	all algae
Chlorophyll c	645	629, 690	diatoms, brown algae
Fucoxanthin	425, 450, 475	675	diatoms, brown algae
Phycoerythrin	490, 546, 576	575, 580	red and blue-green algae
Phycocyanin	618	647, 660	red and blue-green algae

2.4.3 Laser configuration

Flow cytometry (FCM) analysis has been performed using a BD FACSAria II Cytometer (Becton Dickinson) equipped with a blue laser (488 nm excitation), a green laser (532 nm excitation) and a violet laser (405 nm excitation). A fluid system with phytoplankton cells passes through one or more beams of light, and the light scattering, light excitation, and emission of fluorochrome molecules can be measured simultaneously to generate specific multi-parameter data from particles and cells. The multi-wavelength detector system with filters was performed to determine fluorescence emission from algal pigments (**Table 7**).

Table 7 Configuration of flow cytometer. Chl-*a*: chlorophyll a, PC: phycocyanin, PE: phycoerythrin, SSC: side scatter light, LP: long pass filter.

Laser	Channels	Filter
Blue laser (488 nm)	Chl- <i>a</i> (blue)	670 LP, 655 LP
	SSC	488 ± 10
	PC	625 ± 35, 505 LP
Green laser (532 nm)	Chl- <i>a</i> (green)	670 LP, 655 LP
	PE	575 ± 25
	PE (Cy5)	670 ± 14, 635 LP
	PE (Cy7)	780 ± 60, 755 LP
	PE (Texas Red)	610 ± 20, 600 LP
Violet laser (405 nm)	Chl- <i>a</i> (violet)	670 LP, 505 LP

2.4.4 Preparation of freshwater samples

Freshwater samples were concentrated (1.5-liter freshwater to ~10 ml suspension probe), filtered with a net (mesh size 50 µm) and injected into the flowing fluid stream (0.3% NaCl

isoton solution). The fluid droplets passed through a nozzle into a strong electrostatic field, by which algal cells were separated into different tubes. The maximum measurable cell size in an FCM is constricted by the nozzle with 130 μm pore size. As a rule of thumb, the maximum value with respect to the cell diameter is one third of the nozzle diameter. Therefore, the 50- μm net filter was chosen for the sample preparation

2.5 FTIR spectroscopy analysis

2.5.1 Construction and function of FTIR spectrometer

A Fourier spectrometer is developed based on a two-beam interference in a modified Michelson interferometer. The spectrometer essentially consists of a radiation source, an interferometer unit and a detector. The infrared radiation source is a silicon carbide element heated to about 1200 °C. The spectrally continuous light generated by the radiation source is parallelized in the direction of the interferometer. The interferometer consists mainly of a beam splitter and compensator plate. A beam splitter transmits and reflects 50% of the incident radiation. In a Michelson interferometer, one beam passes only once through the beam splitter but the other passes through twice. During the recombination of the light beams at the beam splitter, an interference pattern is generated, which is changed by the displacement of the movable mirror and is detected at the detector as a change in the infrared energy. In addition to the infrared light used for the measurement, the beam of a Helium-Neon laser (632 nm) is reflected into the beam path. The laser light is oriented parallel to the IR light and the interferometer transmits the IR light simultaneously. Correspondingly, the interferences of the laser light occur simultaneously. This light is emitted from the beam path after the interferometer and detected separately. Due to the exact definition and high constancy of the wavelength of the laser, the mirror position of the movable mirror can be calculated very precisely from this interference.

2.5.2 Physical basis of FTIR spectroscopy

The term “infrared” referring to electro-magnetic radiation falling in the region range between 2.5 and 25 μm (4000–400 cm^{-1}) is the most attractive for chemical analysis, which is defined as “mid-IR” radiation region. This mid-IR region includes the frequencies corre-

sponding to the fundamental vibrations of virtually all of the functional groups of organic molecules.

In the mid-infrared range, the absorption bands due to vibration-rotation transitions are referred to group frequencies, which allow the identification of the substance class of molecules (**Table 2.6**). All of the normal vibrations between 4000 and 2500 cm^{-1} can be assigned to stretching vibrations of the type X-H, where X is any element. The vibrations of the O-H (3600–3200 cm^{-1}) and N-H (3500–3000 cm^{-1}) groups are dominant. The C-H vibrations of aromatic and/or unsaturated hydrocarbons are found in the range of 3100–3000 cm^{-1} , and the C-H stretching vibrations of aliphatic hydrocarbons can be found at 3000–2800 cm^{-1} . These vibrations are predominantly caused by lipids in cells, which show high absorbencies due to the chain length of their fatty acids.

Table 8 Band assignments for FTIR spectroscopy summarized by ^[1] Giordano et al. (2001) and ^[2] Coates, (2000).

Wavenumber [cm^{-1}]	Assignments	Classification	Comments
~3000–2800 ^[2]	C-H of methyl groups	lipids	
~1740 ^[1]	C=O of ester groups	lipids and fatty acids	
~1655 ^[1]	C=O of amid-I band	proteins	also C=C groups
~1540 ^[2]	C-N of amid-II band	proteins	also C=N groups
~1455 ^[1]	CH ₃ and CH ₂	proteins	variable wavenumber
~1398 ^[1]	CH ₃ and CH ₂ , C-O of COO ⁻ , N(CH ₃) ₃	proteins, carboxyl acids, lipids	
~1242 ^[2]	P=O of phosphodiester	RNA and DANN	also phosphorylated proteins and polyphosphate
~1200–900 ^[1]	C-O-C of polysaccharides	carbohydrates	high variable wavenumber
~1080 ^[2]	P=O of phosphodiester	RNA and DNA	also phosphorylated proteins and poly-phosphate
~1078 ^[1]	Si-O silicate frustules	silicate	variable wavenumber

The spectral region 1800–900 cm^{-1} is the most important region for spectral interpretation, because it contains all of the specific absorption bands of functional carbon-containing cell components such as lipids, proteins and carbohydrates. Characteristic lipid band based on the C=O oscillation of ester group present at ~1740 cm^{-1} . Proteins are characterized with two

prominent bands depending on vibrations of peptide bonds: the amide I band ($\sim 1655\text{ cm}^{-1}$) and amide II band ($\sim 1540\text{ cm}^{-1}$), from which the former is due to C=O vibrations and the latter is mainly generated by N-H and C-N vibrations. Carbohydrate is a high heterogeneous substance group with absorption bands a broad range from 1200 to 900 cm^{-1} . In addition, Si-O vibrations of the silicate shell of e.g. Bacilliophyceae also present in this region.

2.5.3 Samples preparation and FTIR-spectrum measurements

Cells were harvested by gentle filtration of FCM sorted algal cell suspension ($\sim 10^5$ to 3×10^5 cells in 2–4 ml isoton) on cellulose acetate filters ($0.22\text{ }\mu\text{m}$ pore size, MF-Millipore membrane, Darmstadt, Germany). The pellet was resuspended in 1 ml distilled water and the cells were centrifuged (5000g, 4 min, 5417C, Eppendorf, Germany). The pellet was washed with 1 ml distilled water to remove salt residuals from the isoton which affects the measurement. After another centrifugation, the cell pellet was re-suspended with 5–10 μl distilled water depending on the final cell concentration.

Algal suspension samples were measured by a Vector 22 spectrometer in combination with an HTS-XT microplate reader according to Wagner et al. (2010). Two microliters of the algal suspension were placed on a 384-well silicon microtiter plate (Bruker Optics, Ettlingen, Germany). The algal samples were dried in a cabinet dryer (60 l Heraeus, Thermo Fisher Scientific, Hanau, Germany) at 40°C for 20 minutes to prevent the disturbing effects of water on other absorption bands.

FTIR-spectra were recorded in absorption/transmission mode with 32 scans co-added to enhance the signal-to-noise ratio, in the range $4000\text{--}700\text{ cm}^{-1}$ and at a spectral resolution of 4 cm^{-1} . Cell concentration in the sample was adjusted before the deposition on the plate in order to record spectra with a maximal absorption of ~ 0.2 (Wagner et al., 2010). For each algal sample, 2–5 technical replicates (i.e. 2–5 different spots with dried cells) were measured and finally averaged. All FTIR-spectra were baseline-corrected and smoothed using the OPUS software (OpusLab 5.0; Bruker, Ettlingen, Germany).

2.5.4 FTIR-based quantification models

Spectral reconstruction model

The spectral reconstruction model is based on a multiple linear regression protocol, which has been performed for fitting single reference spectra into the original cell spectra to calculate the amount of each macromolecule (Wagner et al., 2010). The theory basis of the model is Lambert-Beer's law. Since an algal FTIR-spectrum can be considered as a complex spectrum of overlapping bands from all IR-active substances, the optical density of a cell spectrum can be described as the sum of the partial optical densities of all infrared radiation absorbing cellular substances. Wagner et al. (2010) used bovine serum albumin, glucose and glycerol tripalmitate as the reference substances to calculate absolute amounts of cellular proteins, carbohydrates and lipids. Each of the single reference substance is calibrated by correlating the absorption intensity to the substance concentration. By a multiple linear regression algorithm, all reference spectra are then fitted into the cell spectra at once to quantify these macromolecular components. In this study, we used this model to calculate the relative contents of protein, carbohydrate and lipids of field green algae and cyanobacteria in Lake Auensee.

PLSR models based on FTIR-spectroscopy

The growth potential of the field cyanobacterial subcommunity was determined by the PLSR model developed by Jebsen et al. (2012). The model used *M. aeruginosa* (SAG 14.85, Göttingen, Germany) cultured under conditions with different nutrient supply and photon flux density. The PLSR was performed by means of the pls package for statistical programming language R (Mevik and Wehrens, 2007). The method was validated by a strong correlation between the predicted growth rates of *M. aeruginosa* and the measured growth rate according to the cell number ($R^2 = 0.92$).

The PLSR growth model of green algae was developed according to Jebsen et al. (2012). The model establishment used *C. reinhardtii* (SAG 1132b, Göttingen, Germany) cultivated in Kuhl media (Kuhl and Lorenzen, 1964) at 20°C in airlift batch cultures. Cells were illuminated with 100 $\mu\text{mol photons m}^{-2} \text{s}^{-1}$ on a light/dark cycle of 14/10 h. Algal were grown at 25, 50, 75, and 100% N supply, or 25, 50, 75, and 100% P supply of the highest nutrient concentra-

tions available in the full medium. The PLSR model was performed by means of the OPUS software (OpusLab v5.0; Bruker, Ettlingen, Germany). The correlation between the green algal growth rate prediction and the true growth rate in the PLSR model was strong ($R^2 = 0.95$).

The multi-species C:N quota prediction model based on FTIR spectroscopy has been developed by Wagner et al. (2019). The model used six phytoplankton species including Chlorophyceae (*Chlamydomonas reinhardtii*), Cyanophyceae (*Microcystis aeruginosa*), and Dinophyceae (*Amphidinium klebsii*), Chrysophyceae (*Chromulina sp.*), Cryptophyceae (*Cryptomonas ovata*), and Bacillariophyceae (*Cyclotella meneghiniana*), cultivated under N-deplete and N-replete conditions. The PLSR method was conducted by the pls package for R (Mevik and Wehrens, 2007). The model showed well predictive power of cultured microalgae due to a strong correlation between the predicted C:N quota and the real C:N ratio ($R^2 = 0.93$).

2.6 Statistic analysis

The correlation analyses among the environmental factors, algal growth factors and cellular C-allocation traits (**Table 3.2**) were performed by testing Pearson's r correlation coefficients (r -value) and significance levels (p -value) by using "R".

Table 3.2 Measured abiotic and biotic parameters for correlation analysis. Lg, global radiation; Lm, radiation intensity of PAR; T, water temperature; SD, Secchi-depth; DO, dissolved oxygen concentration; EC, electric conductivity; DIN, dissolved inorganic nitrogen; OP, ortho-phosphorus; DIN:TP, mass ratio of DIN and total phosphorus; Chl-*a*, chlorophyll a concentration; %Num, percentage of total cell number; μ , FTIR-predicted growth potential.

Category	Parameters
Environmental factors	Lg, Lm, T, SD, DO, pH, EC, Nutrient (DIN, OP, DIN:TP)
Growth factors	Chl- <i>a</i> , %Num, μ
C-allocation traits	FTIR-predicted relative contents of macromolecules (proteins, carbohydrates and lipids), protein:storage ratio, C:N ratio

In statistics, the Pearson correlation coefficient r -value is a measure of the linear dependence (correlation) between two variables according to Pearson (1895) and Stigler (1989). It has a value between +1 and -1 inclusive, where 1 is total positive linear correlation, 0 is no linear correlation, and -1 is total negative linear correlation. The p -value is used in the context of null hypothesis testing in order to quantify the idea of statistical significance of evidence. Conventionally the 5% ($p < 0.05$, less than 1 in 20 chance of being wrong), 1% ($p < 0.01$) and 0.1% ($p < 0.001$) levels have been used. According to the rule of thumb, the following strengths of relationship are used in this analysis:

Value of r	Strength of relationship
-1.0 to -0.5 or 1.0 to 0.5	strong
-0.5 to -0.3 or 0.3 to 0.5	moderate
-0.3 to -0.1 or 0.1 to 0.3	weak
-0.1 to 0.1	none or very weak

3. Results

3.1 Determination of seasonal environmental changes

3.1.1 Light conditions

The global radiation varied in a range between 400–1200 $\mu\text{mol photons m}^{-2} \text{s}^{-1}$ (Figure 7 A). The declined radiation tendency in the study period was majorly attributed to the frequent rainy and cloudy weather in the summer.

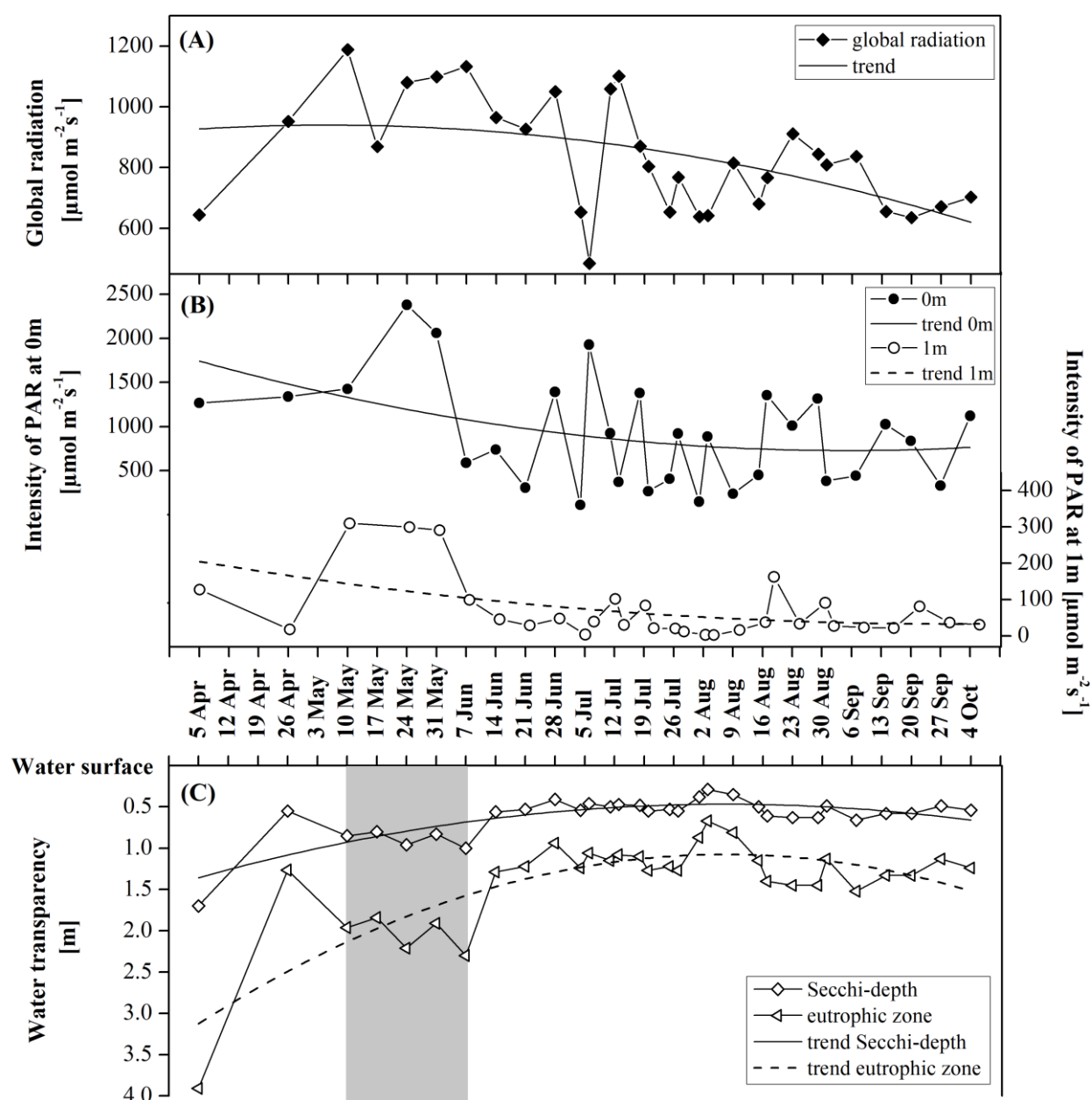


Figure 7 Time-dependent changes of global radiation (A), light intensity at 0m and 1m water depths (B), as all as Secchi-depth and eutrophic zone (C) of Lake Auensee in 2011. The clear-water phase is marked as grey field.

The local intensities of PAR at the 0m surface water varied in a range of 480–2380 $\mu\text{mol m}^{-2} \text{s}^{-1}$, and varied in a range of 0–310 $\mu\text{mol m}^{-2} \text{s}^{-1}$ at 1m water depth (**Figure 7 B**). Similar to the global radiation, the light intensity also showed a decreasing tendency from the spring to the summer and fall.

The average Secchi-depth in the observation term was 0.6 m (**Figure 7 C**), which indicated a eutrophic-hypertrophic status of the lake (according to **Table 1**). The maximal Secchi-depth of 1.7 m was observed during the spring turnover at early-April, when underwater photosynthesis can be performed by autotrophs as deep as 4m (i.e., maximal eutrophic zone). The Secchi-depth declined to 0.6 m at end-April when cryptophytes proliferated in the lake (see **Figure 17**). From mid-May to early-June, a period with higher water transparency was observed, which can be indicated as a “clear-water” phase with Secchi-depth range of 0.8–1 m. During the clear-water phase, the volume of the eutrophic zone was similar to the epilimnion (see **Figure 9**). The turbid water body with extremely low Secchi-depth levels (range 0.3–0.4 m) was detected on 28th June and during 3rd–9th August, when massive cyanobacterial blooms can be observed (see **Figure 17**). In such situations, the eutrophic zone was greatly reduced to <1 m. Below this level, phytoplankton do not have enough light for sustainable growth.

3.1.2 Water temperature

The temperatures of the 0–1 m surface water layer varied between 10–24°C during the observation period (**Figure 8**).

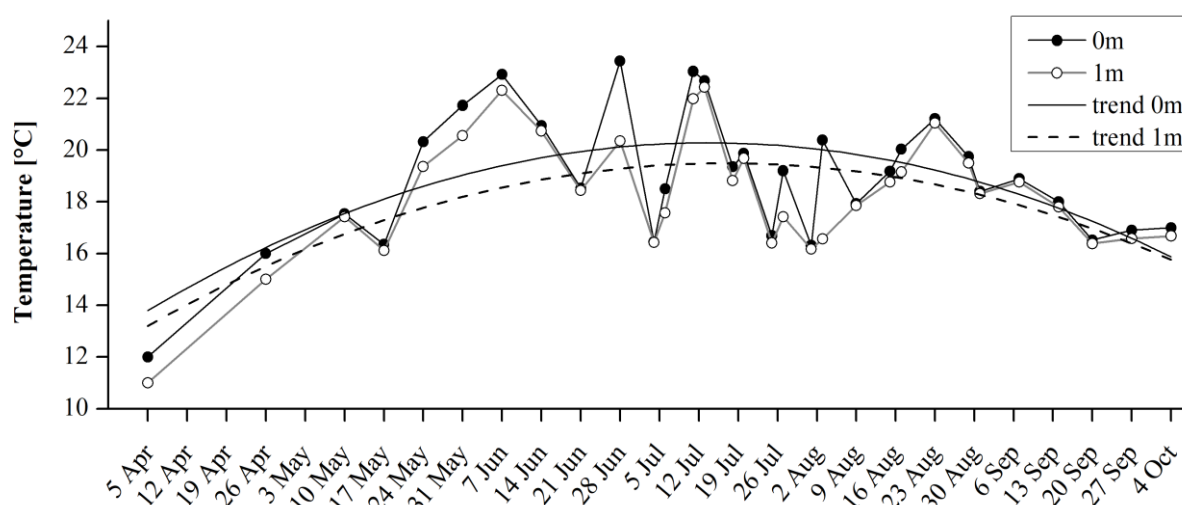


Figure 8 Temperature variation of surface water (0–1 m) in Lake Auensee 2011

The water temperatures showed an increasing tendency from the spring to the summer, followed by a decreasing tendency from the summer to the fall, potentially due to the rainy weathers in July-August. As the solar radiation became intense in the spring (**Figure 7 A**), it heated up the cold surface water that changed the water density. A complete vertical mixing of the water column occurred, when the surface water became denser and sunk into the lower layers. The spring turnover in Lake Auensee can be recognized in April on the basis of relative homogeneous temperature stratification (**Figure 9**). In the process, oxygen and nutrients distributed throughout the water column, when wind mixed the lake from the bottom to the top.

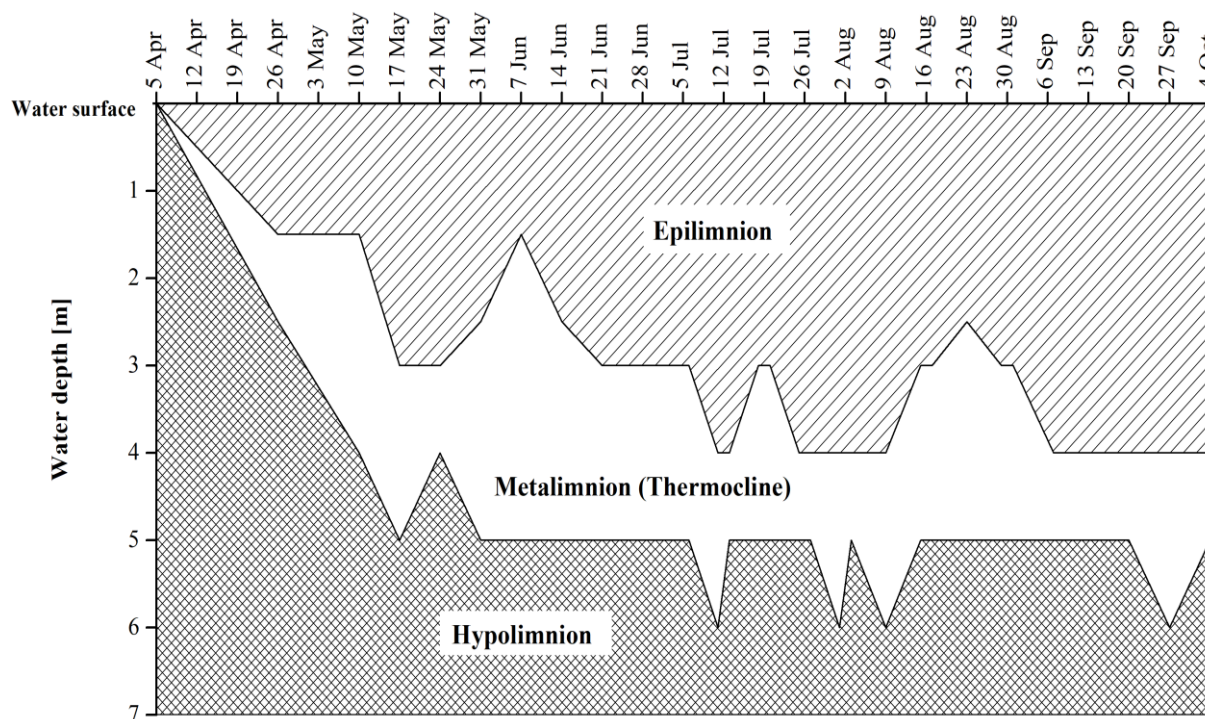


Figure 9 Seasonal thermal stratification in Lake Auensee 2011.

From late-April, the water column became physically stratified into three identifiable layers: epilimnion (upper layer), metalimnion (or thermocline) and hypolimnion (bottom layer) (**Figure 9**). The thermocline is defined as a thermal transition layer between the warmer mixed water at the surface and the cooler deep water below. In this water layer, temperature declines drastically across a small change in water depth. The determination of the thermocline commonly requires the vertical gradient of temperature being larger than a certain fixed value (gradient criterion). However, there is no objective way to determine the gradient criterion for different water systems (Coloso et al, 2011; Hao et al., 2012; Zhang et al., 2014).

Here, we used the criterion of 3°C per meter based on experience regarding the researches of Lake Auensee. Other criterion values are also possible, but we did not compare alternatives in this study. The location of the thermocline was detected relatively shallow in April (0–1.5 m), moderate in May–June (1.5–3 m), and deep in July–October (2.5–4 m).

3.1.3 Dissolved oxygen

The dissolved oxygen concentrations in the 0–1 m epilimnion showed a decreasing tendency from April to September (**Figure 10**). In April, high dissolved oxygen concentrations in the surface water were observed with 21–23 mg O₂ l⁻¹ at 0m and 18–22 mg O₂ l⁻¹ at 1m. Simultaneously, the aerobic zone can reach to the bottom water at 6 m due to the water mixing (**Figure 11**).

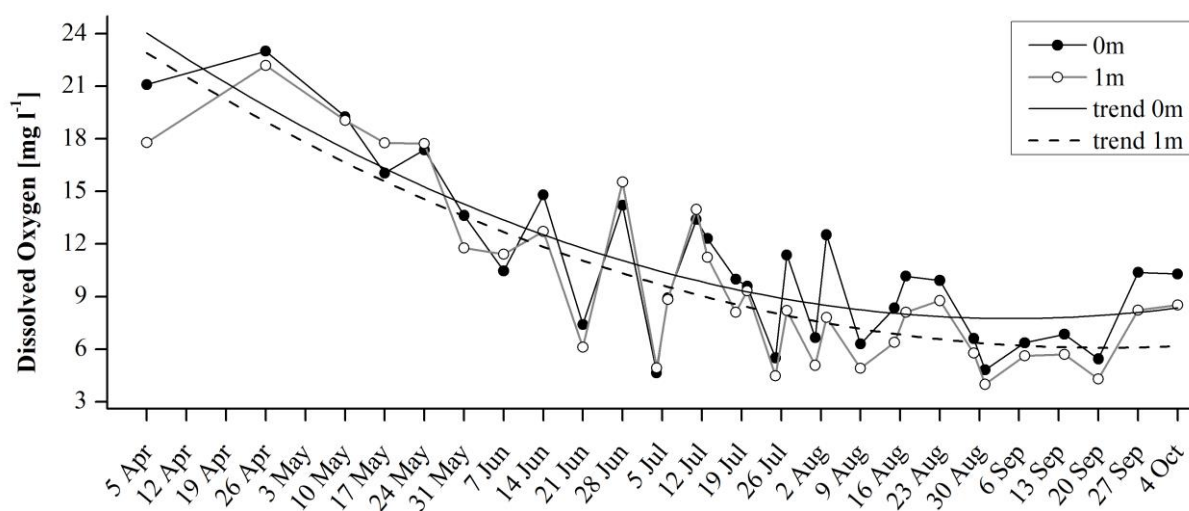


Figure 10 Changes of oxygen concentrations and seasonal variation trends in the 0m and 1m epilimnion of Auensee in 2011

During April and mid-May, both of the epilimnion and metalimnion contained oxygen, and the surface water of 0–2.5 m was over-saturated with oxygen (**Figure 11**). From mid-May, the metalimnion became anoxic, which indicated a lack of photosynthesis in this water layer. The oxygen-saturated zone reduced in the summer and fall, especially in 30th August–20th September, the whole epilimnion was under-saturated with oxygen. In July–October, the volume of the aerobic zone was smaller than that of the epilimnion; especially at mid-August, only the water layer between 0 and 1.5 m in depth contained oxygen. The raising of the anoxic zone to the upper water layer indicated a strong consumption of dissolved oxygen in the

water column.

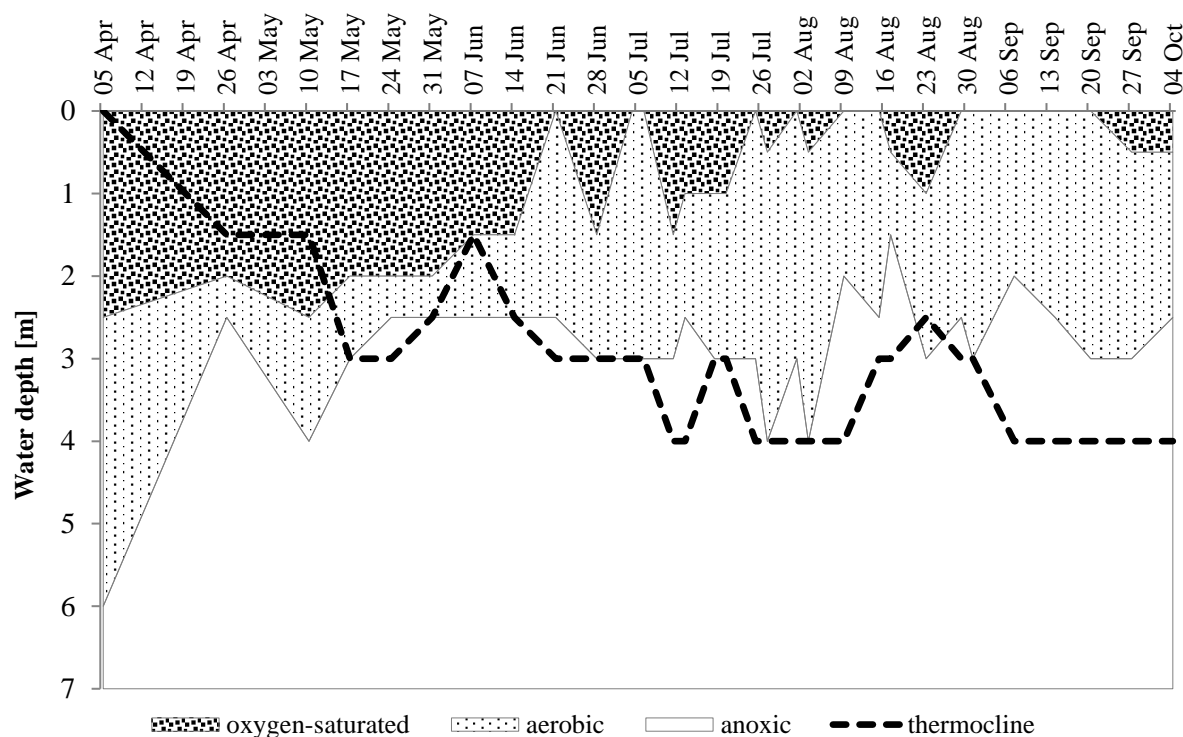


Figure 11 Profile of oxygen saturation in Lake Auensee, incl. the oxygen-saturated zone ($> 100\% \text{ O}_2$, confetti field), the aerobic zone ($0\text{--}100\% \text{ O}_2$, dotted field) and the anoxic zone ($< 0.5 \text{ mg O}_2 \text{ l}^{-1}$, non-filled field). The thick dotted line shows the location of the upper limit of the thermocline.

3.1.4 pH values

In lake Auensee, the mean pH value of both 0m and 1m water samples was 9.9 (**Figure 12**). The high pH level (> 8.3) indicated a high consumption of dissolved CO_2 and an enhancement of alkalinity in this hypertrophic lake. The pH values were lower in the spring and fall, while higher in the summer. A period with extremely high pH > 11 in the summer (with the maximum pH = 11.6 on 13th July) indicated a term of CO_2 -depletion in the surface water, probably due to the high uptake of CO_2 by massive phytoplankton.

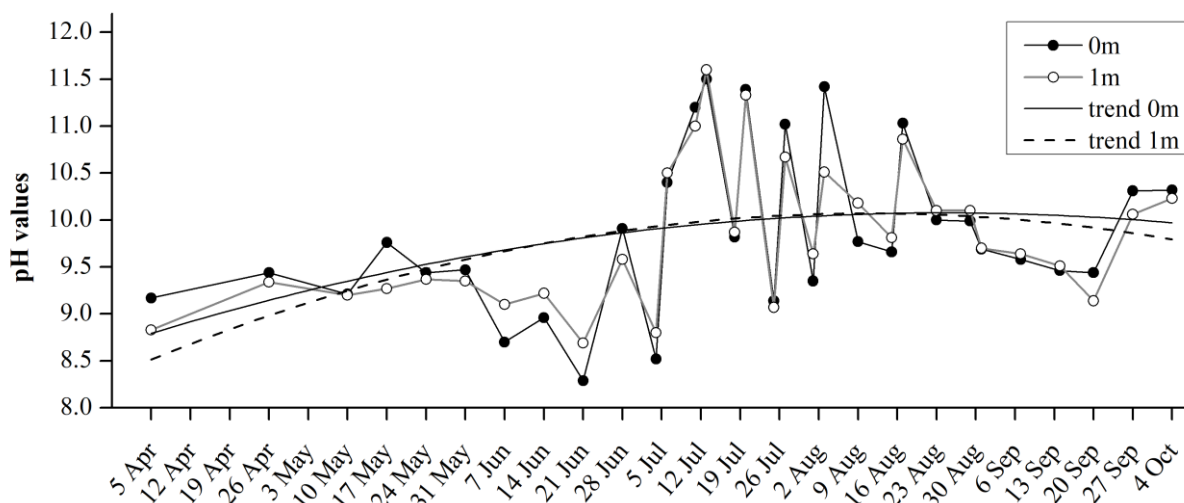


Figure 12 Seasonal variations of pH values of the 0–1m surface water in Lake Auensee 2011.

3.1.5 Electric conductivity

The electric conductivity of the lake surface water showed a slight decreasing tendency from the spring to the summer, followed by an increasing tendency from the summer to the fall (**Figure 13**). Lower conductivity reflected a low level of dissolved ions within the water column during the summer, whereas the increase in conductivity during August–September could be attributed to increased amounts of ions released from sediments into the water column.

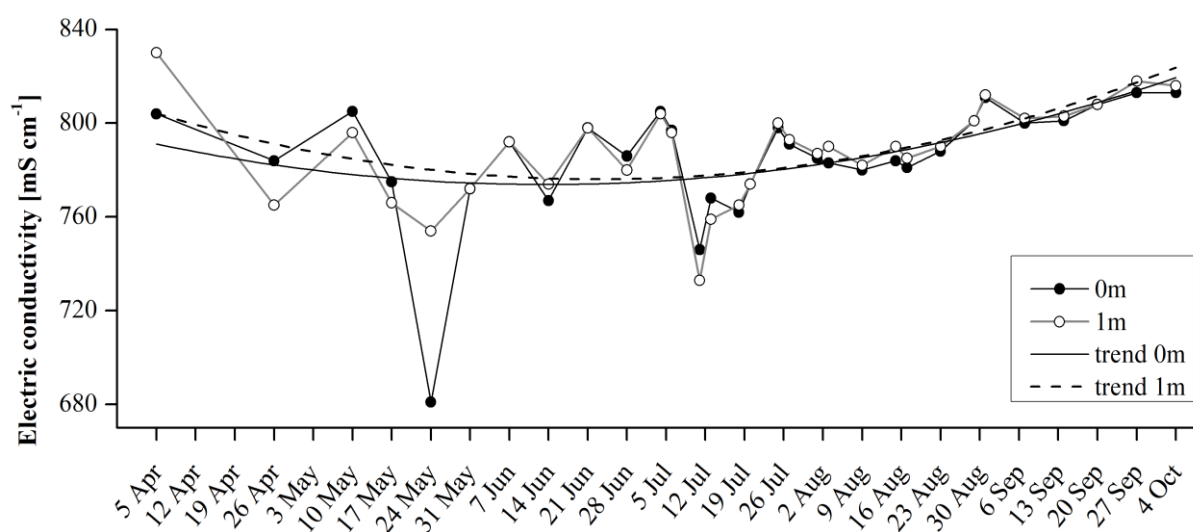


Figure 13 Seasonal variations of the electric conductivity of the 0–1 m surface water in Lake Auensee 2011.

3.1.6 Nutrient conditions

Nitrogen

In this study period, the ammonium (NH_4^+) concentration varied in a range of < 0.05 – 1.85 mg l^{-1} in the 0–3 m epilimnion (**Figure 14 A**). The NH_4^+ availability increased gradually with water depth. Especially on 26th April, the NH_4^+ concentration showed a ~20-fold increase from 0 m to 3 m depth, indicating an accumulation of ions in the lake bottom water. The nitrate (NO_3^-) concentrations can be observed in a range between $< 0.1 \text{ mg l}^{-1}$ and 0.33 mg l^{-1} in the epilimnion (**Figure 14 B**). In April and May, the NO_3^- concentrations decreased with water depth, indicating a higher rate of nitrate conversion in the upper water layer. However, during June–September, the nitrate supply in the whole epilimnion was restricted at a level below the detectable NO_3^- concentration of 0.1 mg l^{-1} . $\text{NH}_4^+\text{-N}$ and $\text{NO}_3^-\text{-N}$ are key forms of DIN for phytoplankton growth. In Lake Auensee, the epilimnion (0–3 m) contained in average $0.24 \text{ mg DIN per liter}$, which evidenced a eutrophic-hypertrophic state in this ecological system (according to **Table 1**). In the 0–1 m surface water layer, the DIN concentrations decreased from $\sim 0.15 \text{ mg N l}^{-1}$ at mid-May to the minimum of $\sim 0.06 \text{ mg N l}^{-1}$ at mid-June (**Figure 15 A and D**), which reflected a strong nutrient consumption in the lake. In September, a recovery of DIN level in the surface water can be observed.

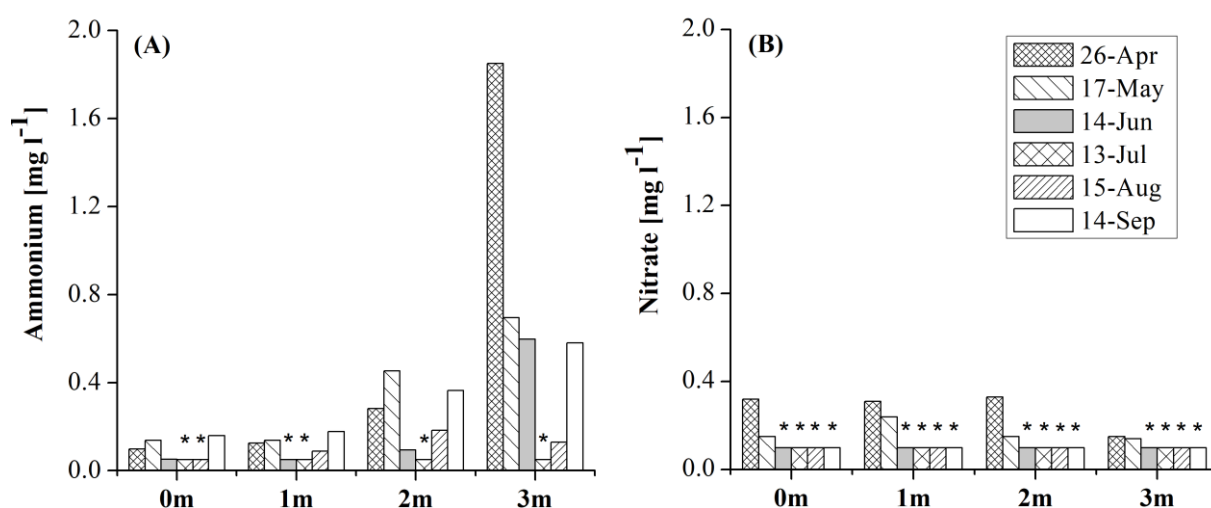


Figure 14 Vertical gradients of ammonium (A) and nitrate (B) concentrations in the epilimnion (0–3 m) of Lake Auensee in 2011. The stars (*) marked the concentrations below the detectable NH_4^+ of 0.05 mg l^{-1} or NO_3^- of 0.1 mg l^{-1} .

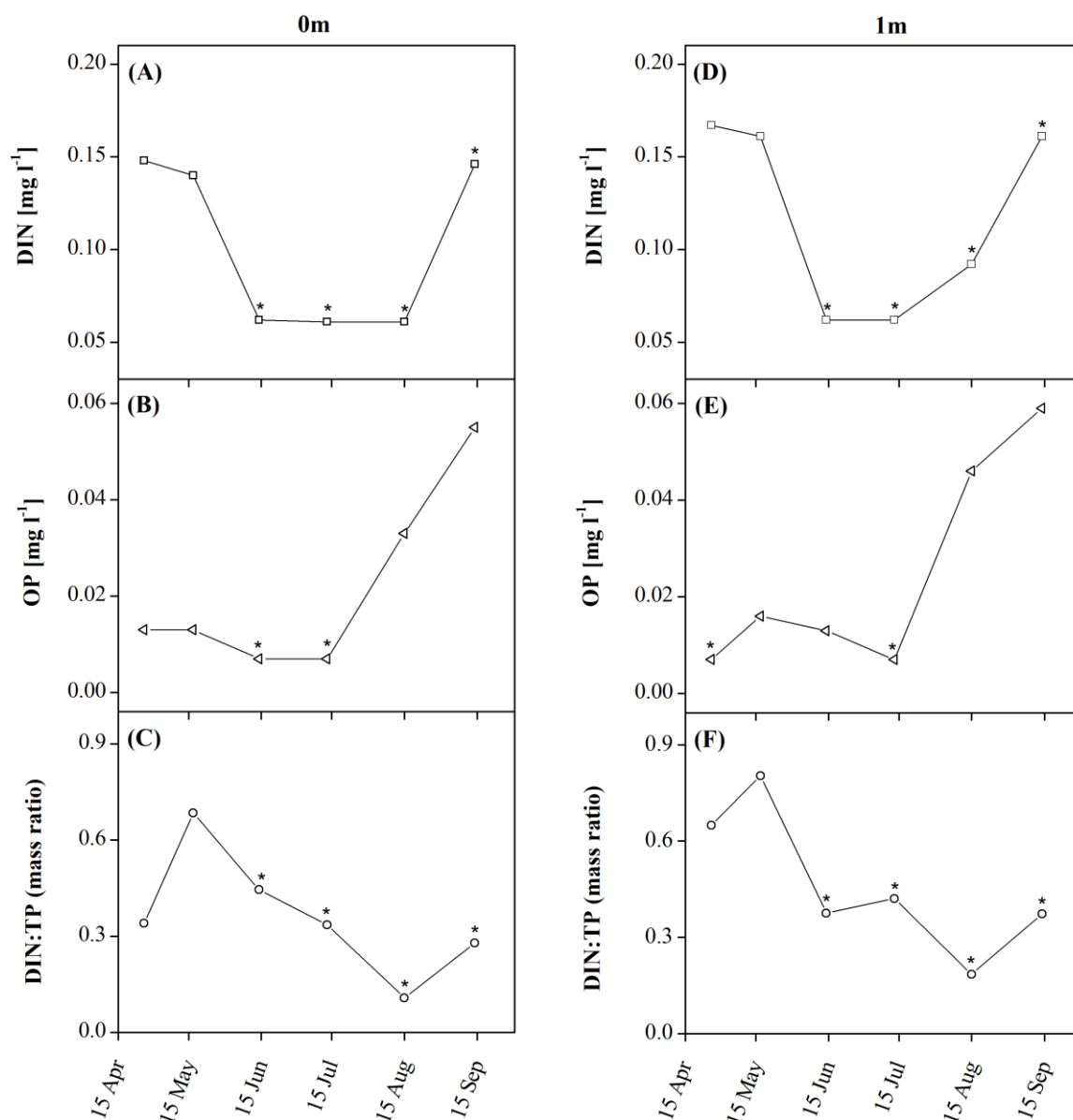


Figure 15 The availability of DIN at 0–1 m (A and D), the OP concentrations at 0–1 m (B and E), and the DIN:TP ratios in 0–1 m (C and F) water layers of Lake Auensee. DIN: dissolved inorganic nitrogen, OP: ortho-phosphorus, DIN:TP: mass ratios of dissolved inorganic nitrogen to total phosphorus. The stars (*) marked the data, whose actual concentrations or ratios should be less than these values.

Phosphorus

In Lake Auensee, the epilimnion contained averagely 0.13 mg l⁻¹ ortho-phosphate (PO₄³⁻) and 0.7 mg l⁻¹ total phosphate during the observation (**Figure 16**). The data demonstrated that the ortho-phosphate only belongs to a small part of the total phosphate. The high phosphate supply, together with excessive N, confirmed the eutrophic-hypertrophic status of the lake (according to **Table 1**), and provided high guarantee of cyanobacterial dominance in the

whole phytoplankton communities (according to **Table 2**). In the 0–1m epilimnion, the OP availability was relatively low from April to mid-July with concentration below 0.016 mg l^{-1} (**Figure 15 B and E**). The OP increased ~8-fold from mid-July with concentration of 0.007 mg l^{-1} to the maximum concentration of 0.06 mg l^{-1} at mid-September, which reflected a dramatic phosphorus release from sediments into the water column.

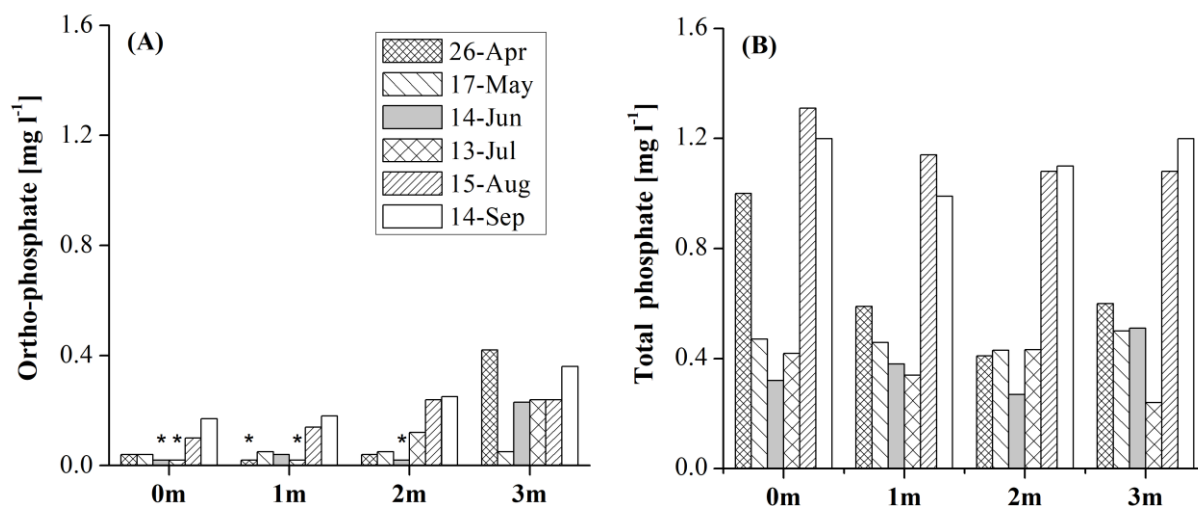


Figure 16 Vertical gradients of ortho-phosphate (A) and total dissolved phosphate (B) concentrations in the epilimnion (0–3 m) of Lake Auensee in 2011. The stars (*) marked the concentrations below the detectable PO_4^{3-} of 0.02 mg l^{-1} .

Determination of N/P-limitations in the 0–1m epilimnion of Lake Auensee

The determination of N/P-limitations was based on the criteria including: absolute concentrations of N and P, DIN:TP mass ratios, and nutrient uptakes of phytoplankton species. In the summer, the DIN concentrations (with $< 0.06 \text{ mg N l}^{-1}$) in the lake surface water were lower than the critical N-limited concentration of 0.1 mg N l^{-1} (Gophen et al., 1999, see **Table 2**), and lower than the N uptakes of green algae and cyanobacteria (see **Table 3**). Furthermore, the DIN:TP mass ratios in range of 0.1–0.8 (**Figure 15 C and F**) during the whole period were lower than the critical N-limited ratio of 1.5 (Bergström, 2010, see **Table 2**). The above data provided the evidence of the potential N-limited growth conditions of phytoplankton during June–August in the 0–1m epilimnion. With the respect to the P supply, the concentrations of OP, ortho-phosphate and TP were much higher than the critical P concentrations and P uptake of microalgae (according to **Table 2 and 3**), which evidenced that P was not limited in the 0–1m epilimnion during our observation period.

3.2 Determination of phytoplankton community structure

3.2.1 Phytoplankton species in Lake Auensee

The most abundant phytoplankton species in Lake Auensee during the observation period in 2011 have been identified with specific adaptation characteristics (**Table 9**).

Table 9 Phytoplankton species determined in Lake Auensee

Phylum	Genus	Preferred bloom conditions
Cyanobacteria (N ₂ -fixing)	<i>Anabaena</i>	P-enriched, arm, stratified, long-residence time, high irradiance, eutrophic
	<i>Aphanizomenon</i>	
(Non-N ₂ -fixing)	<i>Microcystis</i>	N- and P-enriched, eutrophic conditions, warm, stratified, long residence time
	<i>Oscillatoria</i>	
	<i>Gomphosphaeria</i>	
Chlorophyta	<i>Pandorina</i>	Moderate N- and P-enriched, stratified, high irradiance
	<i>Eudorina</i>	
	<i>Closterium</i>	
	<i>Scenedesmus</i>	
	<i>Oocystis</i>	
	<i>Staurastrum</i>	
	<i>Micractinium</i>	
	<i>Coelastrum</i>	
	<i>Crucigenia</i>	
	<i>Tetraspora</i>	
	<i>Pediastrum</i>	
	<i>Selenastrum</i>	
Bacillariophyta	<i>Cyclotella</i>	Silica-enriched, cold water
	<i>Synedra</i>	
	<i>Fragilaria</i>	
	<i>Stephanodiscus</i>	
	<i>Tabellaria</i>	
Dinophyta	<i>Peridinium</i>	N-and P-enriched, stratified, warm
	<i>Ceratium</i>	
Cryptophyta	<i>Chroomonas</i>	N- and P-enriched, eutrophic, stratified, cold water
	<i>Cryptomonas</i>	
Haptophyta	<i>Chrysochromulina</i>	N- and P-enriched, warm
Euglenophyta	<i>Trachelomonas</i>	N- and P-enriched

3.2.2 HPLC-based analysis of seasonal phytoplankton dynamics

We quantitatively analyzed the seasonal dynamics of population biomass of predominant algae groups in Lake Auensee by using HPLC. Fucoxanthin, lutein/Chl-*b*, alloxanthin, peridinin and zeaxanthin were used as marker pigments for families of Bacillariophyceae, Chlorophyceae, Cryptophyceae, Dinophyceae and Cyanobacteria, respectively. The Chl-*a* concentration of each taxonomic group (see **Figure 17**) and the percentage contribution of this group to total Chl-*a* (see **Figure 18**) have been determined.

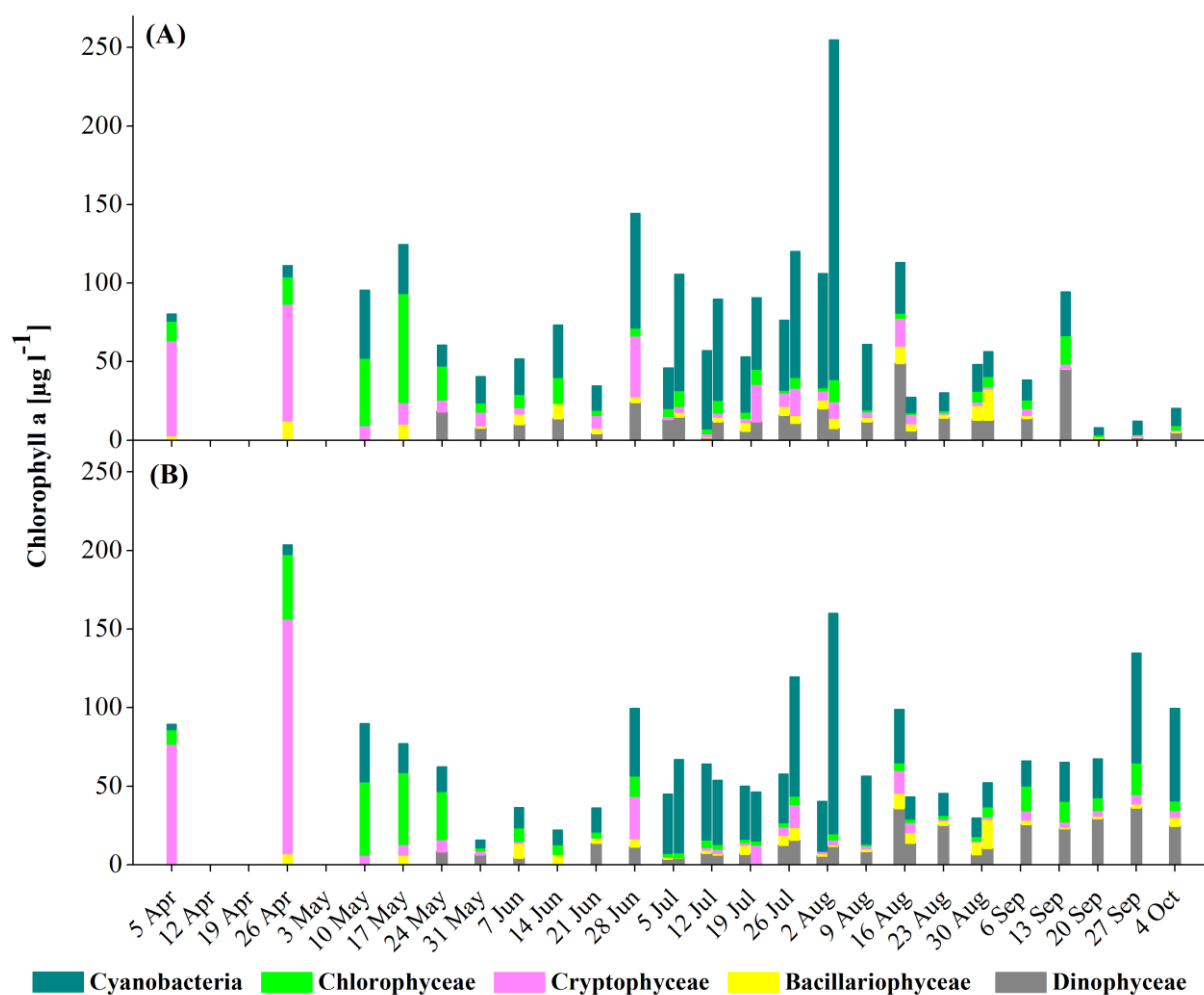


Figure 17 Seasonal dynamics of phytoplankton composition in the 0 m (A) and 1 m (B) epilimnion of Lake Auensee in 2011. The Chl-*a* concentration was estimated by HPLC pigment analysis.

The average Chl-*a* concentration of the 0–3m epilimnion was $61 \mu\text{g Chl-}a \text{ l}^{-1}$ in the study period. The massive growth of phytoplankton further evidenced the nutrient enrichment in the lake (according to **Table 1**). In the 0–1 m surface water, a massive abundance of cryptophytes

can be observed in April with high Chl-*a* concentrations in range of 75–120 $\mu\text{g Chl-}a \text{ l}^{-1}$ per water layer (**Figure 17**). The cryptophyte population, composed mainly by *Cryptomonas* sp. and *Chroomonas nordstedti*, reached ~70–85% of total phytoplankton biomass (see **Figure 18**).

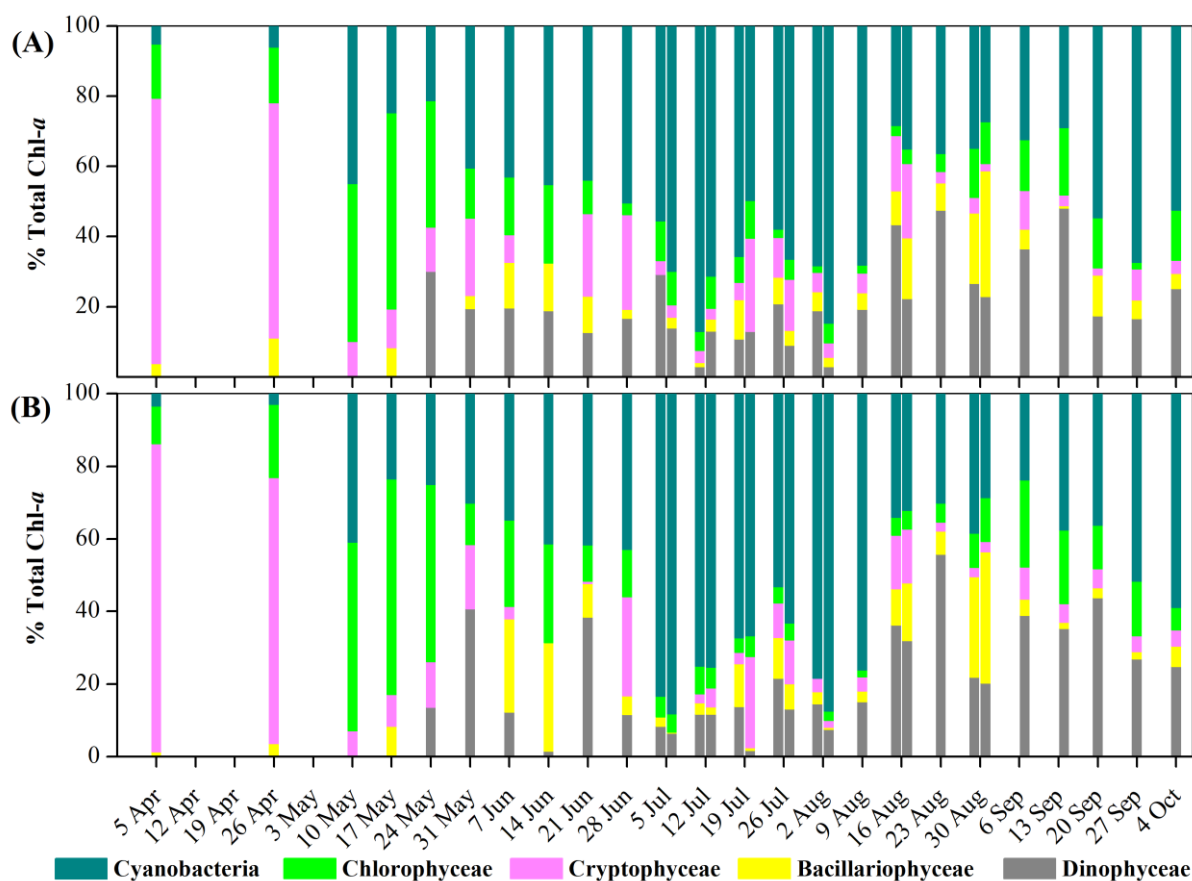


Figure 18 Proportional composition of phytoplankton in the 0 m (A) and 1 m (B) epilimnion of Lake Auensee in 2011, estimated by HPLC analysis. The proportion of single algal group was calculated in % total Chl-*a* concentration.

As the cryptophyte abundance reduced in May, the population of green algae increased and became dominant in 10th–24th May with ~20–70 $\mu\text{g Chl-}a \text{ l}^{-1}$ per water layer. The major dominant species included *Pandorina* sp., *Eudorina* sp., *Scenedesmus* sp., *Pediastrum* sp., *Closterium* sp., *Oocystis* sp. as well as *Trachelomonas* sp., possessing ~35–60% of the total Chl-*a* concentration. During the clear-water phase from mid-May to early-June, the population proportion of green algae reduced distinctly to ~11% of the total Chl-*a*. This subcommunity population kept at a low level of 0–20 $\mu\text{g Chl-}a \text{ l}^{-1}$ (i.e., 0–27% of total Chl-*a*) throughout the summer and fall.

After the clear-water phase, the cyanobacteria became dominated in the summer with a high biomass proportion of 50–90% of the total Chl-*a* contents per water layer. Unlike the green algae peaking only once in the spring, the cyanobacterial growth frequently fluctuated with at least five abundance peaks exceeding 50 $\mu\text{g Chl-}a \text{ l}^{-1}$ from 28th June to 9th August. The maximal bloom exploded during 1st–3rd August with biomass increase from 72 to 216 $\mu\text{g Chl-}a \text{ l}^{-1}$ at 0 m and from 31 to 140 $\mu\text{g Chl-}a \text{ l}^{-1}$ at 1 m depth. The dominant cyanobacterial species included N₂-fixing *Anabaena* sp. and *Aphanizomenon* sp., and non-N₂-fixing *Microcystis* sp., *Oscillatoria* sp., and *Gomphosphaeria* sp. After the collapses of the cyanobacterial blooms, dead cells changed the water colour from green-blue to yellow-brown. The colour changes can be observed during July and August. From mid-August to October, the cyanobacteria and dinophytes were two dominant groups, whose sum proportions contributed about 50–86% of the total Chl-*a* content in the epilimnion. Diatoms can be observed in the whole period with only small content between 0–24 $\mu\text{g Chl-}a \text{ l}^{-1}$ (~0–36% of total Chl-*a*) in the surface water.

The Chl-*a* based prediction of phytoplankton biomass could be inaccurate from the actual biomass in the lake. Since all water samples were filtered immediately after the collection by means of a filter mesh ($\varnothing = 210 \mu\text{m}$) to prevent primarily zooplankton grazing, large cells or aggregates with a size over 210 μm were excluded from the sampling. Thus, the biomass prediction by using HPLC only focused on the phytoplankton cells/colonies with size smaller than 210 μm . Furthermore, HPLC is not able to distinguish Euglenophyceae from Chlorophyceae, because these groups do not contain a taxon-specific xanthophyll (Wilhelm et al. 1995). Thus, the portion of these algal groups was also calculated within the proportion of the green algae.

3.3 Isolation of functional algal groups by flow cytometry

3.3.1 Identification and separation of phytoplankton groups

In this study, the phytoplankton communities in water samples can be separated into four major groups including green algae, cyanobacteria, cryptophytes and diatoms. Because the size of the passing particles is limited by the nozzle size of the flow cytometer, only small cell/colonies with size range 0–130 μm can be analyzed. Consequently, dinophytes with a common cell size between 200–400 μm cannot be considered. Here, the cytogram of a water

sample collected on 17th May as an example showed the isolation procedure of phytoplankton group by FCM (**Figure 19**). A total of 10,000 events displayed in the cytogram. Phytoplankton groups were separated based on light scattering and typical fluorescence properties, and the cell number of individual groups can also be counted. Larger cells and aggregate species have relatively strong signatures that presented in the upper right region, whereas picoplankton species presented in the lower left region. The Chl-*a* vs. PC fluorescence cytogram was chosen to separate the phytoplankton cells into two major clusters depending on their cellular phycobilin contents. Phycobilin-containing taxa (e.g., cyanophytes and cryptophytes) displayed in the upper region with higher phycobilin signals (**Figure 19 A**, Cluster 1), whereas non-phycobilin-containing taxa (e.g., chlorophytes, euglenophytes, haptophytes and diatoms) were clustered in the lower part (**Figure 19 A**, Cluster 2). Further separation of the phycobilin-containing phytoplankton groups was carried out by a PC vs. PE fluorescence cytogram (**Figure 19 B**), which permitted differentiation according to cell size and cellular phycobilin concentration. The cryptophytes (**Figure 19 B**, 1a, pink dots) are larger cells and presented higher fluorescence signals on the upper right of the cyanobacteria (**Figure 19 B**, 1b, blue dots).

The non-phycobilin containing group could be differentiated into diatoms and green algae depending on Chl-*a* vs. PE fluorescence signatures (**Figure 19 C**). The diatoms (**Figure 19 C**, 2a, orange dots) clustered in the upper signature region because they contain fucoxanthin, a light harvesting pigment, which can be excited by the green light and can emit strongly in red fluorescence region. In this group, haptophytes (e.g., *Chrysochromulina* sp.) can also be detected because they are covered with plate-like scales and contain 19' hexanoxyfucoxanthin in cells, which has the same emission region as fucoxanthin. By contrast, the green algae (**Figure 19 C**, 2b, green dots) lack these carotenoids, thus their signatures presented in the lower region of the cytogram. The green algal cluster is a mixture of Chl-*b*-containing groups e.g., chlorophytes and euglenophytes, composed majorly of abundant genera e.g., *Pandorina*, *Trachelomonas* etc. The FCM cannot isolate algal groups because they have similar pigmentation.

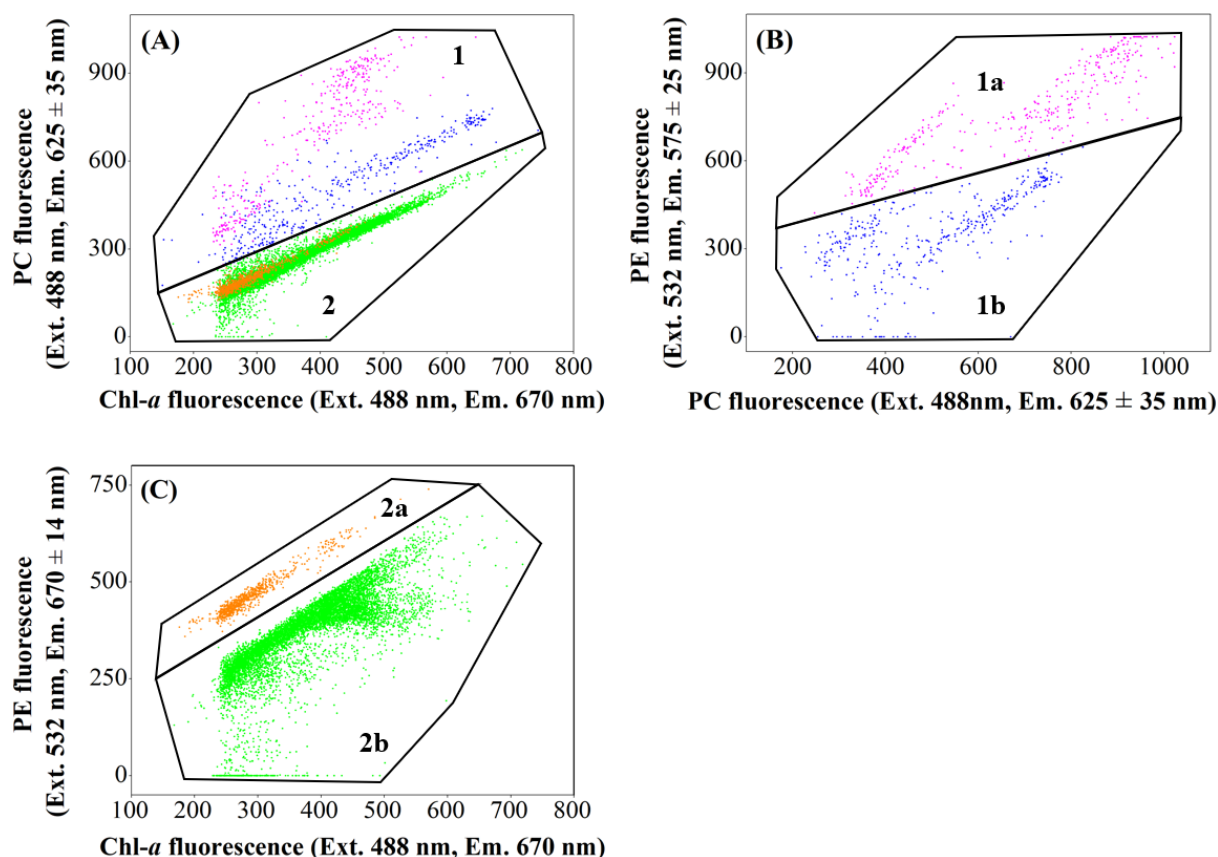


Figure 19 Isolation of phytoplankton groups by flow cytometry. The water samples were collected on 17th May in 2011. The Chl-*a* vs. PC fluorescence cytogram (A) showed the separation of phycobilin-containing (Cluster 1) and phycobilin-lacking (Cluster 2) cells. The PC vs. PE fluorescence cytogram (B) allowed the differentiation of cryptophytes (1a, pink dots) and cyanobacteria (1b, blue dots). And the Chl-*a* vs. PE fluorescence cytogram (C) was used for the separation of diatoms (2a, orange dots) and green algae (2b, green dots). Each dot represented a single algal cell or colony.

The sorted cells will be in the next step used for the measurements by FTIR spectroscopy. Because the FTIR-measurement needs a certain volume of cells to obtain an effective FTIR spectrum (Wagner et al., 2010), about 3,000 to 900,000 cells/aggregates depending on different cell volume have been sorted for individual algal samples. If water samples contain only small cells with less cell number, the FACS (fluorescence-activated cell sorting) process may take a lot of time and more water volume for the sample flow is needed. This problem was particularly serious by the FACS of green algal cells from late-July to early-August, when the population was extremely small (less than 10% of total cell number).

3.3.2 FCM-based analysis of seasonal phytoplankton dynamics

A total of 59 isolations of phytoplankton communities in the surface water samples collected from Lake Auensee have been carried out based on FACS, by which 236 green algal sorts and 221 cyanobacterial sorts have been successfully obtained.

Based on the taxon-specific properties of light scattering and fluorescence, the seasonal population dynamics of green algae and cyanobacteria can be detected in the cytograms (**Figure 20**). The green algal subcommunity dominated in May as a mixture of euglenophytes, charophytes and chlorophytes, showing signatures in an elongated shape due to different cell/aggregate size of species (**Figure 20 A and G**). After the clean-water phase, the green algal population reduced and the elongated clusters became shorter from June to August (**Figure 20 B–D and H–J**), because some colonial species e.g., *Pandorina* sp., *Eudorina* sp., *Scenedesmus* sp., *Micratinium* sp., *Pediastrum* sp., *Coelastrum* sp., etc. disappeared, replaced by some single-cell species of euglenophytes (e.g. *Trachelomonas* sp.) and colonial chlorophytes (e.g. *Staurastrum* sp., *Crucigenia* sp., *Scenedesmus* sp., *Tetraspora* sp., *Selenastrum* sp., *Oocystis* sp., etc.). The cluster became elongated again in September (**Figure 20 E–F and K–L**), composed majorly of e.g. *Pandorina* sp., *Scenedesmus* sp., *Coelastrum* sp., *Trachelomonas* sp., etc.

The cyanobacterial signatures were weaker in May (**Figure 20 A and G**), while became dominant after the clean-water phase. From June to August (**Figure 20 B–D and H–J**), the cyanobacterial cluster was extremely elongated due to the presence of filamentous species (e.g., *Anabaena* sp., *Aphanizomenon* sp., *Oscillatoria* sp., etc.) and larger colonic species (e.g., *Gomphosphaeria* sp., *Microcystis* sp., etc.), which signalled widely in the upper right region of the cytogram. These signatures became decreased in September and October (**Figure 20 E–F and K–L**).

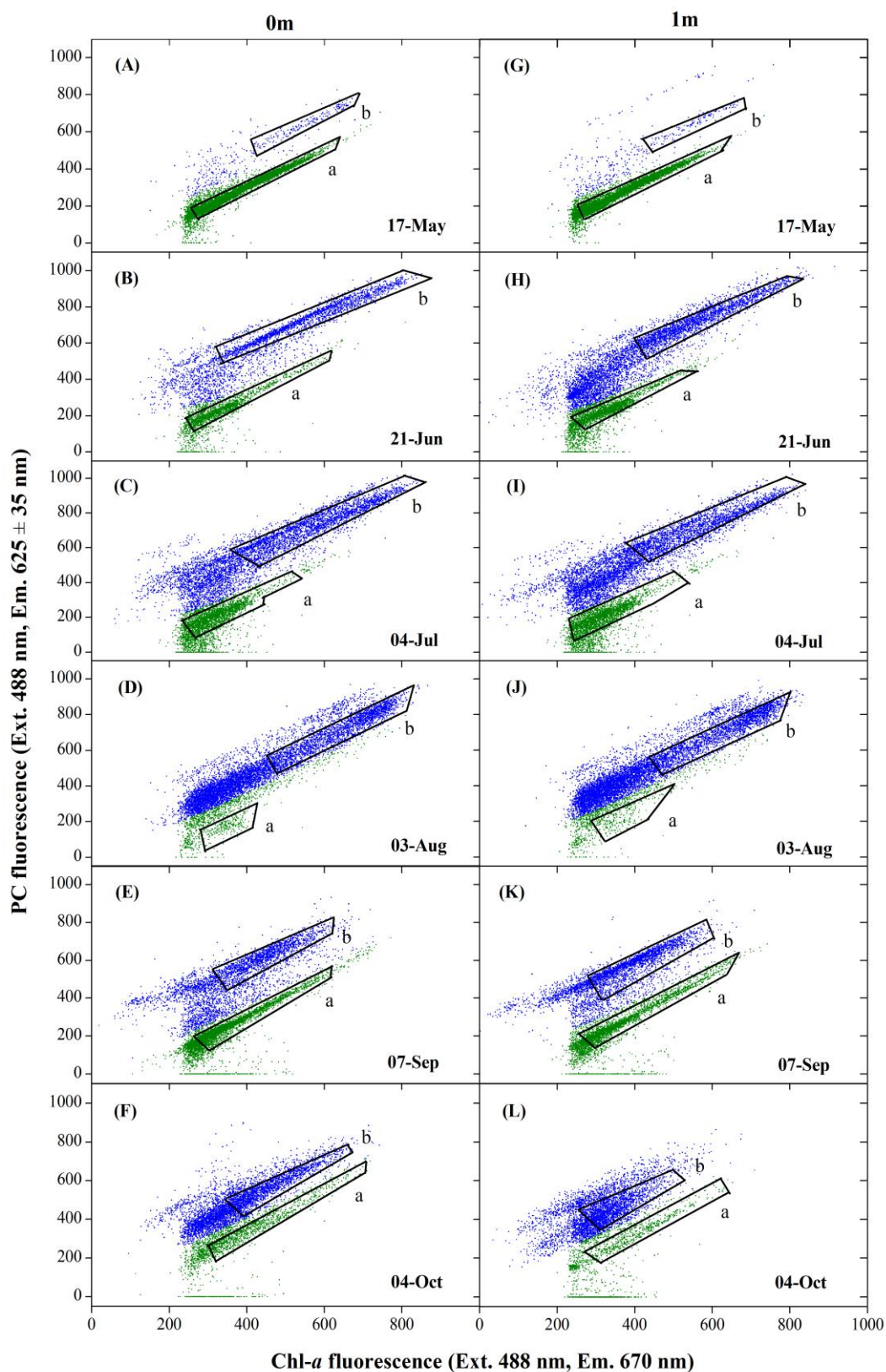


Figure 20 Seasonal dynamics of cyanobacteria (blue spots) and green algae (green spots) populations in 0m (A–F) and 1m (G–L) water samples from Lake Auensee in 2011. The clusters show the areas of FCM sorted cells from the green algal (a) and cyanobacterial (b) subcommunities.

The cell number of green algal and cyanobacterial subcommunities has been counted by FACS. The percentage of total cell number showed that the green algal abundance in May was followed by the dominant cyanobacteria during June–August (**Figure 21**). The detected seasonal dynamic of phytoplankton populations confirmed the determination by HPLC (**Figure 18**).

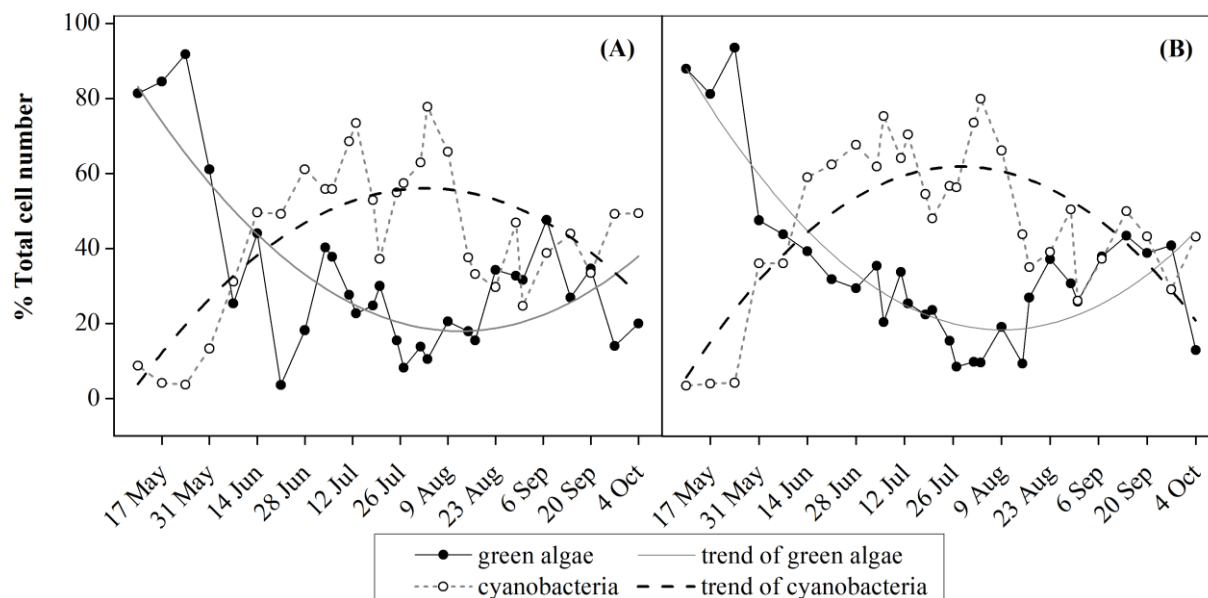


Figure 21 Proportion of cell number of green algal and cyanobacterial subcommunities in 0m (A) and 1m (B) water samples.

3.4 FTIR spectroscopy analysis

A total of 433 effective FTIR spectra have been measured from FACS isolated phytoplankton samples. Cellular C-allocation traits such as macromolecular composition (see **Section 3.4.2**), elemental C:N ratio (see **Section 3.4.3**) and growth potential (see **Section 3.4.4**) have been analyzed by using different FTIR prediction models.

3.4.1 FTIR-spectra of field phytoplankton samples

The FTIR-spectra of field green algal and cyanobacterial sorts by FCM (see **Figure 19**)

were measured. The algal spectra in the range of 1900–700 cm^{-1} showed characteristic molecular absorption bands of protein (amid I and II bands, at ~ 1650 and ~ 1540 cm^{-1}), carbohydrate (polysaccharide bands, at 1200–800 cm^{-1}) and lipid (ester bands, at ~ 1750 cm^{-1}) (**Figure 22**), identified according to **Table 8**. As both spectra were normalized at the amid-II band, green algae showed higher absorbance in the regions of carbohydrate and lipid spectra than cyanobacteria. It suggested that, compared to the cyanobacterial sample, the green algae may have more proportions of carbohydrates and lipids in cell weight.

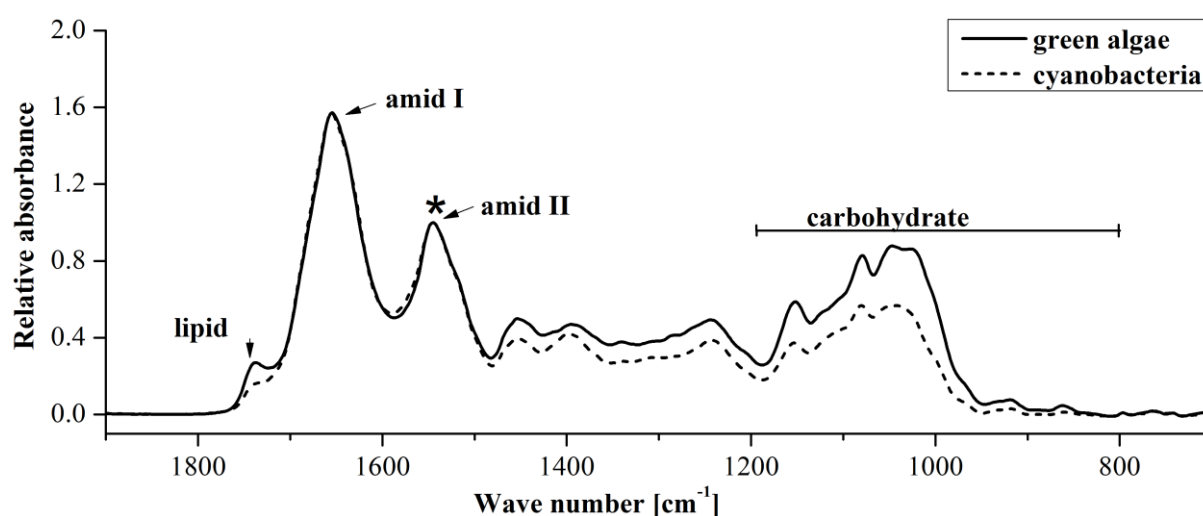


Figure 22 FTIR spectra of field phytoplankton samples sorted on 17th May 2011. The spectra of the green algal (solid line) and cyanobacterial (dashed line) samples were normalized at amid II-band (*).

3.4.2 Determination of cellular macromolecular composition

The analysis of cellular macromolecular composition has been carried out by using a FTIR-spectral reconstruction model according to Wagner et al. (2010). Since the sum of proteins, carbohydrates and lipids can reach 90% of the algal dry weight (Haug et al., 1973), we used this sum value as biomass of a cell and defined it as entire macromolecule pool (eMP). In our study, the relative contents of protein, carbohydrate and lipid were calculated in percentages of eMP (% eMP).

The macromolecular composition of field green algal cells in 0–1 m water was 28–50% eMP (average: 42% eMP) protein, 25–52% eMP (31% eMP) carbohydrate and 19–28% eMP (22% eMP) lipid in the observation period (**Figure 23**). The protein content showed negative correlation with the carbohydrate content (strong r with high significance, **Figure 24 A**),

while showed a lack of linear correlation with the lipid content (**Figure 24 B**). The weak relationship between the protein content and Chl-*a* concentration (**Figure 24 C**) reflected the dependence of green algal growth on the biomass of cellular protein pools.

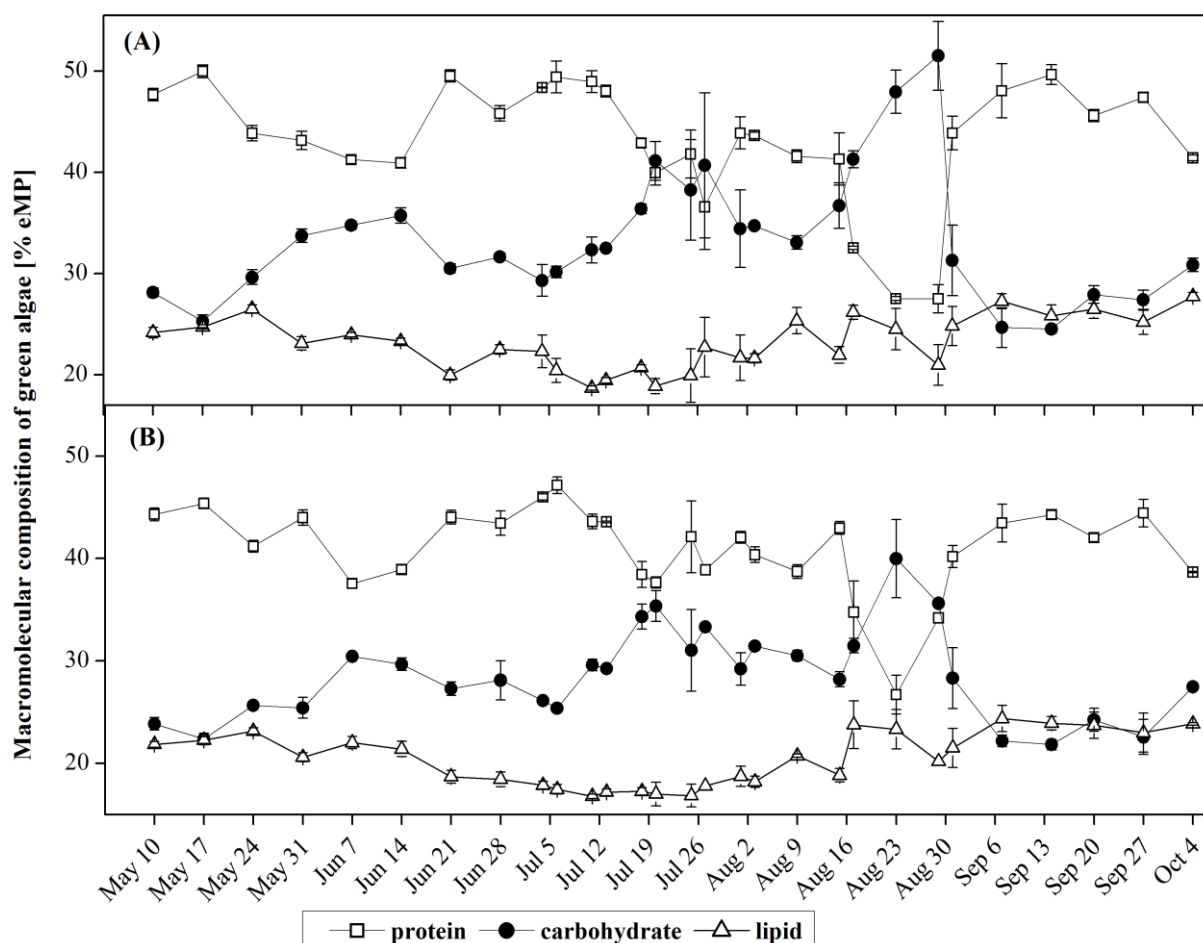


Figure 23 Seasonal variations in relative contents of proteins (solid line with open squares), carbohydrates (solid line with filled circles) and lipids (solid line with open triangles) of green algal cells in 0m (A) and 1m (B) water samples. The relative macromolecule contents were calculated in % eMP.

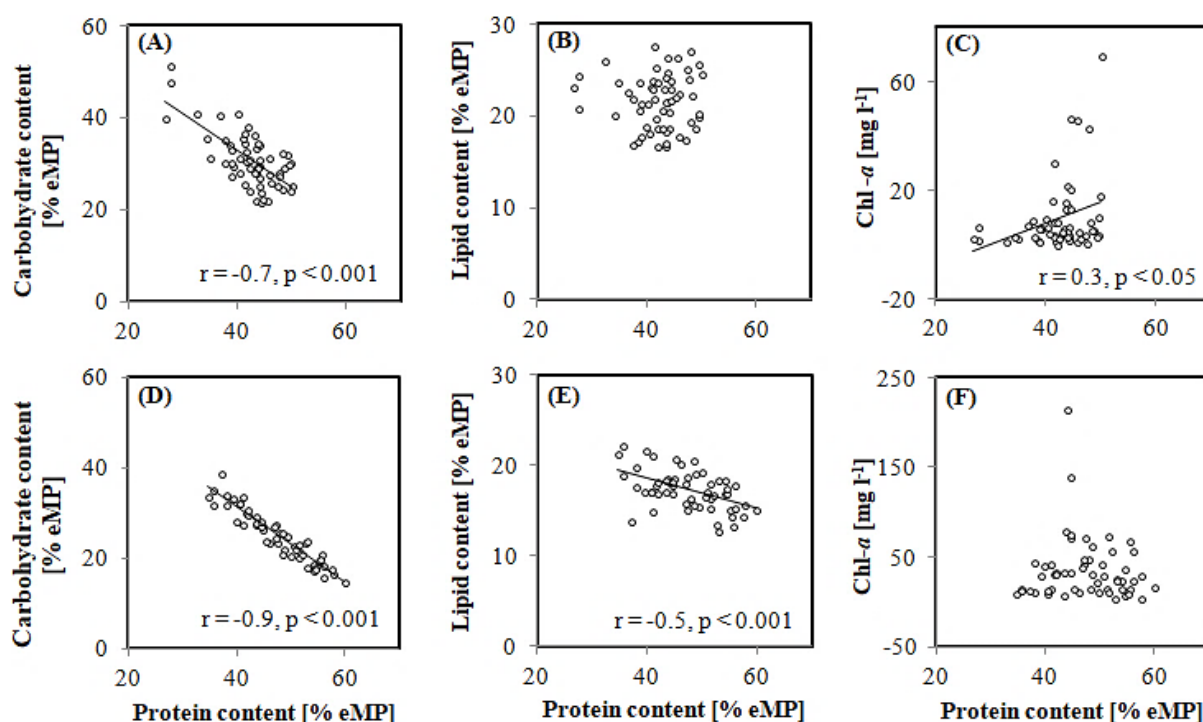


Figure 24 Linear correlations among cellular macromolecule contents (in % eMP) and chlorophyll a (Chl-*a*) concentrations of green algae (A–C) and cyanobacteria (D–F). Lines plotted were from the Pearson's *r* correlation (*r*- and *p*-values are also reported). If there was no linear correlation between the variables, no line was plotted.

In comparison, the field cyanobacterial cells contained more protein (35–60% eMP), less carbohydrate (15–40% eMP) and less lipid (13–22% eMP) (**Figure 25**) than the green algae. The protein contents of cyanobacteria were negatively related with carbohydrate contents (strong *r* with high significance, **Figure 24 D**) and lipid contents (strong *r* with high significance, **Figure 24 E**). The results demonstrated that the decreasing protein fraction was associated with the accumulation of both carbohydrate and lipid storage pools in cells responsible to environmental changes. Unlike green algae, cyanobacteria showed a lack of growth dependence on the cellular protein biomass (**Figure 24 F**).

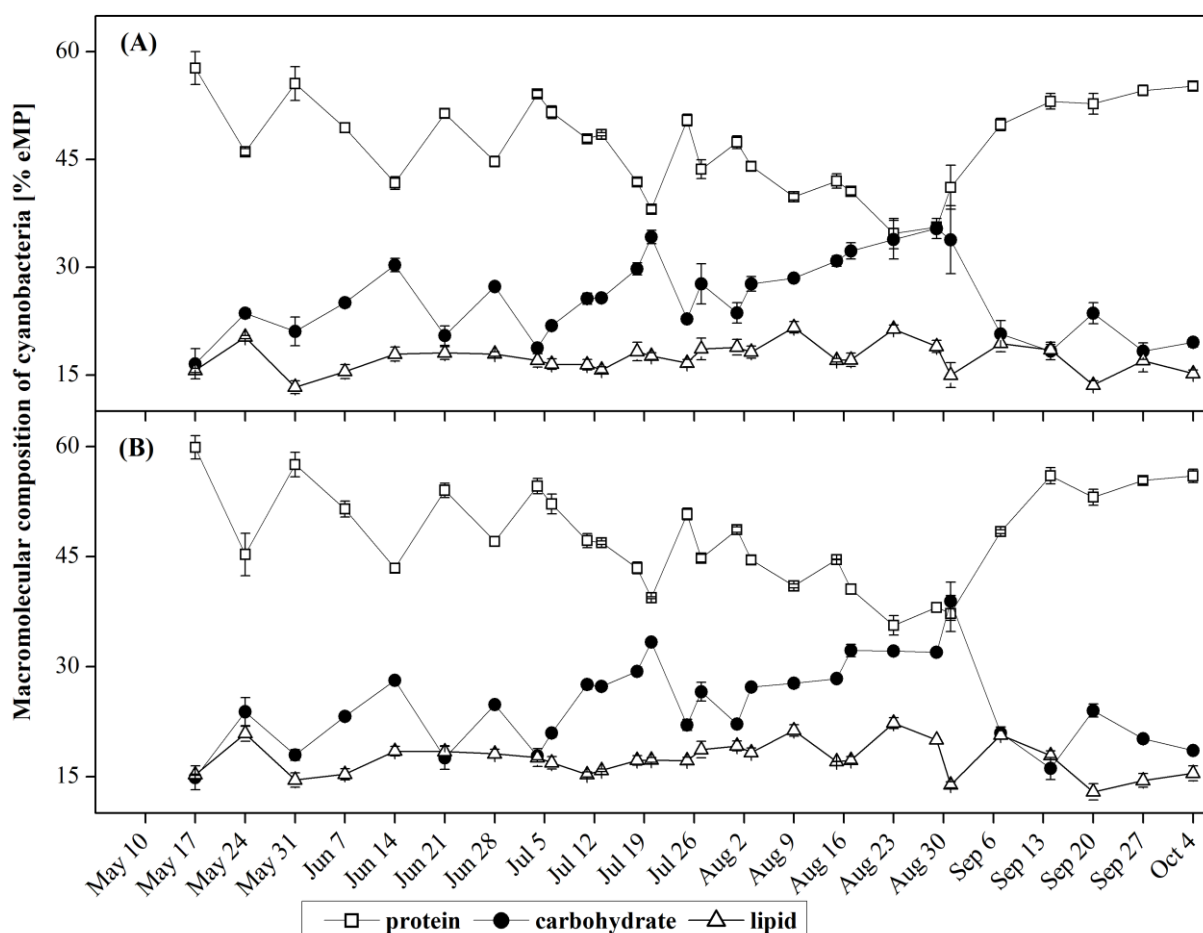


Figure 25 Seasonal variations in relative contents of proteins (solid line with open squares), carbohydrates (solid line with filled circles) and lipids (solid line with open triangles) of cyanobacterial cells in 0m (A) and 1m (B) water samples. The relative macromolecule contents were calculated in % eMP.

3.4.3 Determination of cellular elemental C:N ratios

Based on the FTIR spectra, cellular C:N molar ratios of field green algae and cyanobacteria were predicted by using the PLSR model according to Wagner et al. (2019). The C:N ratios of green algal cells at 0m and 1m showed variations in a range of 5–11.6 (**Figure 26 A**), most of which were higher than the Redfield C:N ratio of 6.6. High C:N ratios reflect relative low N-pools in cells. The cellular C:N ratio above 6.6 was observed mainly from mid-May to end-June and from early-August to early-October. That means the duration of N-limited growth of green algae extended from mid-May to early-October, exceeding the potential N-deficiency period identified during June–August in Lake Auensee (see **Section 3.1.6**). The C:N ratio showed significant correlation with the protein:storage ratio calculated as a ratio of protein content to the sum of storage carbohydrate and lipid contents (**Figure 27 A**). The result indicated that both of C:N and protein:storage ratios can reflect the reallocation of photo-

synthetic energy switching between cellular protein pools and storage pools. Although the C:N ratio had no overall correlation with the population biomass (determined as Chl-*a* concentration) (**Figure 27 B**), a decrease in green algal population from 17th May to 14th June can clearly be observed when the C:N ratio increased from 6.6 to 8.6 (**Figure 26 A**). The results suggested that green algal growth may be restricted by N-limitation in short-term, or limited N regulated the growth development together with other environmental factors.

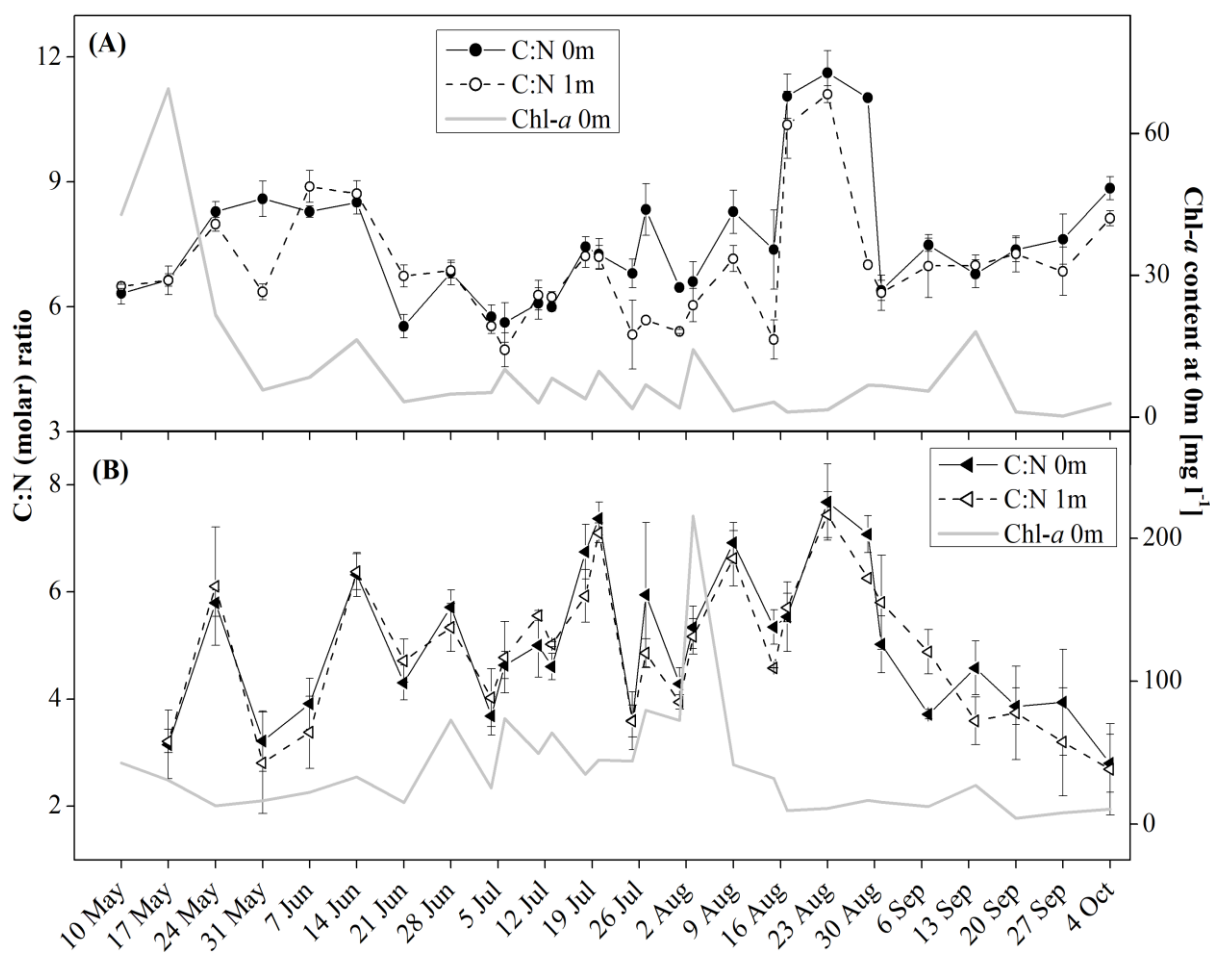


Figure 26 Seasonal variation analysis of carbon to nitrogen ratio (C:N ratio) of green algae (A) and cyanobacteria (B) in 0–1m water samples, respectively. The grey lines showed the Chl-*a* concentration (right axis).

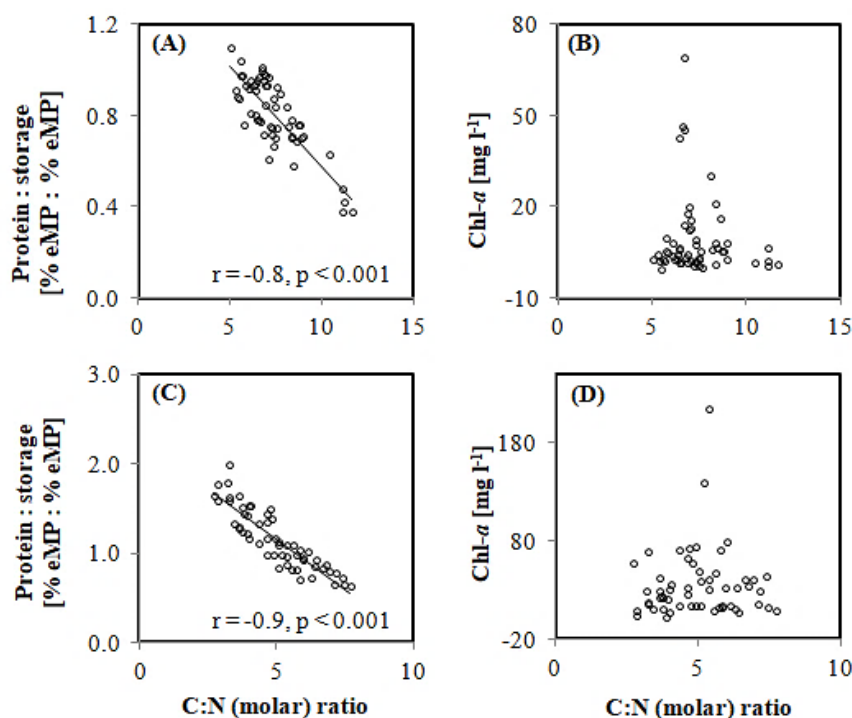


Figure 27 Linear correlations between the carbon-to-nitrogen ratio and protein-to-storage ratio and Chl-*a* concentration of green algae (A–C) and cyanobacteria (D–F), respectively. Lines plotted are from the Pearson’s r correlation (r - and p -values are also reported). If there was no significant correlation between the variables, no line was plotted.

The C:N ratios of cyanobacterial cells in 0–1m water samples showed fluctuations in the range between 2.5 and 8 (**Figure 26 B**), lower than the ratio range of the green algae. The C:N ratio exceeding 6.6 was observed on 20th July, 9th August, and 23th August, which occurred during the determined N-deficiency period of June–August (see **Section 3.1.6**). Similar to the green algae, the cyanobacteria also showed strong negative relation between the C:N and protein:storage ratios (**Figure 27 C**). The cyanobacterial population biomass (determined as Chl-*a* concentration) had no overall linear correlation with the C:N stoichiometry (**Figure 27 D**). However, the population decreased (with 11–45 $\mu\text{g Chl-}a \text{ l}^{-1}$ per water layer) when the C:N ratios exceeded 6.6; whereas cyanobacteria showed high blooms (with 40–216 $\mu\text{g Chl-}a \text{ l}^{-1}$ per water layer) as the C:N ratios were in the range between ~ 4.5 and 6 slightly lower than the Redfield ratio, e.g., on 28th June, 6th July, 13th July, 27th July, and 3rd August (**Figure 26 B**). The results suggested that cyanobacteria proliferated when the cellular C:N slightly lower than the Redfield ratio; while their growth was restricted by N-depletion, which raised the C:N ratio exceeding the Redfield ratio.

3.4.4 Prediction of algal growth potential

We used the PLSR-model based on FTIR-spectra of algal monoculture (Jebsen et al., 2012) to monitor the growth potential μ of field algal groups. The μ value of the green algae in the surface water ranged between 0.1 and 0.32 (**Figure 28 A**). The μ decrease from 0.32 to 0.22 in the period between mid-May to mid-June confirmed the abundance reduction of green algae during the clear-water phase. Furthermore, the μ showed a linear correlation (moderate and significant) with the population biomass (determined as Chl-*a* concentration) (**Figure 29 C**) throughout the observation period. The relationship indicated that the predicted μ based on FTIR-spectroscopy can basically characterize the green algal growth development in relation to seasonal environmental changes in Lake Auensee. In addition, the μ values showed strong and significant correlations with the cellular protein contents (**Figure 29 A**) and C:N ratios (**Figure 29 B**). These relationships evidenced that growth rates depend on the rates of protein synthesis, and increase in C:N ratios associates with growth restriction of green algae.

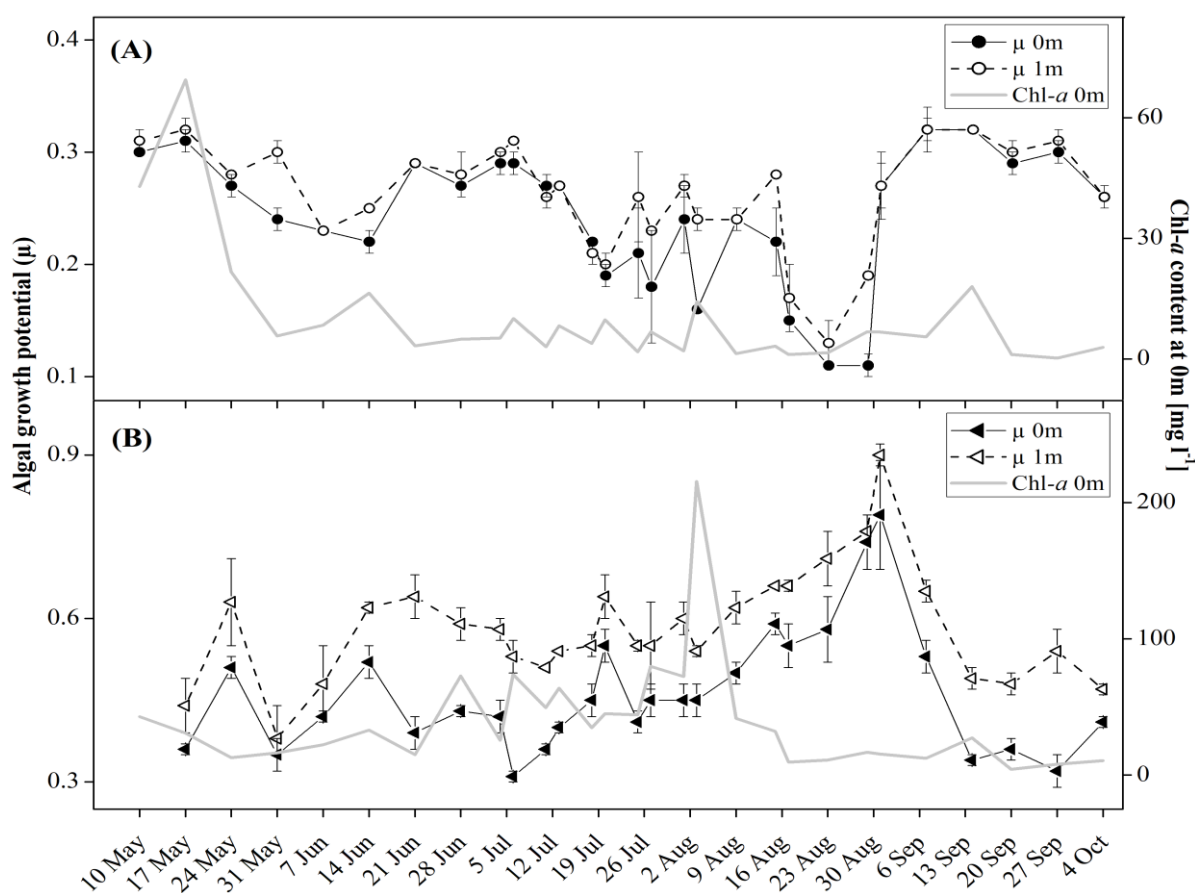


Figure 28 Seasonal variations of algal growth potential of green algae (A) and cyanobacteria (B) at 0m and 1m water depths, respectively. The Chl-*a* concentrations at 0m were also showed (grey lines, right axis).

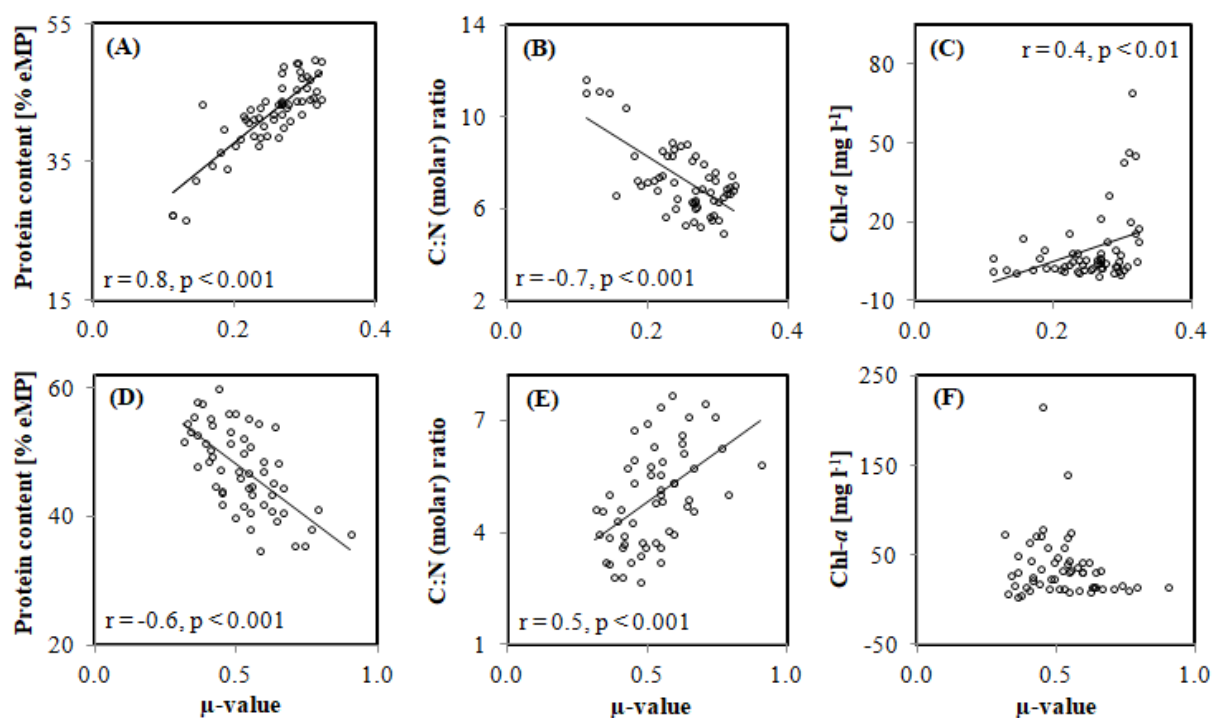


Figure 29 Linear correlations between the growth potential and C-allocation traits and Chl-*a* concentration of green algae (A–C) and cyanobacteria (D–F), respectively. Lines plotted were from the Pearson's r correlation (r - and p -values are also reported). If there was no significant correlation between the variables, no line was plotted.

In comparison to the green algae (μ range 0.1–0.32), the cyanobacteria showed a relatively high μ level (range 0.3–0.9). Furthermore, the μ determined in 1m algal samples (μ range 0.38–0.90) was 30% higher than that in 0m samples (μ range 0.31–0.79) (**Figure 28 B**), indicating better adaptability of this taxonomic group to the underwater environment at 1m depth. Most of the μ peaks, which can be observed on 24th May, 21st June, 20th July and early-August to early September, did not match the cyanobacterial abundance determined by Chl-*a* concentrations, especially, the μ did not provide any indication of the maximal bloom on 3rd August. The lack of linear correlation between the μ and Chl-*a* concentration (**Figure 29 F**) demonstrated that the FTIR-predicted μ cannot characterize the seasonal growth development of the cyanobacterial subcommunity in Lake Auensee. Furthermore, the cyanobacterial μ showed significant negative correlation with the cellular protein contents (**Figure 29 D**), and significant positive relation with the C:N ratios (**Figure 29 E**). These results indicated that cyanobacterial cells can maintain growth rate despite of decreased protein synthesis and increased carbon storage. In comparison to green algae, the cyanobacteria showed different C-allocation and growth strategies in response to environmental changes.

3.5 Statistical correlation analysis

The Pearson's r correlation analysis has been performed to find the relationships among the environmental factors (except nutrient factors, number of samples $n = 31$), the nutrient factors ($n = 6$), the phytoplankton population biomass ($n = 31$), the FTIR-predicted algal growth potential (green algae: $n = 29$, cyanobacteria: $n = 28$), and the cellular C-allocation traits (green algae: $n = 29$, cyanobacteria: $n = 28$).

The environmental factors, which primarily favored green algal abundance (determined as Chl-*a* concentration) in Lake Auensee, include DO, Lm, DIN and DIN:TP (**Table 11**). Furthermore, SD, Lm, Lg, DO and DIN:TP were key factors promoting the dominance of this taxonomic group in entire cell number of the phytoplankton communities. In turn, growth conditions with low Lg, Lm, DO, DIN, DIN:TP and high pH resulted in decreases in algal biomass and cell number proportion. The positive correlation (strong r with significance) between the predicted growth potential μ and DIN confirmed the dependence of green algal growth on N availability. In addition, higher T and pH may reduce the growth potential of green algae (moderate r with significance). With the respect to the environmental affects on C-allocation, decrease in DIN concentration was associated with the increase in carbohydrate content (strong r with significance), as well as the decreases in protein content, lipid content, and protein:storage ratio (**Table 11**). Additionally, high T, pH and SD may also affect the accumulation of carbohydrates in green algal cells.

According to the analysis, the population biomass of cyanobacteria was related with higher pH (moderate-strong and significant r), lower SD (moderate-strong and significant r) and lower DIN (moderate-strong and insignificant r) (**Table 12**). The decreases in Lm, SD, DIN and DIN:TP may majorly affect the cyanobacteria dominance in cell number. Furthermore, the relationship between the μ and DIN (strong and insignificant r) confirmed the cyanobacterial growth independent on the sufficient N supply in water. Furthermore, decrease in DIN showed strong correlation with decreases in the protein content and protein:storage ratio (strong r with significance), and increases in the carbohydrate content (strong r with significance) and C:N ratio (**Table 12**). The DIN:TP ratio had strong and insignificant relation with these C-allocation traits. These relationships demonstrated the effects of the external DIN supply on regulating the C-allocation switching between the cellular N/protein pools and C/carbohydrate pools. In addition, higher T and pH were associated decreases in protein content and protein:storage ratio, as well as increases in the carbohydrate content and C:N ratio.

Table 11 Pearson's *r* correlation (r-value) analysis for green algae. Chl-*a*, chlorophyll a content (by HPLC); %Num, percentage of total cell number (by FCM); μ , predicted growth potential; Pro:Sto, protein to storage ratio; Lg, global radiation; Lm, light intensity; T, water temperature; SD, Secchi-depth; DO, dissolved oxygen concentration; EC, electric conductivity; OP, ortho-phosphorus; DIN:TP, mass ratio of dissolved inorganic nitrogen and total phosphorus. Positive numbers indicate positive relationships, whereas negative relationships are shown as minus numbers. The number of stars is a weighting for the significance level: one star (*) for $p < 0.05$, two (**) for $p < 0.01$, and three (***) for $p < 0.001$. Bold numbers mark the strong ($r \geq 0.5$) and/or significant *r*.

	Green algae 0m								Green algae 1m							
	Chl- <i>a</i>	%Num	μ	Protein	Carbo- hydrate	Lipid	Pro:Sto	C:N	Chl- <i>a</i>	%Num	μ	Protein	Carbo- hydrate	Lipid	Pro:Sto	C:N
Lg	0.3	0.4*	0	0	0	0	0	0.1	0.3	0.5**	-0.1	0.1	0.1	0.1	-0.1	0.3
Lm	0.4*	0.6**	-0.1	-0.1	0	0.2	-0.1	0.3	0.4*	0.8***	0.1	0.1	-0.2	0.3	0	0.2
SD	0.3	0.7***	0.1	-0.1	-0.1	0.3	-0.1	0.3	0.3	0.8***	0.1	-0.1	-0.2	0.5*	-0.1	0.4
T	-0.2	-0.1	-0.3	-0.2	0.3	-0.3	-0.2	0.2	-0.3	0.1	-0.4*	-0.3	0.4*	-0.1	-0.3	0.4*
DO	0.5**	0.6**	0.1	0.1	-0.1	0	0.1	0	0.7***	0.7***	0.1	0.2	-0.2	0.1	0.2	0.2
pH	-0.1	-0.3	-0.4	-0.2	0.3	-0.2	-0.2	0.1	-0.3	-0.4*	-0.4*	-0.3	0.4*	-0.3	-0.3	0
EC	-0.2	-0.4*	0.1	0	0	0.1	0	-0.1	-0.1	-0.2	0.2	0	-0.2	0.4	0	-0.1
DIN	0.5	0.5	0.9*	0.8	-1**	0.8	0.8	-0.3	0.8	0.7	1**	0.7	-1***	0.8	0.7	-0.1
OP	-0.2	-0.4	0.4	0.2	-0.4	0.6	0.2	-0.1	-0.3	-0.3	0.5	0.3	-0.5	0.4	0.2	-0.3
DIN:TP	0.9**	1**	0.5	0.5	-0.6	0.4	0.5	-0.1	0.9*	0.9*	0.5	0.5	-0.5	0.3	0.5	0.2

Table 12 Pearson's r correlation (r-value) analysis for cyanobacteria. Chl- a , chlorophyll a content (by HPLC); %Num, percentage of total cell number (by FCM); μ , predicted growth potential; Pro:Sto, protein to storage ratio; Lg, global radiation; Lm, light intensity; T, water temperature; SD, Secchi-depth; DO, dissolved oxygen concentration; EC, electric conductivity; OP, ortho-phosphorus; DIN:TP, mass ratio of dissolved inorganic nitrogen and total phosphorus. Positive numbers indicate positive relationships, whereas negative relationships are shown as minus numbers. The number of stars is a weighting for the significance level: one star (*) for $p < 0.05$, two (**) for $p < 0.01$, and three (***) for $p < 0.001$. Bold numbers mark the strong ($r \geq 0.5$) and/or significant r .

	Cyanobacteria 0m								Cyanobacteria 1m							
	Chl- a	%Num	μ	Protein	Carbo- hydrate	Lipid	Pro:Sto	C:N	Chl- a	%Num	μ	Protein	Carbo- hydrate	Lipid	Pro:Sto	C:N
Lg	-0.2	-0.2	0.1	-0.1	0.2	0	-0.1	0.2	-0.3	-0.2	0	-0.1	0.1	0	-0.1	0.2
Lm	-0.1	-0.4*	-0.1	0	0	0	0	0.1	-0.3	-0.6**	-0.2	0.1	0	-0.1	0.1	0
SD	-0.4*	-0.8****	0	0.2	-0.2	-0.2	0.2	-0.2	-0.5**	-0.7****	-0.2	0.2	-0.2	-0.1	0.3	-0.2
T	0.3	0.1	0.1	-0.4	0.4*	0	-0.4*	0.4	-0.1	0	0.1	-0.4	0.4*	0.1	-0.4*	0.4*
DO	0	-0.2	-0.2	0.1	-0.1	0	0.1	0.1	-0.2	-0.3	-0.3	0.1	-0.1	-0.1	0.2	0.1
pH	0.5**	0.3	0	-0.3	0.3	0	-0.3	0.3	0.4*	0.3	0.1	-0.4*	0.5**	0	-0.4*	0.4*
EC	-0.1	0.2	0	0.2	-0.1	-0.3	0.2	-0.3	0.1	0	0.2	0.2	-0.1	-0.1	0.2	-0.4
DIN	-0.7	-0.6	-0.8	0.9	-0.9*	0.1	0.9*	-0.7	-0.4	-0.7	-0.7	0.9*	-1*	-0.2	0.9*	-0.9*
OP	-0.2	-0.1	-0.2	0.2	-0.3	0.6	0.1	-0.1	0.3	-0.1	0.1	0.2	-0.3	0.4	0.2	-0.4
DIN:TP	0	-0.6	-0.6	0.7	-0.7	-0.4	0.8	-0.6	-0.5	-0.7	-0.8	0.8	-0.7	-0.6	0.8	-0.5

4 Discussion

According to our analysis of phytoplankton community structure using pigment fingerprinting the following seasonal succession of microalgal groups in Lake Auensee (Leipzig, Germany), could be detected:

Cryptophyte dominance was found in April, during the end phase of the spring turnover. A green algal bloom with only one peak began in early-May, immediately after the collapse of the accumulated cryptophyte population, and ended during the clear-water phase in mid-June. After the clear-water phase, cyanobacteria overgrew the green algae and bloomed in the summer, forming the maximum biomass fraction (> 80% of the total Chl-*a* concentration) and with the bloom of the maximum duration (longer than 3 months) in the lake. More than one peak was observed during the cyanobacterial bloom phase. Dinophytes, together with cyanobacteria, were dominant in the lake during the late summer and fall. Diatoms appeared throughout the observation period, but were never dominant in the epilimnion.

The growth and development of phytoplankton is generally driven one hand by the combination of various environmental factors in an ecosystem. On the other hand, algal growth is also a result of the dynamic balance of changes in cellular elemental and macromolecular composition in response to environmental changes. Therefore, we attempted to explain the seasonal succession mechanisms of the green algal and cyanobacterial subcommunities in Lake Auensee starting from these two aspects of algal growth (see Sections **4.1** and **4.2**). Next, the applicability of predicting algal growth using FTIR spectroscopy within the ecological context of this lake was checked (see **Section 4.3**). Finally, we discussed the methodological advantages and limitations of the measurement techniques used in this study (see **Section 4.4**).

4.1 Effects of seasonal environmental changes on phytoplankton group succession

4.1.1 Nutrient conditions

Lake Auensee can be defined as a eutrophic-hypertrophic lake based primarily on the excessive N and P inputs resulting in a high primary production by its phytoplankton. Fur-

thermore, other factors such as the occurrence of long-lasting stratification, lower Secchi-depth, and an anoxic hypolimnion, reflects the hypertrophic state of this lake ecosystem.

Nitrogen

Nitrogen is one of the most important nutrients for algal growth because it is required in large amounts as an essential component of proteins and other cellular constituents. The bioavailable forms of DIN (sum of ammonium and nitrate) as major N sources for aquatic organisms have been observed in this study. The ammonium contents, which indicate a high rate of ammonification/mineralization of organic nitrogen (tissues from dead plant or animals, and excretes from living organisms) to inorganic ammonium, increased with depths. By contrast, nitrate showed decreasing contents along the vertical gradient of oxygen in the water column, because nitrate is a product of nitrification depending on aerobic conditions.

The DIN concentration in the surface water was observed to be higher in the spring and lower in the summer in the year 2011. The DIN availability increased during the spring turnover due to the mixing of accumulated nutrients from the lake bottom. Conversely, during the summer stratification period, the DIN concentrations in the epilimnion decreased as nutrients were consumed by algae and eventually migrated to the hypolimnion when the algae died and settled out of the surface waters. Furthermore, severe hypoxia in the hypolimnion promotes denitrification processes, by which the nitrate content is reduced and ammonium is formed. However, since the soluble ammonium in the hypolimnion is not available for the phototrophs in the eutrophic zone the distribution of DIN affects the nutritional status and consequently the macromolecular composition of the primary producers.

According to the determination of N-status using a set of nutrient criteria, N-limited growth conditions in Lake Auensee have been identified during June–August in 2011 (see **Section 3.1.6**). However, there were different judgments in previous studies on the occurrence of N-limitations in Lake Auensee. For example, Langner et al. (2004) suggested that the phytoplankton communities in the lake were neither N- nor P-limited during the observation period in 2002. Stehfest et al. (2005) considered the possibility that there was potential N limitation in the lake due to the activities of a cyanobacterial species (*Microcystis* sp.) in the year 2003. To this end, we compared our data in 2011 with data on the previous years' nutrient content (**Table 13**). The results of this comparison showed that the minimum concentrations

of ammonium and nitrate in 2011 were much lower than the minimum N supply in 2002, and similar to the N-limited conditions in 2003. Thus, our findings proved the fact that the degree of N-deficiency in Lake Auensee has gradually increased from 2002 to 2011. Alternatively, short-term deficiency of nitrogen may also occur in systems even where seasonal means give no clear indication (Barica 1990; Matthews et al., 2002), because N₂-fixing cyanobacteria are possible to compensate nitrogen limitation. The short-term nitrogen limitation in freshwater systems is not uncommon when patchy distribution of algal species and nutrient exist and the water column is stratified. In this case, nitrogen limitations occur within microenvironments even when the system average nutrient concentrations do not indicate such condition (Hyenstrand et al., 1998). Accordingly, the above evidence demonstrates the occurrence of N-limited states in phytoplankton cells, or rather a short-term N limitation in our observation period.

Table 13 Availability of ammonium and nitrate at 1 m water depth in Lake Auensee

Year	Ammonium [mg l ⁻¹]	Nitrate [mg l ⁻¹]
2002	1–1.4	1.7–4
2003	0.08–1.5	0.07–3.3
2011	0.05–0.18	< 0.1–0.3
2002–2011 ¹⁾	0.03–2.46	0.05–4

¹⁾ Data summarized by Dunker et al. (2016)

Nitrogen availability significantly affected the abundance and composition of phytoplankton groups depending on their ability to adapt to or tolerate nutrient deficiencies. The green algal abundance showed strong and significant linear dependence on DIN concentrations and DIN:TP ratios (**Table 11**). The linear relationship indicated that nitrogen is one of the limiting factors regulating green algal growth in the lake, that is, sufficient nitrogen supplies due to water circulation benefited rapid growth of green algae that they formed blooms combined with cryptophytes, whereas the spring algal blooms became reduced as a result of N-limitation in the summer, in combination with other factors such as grazing pressure, higher temperature, higher pH values and stability of thermal stratification.

In comparison, the negative (but non-significant) correlation between nitrogen content and cyanobacterial abundance revealed that N-deficiency is likely responsible for cyanobacte-

rial blooms. Under N-limited conditions, diazotrophic cyanobacteria (e.g., *Anabaena*) can fix N₂ from the atmosphere to maintain group productivity, and excrete most of the fixed nitrogen into the environment, which enhances the N content in the whole system (Capone et al., 1994; Hall et al., 2005). The released nitrogen (from diazotrophs) may preferentially facilitate the growth of non-N₂-fixing cyanobacterial species (e.g., *Microcystis*) because some non-N₂-fixers are stronger nutrient competitors due to their higher affinity for nutrient uptake (Paerl and Paul, 2012). The facilitation between N₂-fixing and non-N₂-fixing species can promote the occurrence of intense seasonal cyanobacterial blooms, especially when temperature and light conditions are the most favourable for algal growth (Agawin et al., 2007). This was observed in Lake Auensee when cyanobacteria multiplied dramatically (more than 3-fold) within two days (from 1st–3rd August) and formed “scums” or “mats” in the surface waters. Finally, if nutrients are depleted in the lake water, the magnitudes of cyanobacterial blooms may be reduced. For example, N-depletion can result in decreases in the chlorophyll and phycobilisome (PBS) content of algal cells, and even cell death, leading to a dramatic change in cell colour from the normal blue-green to yellow-green, which is known as bleaching or chlorosis (Richaud et al., 2001). Dead cells and materials released from them may then serve as a nutrient source for the development of the next bloom, especially under high temperatures which allow high microbial activities. Therefore, variation in nitrogen content not only affects changes in standing crop of biomass, but also drives changes in species composition.

Phosphorus

Phosphorus is essential for phytoplankton growth because it is a key component of DNA, ATP, and phospholipids. In our study, by comparing the P uptake of algal species with the high P input to the system, phosphorus was demonstrated to not be a limiting factor for the growth of green algae and cyanobacteria in Lake Auensee (see Section 3.1.6). This finding was in agreement with the results of Langner et al. (2004), who found that excessive phosphorus in the lake can be utilized by these algal groups in sufficient quantities without bottlenecks throughout the year.

Although there was no significant relationship between the algal growth and phosphorus contents (**Table 11** and **12**), changes in P-loading may play important roles in driving the seasonal phytoplankton succession in the lake. From mid-July to September, a dramatic increase

in OP was observed (**Figure 15**). The high amount of phosphorus released from the bottom sediments into the water column is generally regulated in summer by increasing pH and wind-generated surface waves, as has been observed in many eutrophic lakes (Phillips et al., 1994; Welch and Cooke, 1995; Jeppesen et al., 1997; Ramm and Scheps, 1997; Kozerski and Kleeberg, 1998). As a consequence, the DIN:TP ratio declined in the epilimnion. The imbalance between nitrogen and phosphorus supplies, which results in N-limitation in freshwater systems, can lead to eutrophication (Vollenweider and Kerekes, 1982; Linkens, 1972) and harmful cyanobacterial blooms, especially when the affected waters have relatively long residence times and thermally strong stratification (Schindler, 1977; Fogg, 1969; Reynolds and Walsby, 1975; Paerl, 1988; Shapiro, 1990). Therefore, low N:P (such as DIN:TP and TN:TP) ratios can increase the probability of cyanobacterial blooms occurring, which may account for our observation that massive blooms occurred frequently during the summer in Lake Auensee.

In conclusion, our findings suggest that the changing availability of different nitrogen and phosphorus sources can regulate the growth development of the green algal and cyanobacterial subcommunities in Lake Auensee, and play key roles in driving the seasonal succession of these algal groups, and even species composition dynamics within these algal groups. The strong stratification indicates that a great amount of deposited gross P is released back into the water column and P is recovered mainly on short term recycling in sediment. Thus, the imbalanced N and P supply due to existence of excessive P concentration is likely a causative agent of N-limitation in this aquatic ecosystem.

4.1.2 Light conditions

Light, similarly to nutrients, often limits the growth of primary producers (Sterner and Elser, 2002). Conditions with light levels that are too high or too low can inhibit phytoplankton growth. For example, in Lake Auensee, the light intensity at the water surface (0 m depth) (ranging between 100–2400 $\mu\text{mol m}^{-2} \text{s}^{-1}$) during the study period was often above the optimal intensity range of 33–400 $\mu\text{mol m}^{-2} \text{s}^{-1}$ (Singh and Singh, 2015), which may have reduced phytoplankton growth via photoinhibition and photorespiration. In contrast, light limitation may occur at the 1 m water depth layer during July-August, where L_m values below the optimal irradiance intensity could have restricted the population's production of new biomass.

Our findings showed that the green algae favoured illumination conditions with higher

SD, Lg, and Lm (**Table 11**). Furthermore, green algae can adapt to fluctuating light as a consequence of spring water circulation probably due to higher capacity to partition excess energy towards e.g. NPQ (Wagner et al., 2006; Lavaud, 2007; Fanesi et al., 2016). The energy dissipation process is important for the mechanisms to maintain growth rates and cellular photostasis, i.e. the balance between energy absorption and consumption (Ensminger et al., 2006; Fanesi et al., 2016). In turn, the strong dependence of growth on illumination implies that the population decrease observed in the summer can be partly attributed to the decreased Lm and SD during the summer cyanobacterial blooms. The massive accumulation of cyanobacterial colonies at the water surface can decrease light penetration through the epilimnion, which may induce the light limitation of other algal groups. Thus, we suggest that low light is one of the key limiting factors for green algal abundance in the lake. Furthermore, the short-term oscillations in PAR and Chl-*a* concentration e.g. in windy and rainy weather, indicated wind mixing which alters the light climate in the euphotic zone with the consequence that the cells cannot achieve homeostatic states. This may prevent the prediction of *in situ* growth rates.

From mid-May to mid-June, a clear-water phase with a very small amount of phytoplankton cells present and a higher SD (up to 1.2 m) was observed (**Figure 7 C**). The phytoplankton population decline at this time could be attributed to intense grazing during the spring peak of zooplankton (e.g., cladocerans) abundance as temperatures increased (Lampert et al., 1986; Deneke and Nixdorf, 1999). Due to selection by grazers, together with other selective pressures, such as fluctuating nutrient supplies and light availability, changes in the composition of these natural communities can be observed (Sommer et al., 1986). Accordingly, the clear-water phase is a turning point in the seasonal succession of phytoplankton groups, in that a period when the community was dominated by small, edible spring species (e.g., single-celled or small colonial green algae, cryptophytes) was succeeded by a period of greater abundances of grazing-resistant summer species (e.g., colonial green algae, filamentous and colonial cyanobacteria, dinoflagellates). Therefore, the standing crop of biomass at different time points is not only influenced by growth rates but also by grazing intensity which could not be measured in the study.

Cyanobacterial dominance in the epilimnion was determined associated to conditions with lower SD and Lm values (**Table 12**). Cyanobacteria are thought to have tolerance of and the ability to adapt to both high and low light levels (Paerl et al., 2001; Moustaka-Gouni et al.,

2010). There are different possible explanations of the high competitiveness of cyanobacteria for light. Several studies demonstrated that cyanobacteria are strong competitors under limiting light conditions due to their photosynthetic accessory pigments and the structural organisation of their light-harvesting antennae (phycobilisomes) (Osborne and Raven, 1986; Passarge et al., 2006). Phycobilisomes can harvest light of a wide range of wavelengths across the electromagnetic spectrum; for example, cyanobacteria can use green light for growth, and can also utilize blue and red light. Therefore, species with a higher competitive ability for light (or a high tolerance of low light) may also dominate under light-limited conditions, such as when there are deep mixing depths or high dissolved organic matter content (Edwards et al., 2013). Mur et al. (1978) performed a competition study of a cyanobacterial species *Oscillatoria agardhii* and a green alga *Scenedesmus protuberans* and demonstrated that the cyanobacteria grow more slowly at high irradiance, while grow faster than green algae at decreased irradiance as a result of self-shading in the mixed culture. Such high competitiveness for light could account for the succession from green algae to cyanobacteria during the summer in eutrophic lakes that support dense phytoplankton populations. However, the observed dominance of cyanobacteria in eutrophic waters cannot be explained solely by competition for light because some of the bloom-forming species (e.g., *Microcystis* sp.) are not particularly strong competitors for light in a well-mixed environment (Huisman et al., 1999; Reynolds, 2006). Other highly adaptable eco-physiological traits of cyanobacteria, such as buoyancy and the ability to compete well under conditions of high pH, high temperature, low nutrients, and strongly enhanced water column stability, also play important roles in driving their bloom development (Carey et al., 2012).

4.1.3 Water temperature

During the season, the green algae bloomed in Lake Auensee when T ranged between 16–18 °C, and the cyanobacterial blooms occurred when T ranged between 16–24 °C (**Figure 8**). It suggested that these algal groups can form blooms in natural environments with temperature much lower than their optimum growth temperatures (ranging between 25–35 °C) measured in the laboratory (Robarts and Zohary, 1987; Cho et al., 2007; Zargar et al., 2006; Bouterfas et al., 2002; Sosik and Mitchell, 1994). Possible reason is that temperature commonly affects growth rate and photosynthetic production of natural samples in combination with other factors such as light intensity (Konopka and Brock, 1978).

Although there was no overall linear relationship between the T changes and the standing crop in the study period (**Table 11**), the green algae tended to perform better in colder water. At low temperatures, microalgae usually have lower photosynthetic efficiency in converting absorbed light energy into growth (Fanesi et al., 2016), especially under the fluctuating light conditions. Growth conditions with excessive light energy and fluctuating light in the upper epilimnion may result in damage to the photosynthetic apparatus and restricted growth rates. Green algae having relatively high capacity to dissipation excess energy can cope with such conditions with low T and fluctuating light during the spring turnover (Wagner et al., 2006; Lavaud et al., 2007; Fanesi et al., 2016).

Many species of planktonic cyanobacteria can proliferate at higher temperature because they have specific physiological features to cope with thermal stratification, including buoyancy. Buoyancy regulation allows cells to perform photosynthesis in the light and respiration in the dark (Kromkamp and Walsby, 1990) when they migrate in stratified lakes between the light-flooded surface layer and the nutrient-rich bottom water (Ganf and Oliver, 1982). The stratification of Lake Auensee (including epilimnion, metalimnion, and hypolimnion layers; **Figure 9**) was established for more than five months from the early spring to the fall, which led to reduced turbulence in the water column and fluctuating nutrient supplies in the bottom water layer (e.g., a decreased DIN supply due to denitrification). The long-lasting stratification, together with the higher temperatures during this period, altered nutrient loading in ways that are considered to favour cyanobacteria over other phytoplankton (Paerl et al., 2001; Carey et al., 2012). Therefore, the cyanobacteria could compete with other algal groups and dominate the whole phytoplankton community throughout the summer.

In conclusion, water temperature was found to be an important factor driving seasonal variations in the community structure and abundance of phytoplankton in Lake Auensee. From the perspective of future climate warming, increasing temperatures along with changes in other related factors, such as nutrient loading, may elevate the degree of eutrophication and preferentially promote harmful cyanobacterial blooms in the lake.

4.1.4 Dissolved oxygen

The concentration of dissolved oxygen in a natural lake can change daily and seasonally. The level of dissolved oxygen in lakes reflects the balance of oxygen supply (i.e. by diffusion

and photosynthesis) and oxygen consumptions (i.e. by respiration and decomposition). High DO level in the spring is mainly attributed to low temperature and water turbulence as a result of the spring turnover. In April, water mixed around the lake and delivered DO to lower depths, which led to oxygen oversaturation ($> 100\% \text{ O}_2$) in the 0–2.5 m surface water layer (**Figure 11**). Furthermore, massive abundances of spring bloom-forming cryptophytes and green algae can release oxygen into the water column that enhanced the oxygen contents and deepened the oxygen-containing zone into the bottom water (at maximal 6m depth). In such situations, “more oxygen supply than consumption” can account for the oxygen sufficient conditions in the epilimnion, and a strong correlation between the green algal abundance and higher DO concentration can be observed (**Table 11**).

As the thermal stratification became stable along with the season, the distribution of DO in the water column changed (**Figure 11**): in April, both epilimnion and metalimnion contained oxygen; from May to June, only the epilimnion was aerobic; and from July to October, the aerobic zone had smaller volume than the epilimnion. In the summer, the volume ratio of the eutrophic to the aphotic zone decreased and oxygen oversaturation at the surface led to a loss of oxygen into the atmosphere, therefore, an oxygen deficit for the whole basin was formed. Furthermore, oxygen utilization by biological processes (i.e. respiration and decomposition) may also accelerate the oxygen depletion in context of the cyanobacterial blooms. Intense accumulation of cyanobacterial aggregates at the surface water can block sunlight for photosynthesis, thus decrease the oxygen productivity, and the demand for oxygen in dark respiration (uptake O_2) is also enhanced not only during night but also in the daytime. Oxygen is also required for bacterial decomposition of massive particulate organic matters released from the dead cells. The enhanced oxygen requirement may account for a fact of “less oxygen supply than consumption”, resulting in the shifting of the depth of the anoxic zone from deeper layers to higher layers. The reduced anoxic zone narrowed the habitat of aerobic zooplankton and fish and may regulate the nitrogen concentration due to denitrification processes, in which inorganic N is removed from the water ecosystem under anaerobic conditions. Therefore, the increasing size of the oxygen-depleted zone represents a further danger of increasing eutrophication and frequency of HABs to the hydrological habitat of a lake.

4.1.5 pH value

The pH of the water in an aquatic system reflects the balance between bicarbonate-carbonic acid buffering in it. In Lake Auensee, there was likely no free carbon dioxide in the 0–1 m epilimnion during the study period because almost all pH values measured were above 8.3. High alkalinity can reduce CO₂ availability in the water, resulting in the decreased ability of phytoplankton to photosynthesise (Singh, 1974). Thus, CO₂ may have been a limiting factor for photosynthesis when massive blooms of algae occurred in the upper epilimnion.

Freshwater studies have suggested that species succession is determined by the ability of certain species to proliferate at high pH, presumably due to their tolerance to low CO₂ levels (Brock, 1973; Goldman and Shapiro, 1973; Shapiro, 1973). In our study, higher pH in the epilimnion was related to the decreased abundance of green algae and the increased abundance of cyanobacteria (**Table 11** and **12**). Dense blooms occurring at higher pH values provide evidence that cyanobacteria have a higher tolerance of CO₂ limitation than other algae, and they can thus dominate the phytoplankton communities in waters in which the dissolved CO₂ concentration has been depleted (Shapiro, 1990, 1997; Caraco and Miller, 1998; Low-Décarie et al., 2011, 2015). Cyanobacteria are strong competitors under CO₂ restriction at high pH because they can take up CO₂ and bicarbonate as an inorganic carbon source through the development of highly efficient CO₂-concentrating mechanisms (CCMs). This specific feature can increase the free CO₂ level around the RuBisCO enzyme responsible for carbon fixation and saturate the photosynthetic apparatus (Price et al., 2008; Raven et al., 2012; Burnap et al., 2015), which allows cyanobacteria to cope with harsh alkaline environmental conditions (Pikuta and Hoover, 2007; McGinn et al., 2011). Therefore, the highly alkaline epilimnion that occurs in the summer may play a key role in driving the succession of dominance in the phytoplankton community from green algae to cyanobacteria in Lake Auensee. In addition, pH can influence the nutrient stoichiometry in the lake by means of enhancing phosphorus release from sediments into the water column under alkaline conditions (Moore and Reddy, 1994; Penn et al., 2000). Thus, higher pH may promote the eutrophication development and cyanobacteria dominated HABs in the lake.

4.1.6 Electric conductivity

Electric conductivity reflects the water's capability to pass electrical flow, which is di-

rectly related to the concentration of ions in the water. In our study, the EC increase from summer to fall may be attributed to the release of dissolved salts and inorganic materials from bottom sediments such as ammonium and phosphate, regulated by seasonal environmental changes such as temperature, pH, dissolved oxygen etc.

One reason conductivity had negative relation with green algal dominance (%Num) could be that the spring abundance have almost exhausted the dissolved inorganic nutrients (such as nitrogen), thus reduced the EC in the epilimnion. In turn, green algae may have been unable to tolerate a conductivity increase, while some cyanobacterial species e.g. *Anabaena* are saltwater resistant (Apte and Bhagwat, 1989; Flöder et al., 2010; Chakraborty et al., 2011). This may account for the lack of a relationship between conductivity and cyanobacterial abundance. Another possible reason is that conductivity changes may result in decreased zooplankton populations that would affect phytoplankton concentration or species composition.

4.1.7 Regulation of seasonal phytoplankton succession by environmental factors

Green algae

The green algal bloom occurred in May, immediately after the collapse of the earlier cryptophyte bloom. Our results demonstrated that green algal abundance was significantly and linearly related to higher nitrogen availability. This supports the findings of Dunker et al. (2016) that chlorophytes, including cryptophytes, are the classes of phytoplankton with the highest nutrient requirements, while the fact that green algal dominance superseded that of cryptophytes may have been due to the gradually increasing water temperature over the course of the season. According to the results of the correlation analysis, low nutrient availability, in combination with increasing pH, and decreasing SD and DO under well-stratified conditions with the progression of the season may result in the reduction of green algal blooms. In addition, grazing pressure is also an important factor reducing the green algal population because of the occurrence of a clear-water phase from mid-May to early-June. Although the nutrient-rich water during the late-summer and fall led to phosphorus and nitrogen being abundant, the population biomass of green algae was repressed to a relatively low level during this time, perhaps due to such other stress factors as low light conditions.

Cyanobacteria

Cyanobacteria overgrew green algae and dominated in the summer with the maximum biomass fraction (> 80% of the total Chl-*a* concentration) and duration (longer than 3 months) observed in Lake Auensee because they can adapt to grow in conditions of higher phosphorus supply, pH, and T, as well as lower SD and DO content (Dunker et al., 2016). Cyanobacteria are considered to have unique and highly adaptable eco-physiological traits, including: 1) a high affinity for, and ability to store, phosphorus; 2) the ability to take up HCO₃⁻ under high-pH conditions (Price et al., 2008); 3) adaptation to higher temperatures (Paerl and Huisman, 2009); 4) light capture at low intensities and over a wide wavelength range due to their possessing accessory pigments and due to the structural organization of their light-harvesting antennae (e.g., Osborne and Raven, 1986); and 5) nitrogen fixation. Additionally, cyanobacteria may also possess many other traits outside the scope of our work, such as buoyancy due to the production of gas vesicles, toxin production, and grazing resistance (through changes in the morphology of filaments and colonies). Dunker et al. (2016) summarized the data of three German freshwater lakes including Lake Auensee and demonstrated that low P and N availability, together with high pH values and water temperature, are key conditions driving cyanobacterial dominance in these lakes. These specific adaptations may allow harmful cyanobacterial blooms to occur with greater frequency and intensity in the future in combination with climate changes, such as higher temperatures (Parry et al., 2007), stronger and longer periods of stratification (Jeppesen et al., 2007), etc.

According to the Leibig's law of the minimum, the growth rate of an algal cell is limited by the factor or factors present in the lowest supply that is required for synthesizing the cellular constituents. In our study, the limiting factor for phytoplankton growth can be nutrient, light, temperature, pH, DO, EC, or a complex of them; as well as other factors not measured in this work like grazing, wind and toxin. The seasonal changes of environmental factors have driven the phytoplankton succession in Lake Auensee, from a spring green algal bloom to harmful cyanobacterial blooms in the summer. However, some of the environmental factors did not show clear linear correlation with Chl-*a* concentration, probably because one hand, combined effects of different environmental factors and interaction among them may influence the correlation. On the other hand, the lack of (or weak) correlations can be explained by the unstable ratios of Chl-*a* to biomass, with Chl-*a* concentration strongly depending on light and nutrient status (Yacobi and Zohary, 2010; Dunker et al., 2016). To this end, we attempted

to explain the responses of algal growth to environmental changes from a molecular perspective of cellular traits.

4.2 Effects of seasonal environmental changes on C-allocation in algal cells

4.2.1 Macromolecular composition dynamics in response to nutrient limitation

In this study, the macromolecular composition of proteins, carbohydrates and lipids of field phytoplankton cells was determined using a chemometric model. The model was based on a reconstruction of a whole algal spectrum by the FTIR-spectra of these macromolecular components with relative contribution (Wagner et al. 2010). These calculated relative contents of major macromolecules reflected the allocation profile of photosynthetically yielded energy and carbon in response to environmental changes. The main questions addressed in this analysis concerned whether the C-allocation stoichiometry could explain the influences of these environmental changes on standing crop and seasonal succession of phytoplankton communities in this hypertrophic lake.

Effects of nitrogen limitation on the C-allocation of green algae

Under conditions of low N content and N:P ratios, green algae showed declines in their Chl-*a* concentrations, cellular protein content, and protein:storage ratios, while their carbohydrate content increased (**Table 11**). These results demonstrated that the algal cells adapted to N-limited conditions by switching their metabolic balance from a state of high biosynthesis with active cell division and C being allocated mainly into proteins, to one of low biosynthesis and minimal biomass increase with C allocated mainly into storage pools (Stehfest et al., 2005; Beardall et al., 2001a; Dean et al., 2012). The linear dependence of biochemical composition on nitrogen availability confirmed the C-allocation hypothesis (see **Section 1.4.2**). Accordingly, the CAH can explain the C-allocation strategies of green algae responding to N-stresses not only for lab-cultured cells, but also for natural samples.

Furthermore, our results confirmed that expressing the composition of cellular proteins, carbohydrates, and lipids as a carbon allocation profile can mirror the changes in growth patterns that occur in response to variations in abiotic factors and nutrient conditions (Rhee, 1978;

Goldman et al., 1986; Palmucci et al., 2011; Vrede et al., 2004; Flynn et al., 2010; Jebsen et al., 2012). Therefore, macromolecular stoichiometry can be used as a marker to reflect the physiological status of phytoplankton in a given ecological niche.

Effects of nitrogen limitation on the C-allocation of cyanobacteria

According to the results of correlation analysis, lower N content and N:P ratios in the epilimnion can also influence the macromolecular composition of cyanobacterial cells, similarly to their impacts on the metabolic reactions in green algae. The field cyanobacteria responded to conditions with lower DIN content and DIN:TP ratios in the epilimnion by increasing cellular carbohydrate contents, as well as decreasing protein contents and protein:storage ratios (**Table 12**).

These metabolic reactions with decreases in protein pools may be attributed one hand to the degradation of phycobilinprotein (PBP) and chlorophyll under N-limitations (Allen and Smith, 1969; Wood and Haselkorn, 1980; Stevens et al., 1981; Elmorjani and Herdman, 1987; Foulds and Carr, 1977; Richaud et al., 2001). PBP, as an essential component of the light-harvesting antennae in the photosystems of cyanobacteria, constitutes up to 50% of the total cellular protein, and also acts as a nitrogen store. Under N-limitations, PBP can be progressively, rapidly, and almost completely degraded and release N for new polypeptide synthesis to maintain growth (Allen and Smith, 1969; Richaud et al., 2001). On the other hand, diazotrophic cyanobacteria shift their C-allocation pathways from protein synthesis to energy storage, when the nitrogen uptake strategy switching from assimilating NH_4^+ and NO_3^- under N-sufficient conditions to N_2 -fixing under N-deficiency (Molot, 2017). It is detected that diazotrophs accumulate photosynthetic energy in forms of lipids and carbohydrates for dark N_2 -fixation (Molot, 2017), because the N_2 -fixing processes require more energy. This phenomenon has been observed by some laboratory cultures growing under conditions with N_2 as the sole source of extracellular nitrogen, including species of *Anabaena* (Sanz et al., 1995) and *Nostoc* (Bagchi et al., 1985; Vargas et al., 1998).

Our results supported the above findings that field cyanobacteria adapted to nutrient stresses in terms of photosynthetic carbon/energy allocation shifts from protein to storage pools. Nevertheless, they were able to maintain growth rate and population dominance under N-deficiency conditions, which did not match the CAH.

One possible reason is that the growth response of cyanobacterial species is more variable and species-specific (Stehfest et al., 2005; Molot, 2017). For example, N₂-fixing cyanobacteria do not significantly change their biomass productivity when grown under diazotrophic conditions (Vargas et al., 1998). This may be attributed to: first, the N₂-fixation rates may not be able to support very high cellular growth rates, although N₂-fixation can meet the N requirements of most metabolic processes in cyanobacteria (Kenesi et al., 2009; Molot et al., 2017). Second, N₂-fixing cyanobacteria can store nitrogen as cyanophycin, a polypeptide which is not ribosomally synthesized. Cyanophycin is measured in the FTIR spectroscopy as a protein, although they are storage and do not contribute to growth. Third, cyanobacteria can store polyphosphates and therefore realize high growth rates even with low P supply. In such situations, diazotrophs respond to N deficiency with less change in their growth rate. Some bench top studies found that heterocystous N₂-fixing cyanobacteria can exhibit very modest changes in growth rates under N-starvation conditions (Vargas et al., 1998; Allen and Arnon, 1955; Kenesi et al., 2009).

By contrast, non-N₂-fixing cyanobacteria grow faster under sufficient nutrient, whereas decrease growth rates and accumulate carbohydrates and storage lipids when N or P is limited, observed by i.e. lab-cultured *Microcystis aeruginosa* (Stehfest et al., 2005; Jebsen et al., 2012). Moreover, comparisons between experiments have demonstrated that the kinetics and amplitudes of changes in the macromolecular composition under N depletion differ significantly among different species of cyanobacteria, as previously determined using FTIR spectroscopy (Stehfest et al., 2005). Therefore, the species-specific dependence of growth patterns on biochemical responses to nutrient changes (Stehfest et al., 2005; Molot, 2017) may complicate the establishment of growth models for the whole cyanobacterial subcommunity based on their taxonomic FTIR spectra.

Another finding of this study was that increased lipid content was correlated with decreased protein content in cyanobacterial cells, whereas this relationship was not obvious in green algal cells. This fact can be attributed to the fact that lipid analysis is only focused on the determination of the content of neutral lipids because the quantification model was based on the reference FTIR spectrum of a neutral lipid (palmitic acid), thus, the contents of other lipid components such as polar lipids would be ignored. Generally, when algal growth slows under N-deficiency, the requirement for the synthesis of new cell membrane compounds is also decreased. As a consequence, the cells convert and deposit polar lipids (e.g., phospholip-

ids) into neutral lipids (Sharma et al., 2012; Widjaja et al., 2009). Since cyanobacteria contain higher concentrations of polar lipids (Sallal et al., 1990), an obvious accumulation of neutral lipids deposited from the polar lipids under N-limited conditions can be observed. By contrast, green algal cells usually have fewer polar lipids and a higher fraction of neutral lipids (Choi et al., 1987), and thus the C-allocation response to N-deficiency with increased lipid content in them may not be clearly detected by FTIR spectral analysis. Therefore, cyanobacteria appear to react to environmental stress with increases in their energy/carbon storage in both the lipid and carbohydrate pools, whereas green algae appear to restore energy/carbon levels, mainly in the form of carbohydrates, under stressful conditions.

Effects of pH and water temperature on C-allocation

Higher pH and T values were correlated with increased carbohydrate and decreased protein content, which confirmed the results of previous studies (Taraldsvik and Mykkestad, 2000; Al-Safaar et al., 2016; Touloupakis et al., 2016). A major portion of metabolic regulation can be attributed to the influences of pH and T on the activity of enzymes involved in C fixation and membrane transport processes (Raven, 1993; Taraldsvik and Mykkestad, 2000; Davidson, 1991; Fanesi et al., 2016; Wagner et al., 2016). For example, higher pH may affect the biosynthesis of amino acids and sugars, which would change the macromolecular composition of a cell (Taraldsvik and Mykkestad, 2000; Al-Safar et al., 2016; Touloupakis et al., 2016). Higher T may decrease cellular quotas of ribosomes (Toseland et al., 2013; Yvon-Durocher et al., 2015; Yvon-Durocher et al., 2017), potentially leading to decreased protein levels.

The green algae and cyanobacteria in the lake similarly reacted to higher pH and T variations with changes in their C allocation from protein to storage pools. However, they showed opposite growth responses: there was a strong restriction of green algal growth, but increased cyanobacterial abundance, in the summer. These differences in their methods of physiological adaptation may be attributed to taxon-specific metabolic features, such as cyanobacteria having the ability to sustain their growth rates with low energy requirements at high T (Fanesi et al., 2016) and being strong competitors for CO₂ under higher pH conditions (Price et al., 2008).

Effects of light, electric conductivity, and dissolved oxygen on C-allocation

Light conditions, together with temperature and nutrient levels, play key roles in driving seasonal algal succession. However, no direct effects of light on the macromolecular composition of either algal group were found in the correlation analysis performed (**Table 11** and **12**). Some possible reasons include: 1) the effects of fluctuating light regimes on the photosynthesis and growth rates of microalgae are highly variable, depending on species-specific physiological adaptations (Elliott et al., 2001; Fietz and Nicklisch 2002; Wagner et al., 2006); and/or 2) the effects of light on metabolism can be weakened or superimposed by other environmental factors in the aquatic environment. For example, the decreased content of storage carbohydrates and lipids under light limitation may be offset by the increases in these storage pools caused by N-deficiency (Jebsen et al., 2012) when both environmental stressors co-occur in the system. Thus, strong fluctuations in light levels in combination with variations in nutrients, temperature, etc. may alter the metabolic performance of algae in a complex manner.

Similar to the light conditions, the electric conductivity and dissolved oxygen supply also showed no/weak linear correlations with the macromolecular composition of phytoplankton cells. Nevertheless, we surmise that these environmental factors must have direct or indirect influences on metabolism, as they may change the nutrient supply in the environment, or that their influences are usually interfered with by other environmental factors. The interaction and combination of environmental factors may complicate the monitoring of environmental changes using cellular C-allocation traits.

4.2.2 Cellular C:N ratio as an indicator of algal growth under N-limitations

The FTIR-based C:N prediction model is a partial least squares regression model built for species from six phytoplankton species from among different phylogenetic groups under different nitrogen supply conditions (Wagner et al., 2019). This multi-species model is useful to analyse cellular traits as the mean value of a group of interest to minimize taxon-specific differences in C-allocation dynamics.

C:N ratio reflects how energy is allocated to carbohydrates and to RubisCo; in other words, C:N ratio is connected to the “nitrogen-use efficiency” (Vitousek, 1982). Both green algae and cyanobacteria in Lake Auensee showed stronger correlations between increases in

the C:N ratio in cells and decreases in the nitrogen availability in the epilimnion, which indicated that the cellular N pool is dependent on the external N availability (Droop, 1973; Caperon and Meyer, 1972). Similar to macromolecular traits, the C:N ratio can also reflect the shift in C-allocation from the N-rich protein pool to the storage pools (carbohydrates and lipids) when N is limiting. As a cellular trait of the N quota, the C:N ratio provides evidence that the green algae have a higher sensitivity to and requirement for nitrogen than the cyanobacteria (Dunker et al., 2016). For example, the first occurrence of a C:N above the Redfield ratio of 6.6 in the green algal cells was observed early, on 10th May, when the nitrogen concentration was above the critical value for N limitation (0.1 mg N l^{-1} , Gophen et al., 1999). In comparison, a C:N > 6.6 first occurred in the cyanobacterial cells on 18th July, when the nitrogen concentration was below 0.05 mg N l^{-1} , which is much lower than the critical N concentration. The higher level of biochemical homeostasis in cyanobacteria indicates that they have a higher tolerance to N-deficient conditions than the green algae do.

Our study showed for the first time that the regulatory mechanisms found under lab-conditions can be also identified in the field. Although the same mechanisms can be found in the field, other factors should also be considered, e.g. the use of the Redfield C:N ratio as a criterion to determine the N-limited growth conditions for algal cells in Lake Auensee. The analysis demonstrated that when the cellular C:N ratio was far above the Redfield ratio, both of green algae and cyanobacteria in the lake decreased their population biomass (determined as Chl-*a* concentration) significantly, or restricted their growth to a low level. Therefore, the Redfield C:N level may be able to indicate the growth restriction of phytoplankton under N-depletion. Interestingly, the cyanobacteria often proliferated when the C:N ratio was between 4.5 and 6, slightly lower than the Redfield C:N ratio. This phenomenon provides a possibility that the non-N₂-fixing cyanobacteria benefit from fixed nitrogen supplied by diazotrophic cyanobacteria. Thus, at this nitrogen level, the species interaction between diazotrophic and non-N₂-fixing cyanobacteria is transformed from competition into facilitation that eventually cause outbreak of cyanobacterial blooms (Agawin et al., 2007).

However, the critical C:N ratio should be used with caution because the optimal C:N ratios of cells are usually species-specific (Rhee and Gotham, 1980; Hecky and Kilham, 1988; Geider and La Roche, 2002), and highly variable depending on growth rates (Vrede et al., 2004; Klausmeier and Litchman, 2004). Previous studies demonstrated that the average C:N ratio of nutrient-replete marine phytoplankton cultures has a typical value greater than the

Redfield ratio (Geider and La Roche, 2002). Healey (1975) provided evidence that freshwater microalgal cultures are moderately N-deficient (20-50% of maximum growth rate) at $8.3 < \text{C:N} < 14.6$, extremely N-deficient (less than 20% of maximum growth rate) at $\text{C:N} > 14.6$, and have no N deficiency at $\text{C:N} < 8.3$. However, for field phytoplankton cells, the C:N ratio can be constrained to values lower than the Redfield ratio, especially in cyanobacteria. Several studies found cyanobacteria (*Anabaena* and *Microcystis*) that grew in highly eutrophic lakes had low average C:N ratios around the Redfield ratio (Aizaki and Otsuki, 1987; Tezuka, 1989). Therefore, the ability of algal growth responses to nutrient status in natural environments to be predicted solely by macromolecular and C:N stoichiometry is limited, so these critical C allocation traits should be combined with other criteria, such as absolute nutrient concentrations, algal affinity for nutrients, TN:TP ratios, etc.

Although a linear relationship between C:N ratios and growth rates has been found in algal cultures (Vrede et al., 2004), this does not necessarily hold true in field algal samples; for instance, no overall correlation was found in this study between the C:N and Chl-*a* of both green algae and cyanobacteria in Lake Auensee (**Figure 27 B and D**). Because the actual conditions *in situ* are more complex, this relationship is influenced by a combination of environmental factors. The use of solely nutrient-based models clearly cannot adequately interpret the relationship between algal biochemical stoichiometry and growth rates in an ecological context. Nevertheless, focusing on the biological basis of macromolecular and elemental stoichiometry may provide possibility to mechanically link growth and C-allocation strategies of biota to major ecological consequences.

4.3 Prediction of phytoplankton growth using FTIR spectroscopy

We tested the applicability of PLSR models (according to Jebsen et al., 2012) for monitoring the phytoplankton succession in Lake Auensee. Our results demonstrated that the growth prediction model, which has been established with a monocultured algal species, was applicable to determine the growth development of field green algae because the predicted algal growth potential, μ , has a moderate and significant relationship with the population biomass determined using HPLC.

The μ is able to predict growth due to its strong correlation with the cellular protein content (**Figure 29**). The protein abundance reflects protein synthesis rate of a ribosome. Ribo-

some consist mainly of P-rich ribosomal RNA and structural proteins. The GRH suggests that growth rate depends on the protein-synthesis rate and the number of ribosomes (Sterner and Elser, 2002; Vrede et al., 2004; Flynn et al., 2010). Since the FTIR-based growth model defines a μ as depending on a relative absorption in protein (amide I and II) and phosphate ester bands, μ can explain the growth rate. The growth prediction was particularly applicable to describe the growth tendency of green algae in response to N-limitation in the lake. Due to the strong dependence of cellular N pool on the external N source, the decrease in N supply in water can affect the protein synthesis rate, leading to μ decrease.

The cyanobacteria had higher μ (0.30-0.75) than the green algae (0.15–0.35), which may be attributed to that cyanobacteria (e.g., colonial species) have smaller cell size than green algae. Smaller cells have higher surface-to-volume ratio, and hence, presumably the light absorption and rate of nutrient uptake per cell volume per time than larger cells. Many studies demonstrate that growth rate is negatively correlated with cell size that smaller species grow faster than larger cells under continuous illumination (Fogg, 1975; Banse, 1976; Foy et al., 1976; Foy, 1980). Although cyanobacteria showed a higher μ in the spring, their abundance was in fact much lower than that of the green algal bloom. This suggested that μ can only reflect the relative variation in trends in growth and development, but cannot determine the absolute growth rates of these algae. This may be attributed to that in field studies, the standing crop of biomass is often underestimated due to other factors such as grazing and sinking. However, these factors do not play roles in lab-studies.

In a previous study, Jebsen et al. (2012) indicated that there was a very strong correlation between the predicted and the actual species-specific growth rates of *Microcystis aeruginosa*. However, the predicted growth potential had no linear correlation with the cyanobacterial abundance in water samples from Lake Auensee. Furthermore, the μ was negatively related to the cellular protein pool, and positively related to the C:N ratio, which was inconsistent with the results of the previous studies by Jebsen et al. (2012) and Fanesi et al. (2017). Some possible reasons for this discrepancy may be the following:

- 1) The specific tolerances and abilities of cyanobacteria (e.g., N fixation) can complicate the interpretation of their metabolic strategies, leading to deviations from the predictions of the C-allocation hypothesis. The mismatch between the predicted and actual growth may be attributed to the lack of a relationship between the macromolecular composition and cyanobacterial growth in the field, as discussed in **Section 4.2.1**.

- 2) Another important potential reason that cannot be ruled out is the interaction among cyanobacterial species. Agawin et al. (2007) performed competition experiments with a mixed culture of simultaneously growing N₂-fixing and non-N₂-fixing cyanobacterial species. That experiment showed that: 1) non-N₂-fixers dominated at high nitrate input concentrations, whereas the two species coexisted at low nitrate input concentrations; 2) the release of fixed nitrogen by diazotrophs facilitated their competitors (non-N₂-fixers), and thereby changed their interaction from competition to facilitation; 3) non-N₂-fixers showed distinctly different growth rates in monoculture and mixed cultures (i.e., non-N₂-fixers reached a population with four times higher density than their corresponding population density in monoculture). Therefore, the interactions between N₂-fixing and non-N₂-fixing cyanobacterial species may shift the nature of the predicted relationship between growth patterns and nutrient supply (as well as other environmental factors) and increase the difficulty of establishing a taxon-specific growth model for field studies.
- 3) The filtration of samples in the preparation process may lead to losses of large amounts of filamentous and large colonial cyanobacteria. Consequently, the predicted growth potential may deviate from the actual growth rates.
- 4) Cyanobacterial growth can benefit from their other physiological traits, such as buoyancy control and grazing resistance, the relationships of which to C-allocation traits are still unclear.

In conclusion, our model and experiments demonstrated that the FTIR model can be used to predict the growth potential of green algae under seasonal environmental changes, whereas the growth potential of cyanobacteria cannot be accurately predicted by this model. The specific physiological traits of cyanobacteria (e.g., nitrogen fixation) may complicate the prediction of their metabolic strategies. Thus, as a next step, the use of species-specific models for some major bloom-forming species (e.g., *Microcystis* and *Anabaena*) may be more suitable for use in water monitoring and early warning for the occurrence of HABs. These species-specific predictions can be achieved by using microscopy coupled with FTIR spectroscopy. Dean et al. (2012) used synchrotron-based FTIR micro-spectroscopy to selectively analyse target species within mixed populations. The combination of synchrotron-based-FTIR spectroscopy and the PLSR model of the whole-cell spectra is very promising for use in future water monitoring.

4.4 Technique advantages and limitations

4.4.1 Flow cytometry-coupled FTIR spectroscopy for phytoplankton monitoring

The use of flow cytometry in combination with FTIR spectroscopy stands out for its high accuracy, sensitivity, and rapid speed (Rutten et al., 2005; Hofstraat et al., 1994; Cellamare, 2010) when used to select (or sort) cells of interest from natural water samples. This combined method supports the measurement of FTIR spectra from target functional algal species or groups in natural phytoplankton communities. The identification and separation of algal groups were addressed based on the combination of information on the characteristics of cells, such as FSC (cell size), SSC (granularity or internal complexity), and fluorescence emission from such pigments as phycocyanin, phycoerythrin, fucoxanthin, and chlorophyll. Four major phytoplankton groups forming well-defined clusters were identified in Lake Auensee, including cryptophytes, cyanobacteria, diatoms, and green algae, by comparing these against each other in terms of their fluorescence and light-scattering signatures.

Since algae are sensitive to changing environments, a rapid separation method is particularly essential to avoid extra physiological changes in cells after sample collection. Compared to conventional methods (e.g., selection under the microscope), this combined method allows a delay of less than 12 hours between sample collection and analysis that minimizes the impact of post-collection conditions on phytoplankton. In these processes, cells were only ice-cooled in the dark and persevered without fixation with paraformaldehyde (Marie et al., 2001) or with techniques targeting them with specific dyes (Eschbach et al., 2001) because all forms of aldehyde preservation may cause artificial changes to cell structure and interference with the chemicals used in FTIR spectroscopy. These operations are beneficial to keep algal cells in a physiological state as close to their “original” state in the natural environment as possible, which will be characterized by the FTIR spectra.

Flow cytometric analysis allowed the phytoplankton community structure to be closely studied, and illustrated the detailed population development throughout the observation period. This approach indicated that the bloom patterns and seasonal succession of phytoplankton were dependent on seasonal environmental changes. For example, FCM demonstrated that the spring bloom biomass was dominated by green algae, whereas after the clear-water phase cyanobacteria succeeded green algae and dominated the community in the summer. This confirmed the determination of phytoplankton bloom dynamics by HPLC pigment fingerprinting.

According to the signature distribution of algal groups on the FCM cytogram, the green algal population was distinctly reduced and cyanobacteria became more abundant, forming larger aggregates, after the clear-water phase. This confirmed the shift in the phytoplankton species composition (Sommer et al., 1986) from being dominated by small species (i.e., cryptophytes, chlorophytes, and diatoms) to grazing-resistant summer species (i.e., filamentous/colonial cyanobacteria).

However, there are some limitations to the combined technique used, including:

- 1) Shearing forces can break large single cells/aggregates ($> 130 \mu\text{m}$ nozzle) and wall-less cells, such as cryptomonads or dinoflagellates; therefore, samples have to be size-fractionated/filtered to prevent plugging the stream flow (Wagner et al., 2012; Cellamare et al., 2009; Rutten et al., 2005). Consequently, large cells can be under-represented, so that the FTIR spectra obtained were only contributed to by the small-sized components of algal subcommunities. The lack of large-sized species may be one of the reasons for the inconsistency in seasonal variations detected between the FTIR-predicted growth potential and the Chl-*a* concentration.
- 2) Chlorophytes can only be isolated together with euglenophytes and other groups because of similar pigmentation or light-scattering features. Thus, the sorted green algal subcommunity was a mixture of these groups.
- 3) The isolation of green algae is not always successful if the population fraction is very small. For example, from late- to end-August, the green algal fraction was much smaller compared to that of the dominant fucoxanthin-containing diatoms and haptophytes in the non-phycobilin-containing cluster. Because green algae have similar cell sizes to those of diatoms, this increased the possibility of errors in separating diatoms from green algae based on the FCM cytogram. The silicate shell of diatoms may also have a serious impact on the FTIR spectra, especially by resulting in overestimation of the carbohydrate content by macromolecular quantification (Jungandreas et al., 2012).

Therefore, it was suggested that taxonomic identification based solely on light-scattering and fluorescence data may not be feasible with FCM alone (Göröcs et al., 2018). There have been some studies that used flow cytometry coupled with additional microscopic image analysis (Leroux et al., 2018) or enhanced with some form of imaging technique (Olson and Sosik, 2007; Thyssen et al., 2015). The imaging of flow cytometry allows phytoplankton to be identified from high-quality images, and has the advantages of being high-throughput, with a very

large dynamic range in terms of the object size that can be examined, from microns to several hundreds of microns, and this approach is also relatively inexpensive (Göröcs et al., 2018). Therefore, despite the fact that at present the method has some limitations, the combination of FCM and FTIR spectroscopy provides the prospects to monitor physiological changes in target phytoplankton groups/species, as well as to study or predict the processes controlling changes in phytoplankton growth and community composition in response to environmental changes.

4.4.2 FTIR spectroscopy for freshwater phytoplankton monitoring

FTIR spectroscopy has striking advantages that overcome the limitations of traditional biochemical methods due to its high sensitivity, reliability, reproducibility, and the speed of the measurement procedure. The method is fast, only requiring the measurement of a single infrared spectrum (< 2 min), allows high-throughput measurements of many algal probes, and only requires a small amount of dry matter, which is typically all that is available for small-volume cultures or phytoplankton field samples. Our study also showed that FTIR spectroscopy combined with flow cytometry can be used to study macromolecular and elemental composition in natural populations of phytoplankton, allowing the taxon-level determination of shifting carbon allocation in cells, which is difficult or impossible to quantify with conventional biochemical methods.

However, FTIR spectrometry has some limitations. Wagner et al. (2010) pointed out that the sample thickness is a crucial parameter that influences the spectral quality. In sample preparation, algal cells in the suspension drop can collapse to form a thin film of biomolecules on the microtiter plate throughout the drying procedure. If the partial particle size is equal to or larger than the wavelength of infrared radiation entering the sample, this can lead to non-linear deviations from Beer's law by light scattering. Wagner et al. (2010) suggested that deviations due to attenuation artefacts can be minimized by applying limited cell numbers, forming a sample film which yields a maximum absorption value of 0.1–0.2. If the range of cell amounts analysed is restricted to this absorption range, then Beer-Lambert's law is valid for the FTIR spectra of microalgal cells, and the influence of “package effects” on the spectra is negligible. However, for natural phytoplankton samples, the sample thickness is particularly difficult to control. Because these cells have very different biovolumes within and among

taxonomic groups, the dilution of a concentrated cell suspension can be highly variable. Therefore, the amount of probe material used has to be kept within a narrow range and handled with care.

In addition, the use of FTIR spectroscopy is restricted for diatoms, since diatoms have siliceous walls. Silica usually forms bands with high absorption signatures that overlap with the absorption bands for quantification of carbohydrates (Wagner et al., 2010). Thus, the macromolecular quantification of diatom composition could not be accurately addressed when diatoms were involved in the FACS sorting fractions of green algae during mid- and end-August. Some studies have proposed a combination of FTIR spectral analysis and measurements of the elemental composition of the algae, such as the C:N (Su et al., 2012) and Si:C ratios (Jungandreas et al., 2012), to quantify the content of carbohydrates, proteins, and lipids in diatoms without the use of the Si and carbohydrate absorbance bands. However, these methods have not been tested on natural phytoplankton groups including diatoms.

5 Reference

1. Abell, J., Oezkundakci, D., Hamilton, D. (2010). Nitrogen and phosphorus limitation of phytoplankton growth in New Zealand lakes: implications for eutrophication control. *Ecosystems* 13:966–977.
2. Agawin, N.S., Rabouille, S., Veldhuis, M.J., Servatius, L., Hol, S., van Overzee, H.M., Huisman, J. (2007). Competition and facilitation between unicellular nitrogen-fixing cyanobacteria and non—nitrogen-fixing phytoplankton species. *Limnol. Oceanogr.* 52(5):2233–2248.
3. Ahlgren, G. (1987). Temperature functions in biology and their application to algal growth constants. *Oikos*, 177–190.
4. Aizaki, M. and Otsuki, A. (1987). Characteristics of variations of C:N:P : Chl ratios of seston in eutrophic shallow Lake Kasumigaura. *Jpn. J. Limnol.* 48:99–106.
5. Allen, M.B. and Arnon, D.I. (1955). Studies on nitrogen-fixing blue-green algae. I. Growth and nitrogen fixation by *Anabaena cylindrica* Lemm. *Plant Physiol.* 30:366–372.
6. Allen, M.M. and Smith, A.J. (1969). Nitrogen chlorosis in blue-green algae. *Arch. Mikrobiol.* 69:114–120.
7. Al-Safaar, A.T., Al-Rubiaee, G.H., Salman, S.K. (2016). Effect of pH condition on the growth and lipid content of Microalgae *Chlorella vulgaris* & *Chroococcus minor*. *IJSER* 7(11):1138–1143.
8. Anthor, J.S. and Baldocchi, D.D. (2001). Terrestrial Higher Plant Respiration and Net Primary Production. In *Terrestrial Global Productivity*, Academic Press, 33–59.
9. Anderson, O.R. (1988). *Comparative Protozoology*. Springer.
10. Anthoni, J.F. (2000). Oceanography: waves. (www.seafriends.org.nz/oceano/currents.htm)
11. Apte, S.K., and Bhagwat., A.A. (1989). Salinity-Stress-Induced Proteins in Two Nitrogen-fixing *Anabaena* Strains Differentially Tolerant to Salt. *J. Bacteriol.* 171(2):909–915.
12. Bagchi, S.N., Sharma, R., Singh, H.N. (1985). Inorganic nitrogen control of growth, chlorophyll, and protein level in cyanobacterium *Nostoc muscorum*. *J. Plant Physiol.* 121:73–81.
13. Bansen, K. (1976). Rates of growth, respiration and photosynthesis of unicellular algae as related to cell size—A review. *J. Phycol.* 12:135–140.
14. Barica, J. (1990). Seasonal variability of N:P ratios in eutrophic lakes. *Hydrobiol.* 191:97–103.
15. Barker, T., Hatton, K., O'Connor, M., Connor L., Moss, B. (2008). Effects of nitrate load on submerged plant bio-mass and species richness: results of a mesocosm experiment. *Fundam. Appl. Limnol.* 173:89–100.
16. Beardall, J. and Raven, J.A. (2004). The potential effects of global climate change on microalgal photosynthesis, growth and ecology. *Phycologia* 43:26–40.
17. Beardall, J., Berman, T., Heraud, P., Kadir, M.O., Light, B.R., Patterson, G., Roberts, S., Sulzberger, B., Sahan, E., Uehlinger, U. (2001 b). A comparison of methods for

- detection of phosphate limitation in microalgae. *Aquat. Sci.* 63:107–121.
18. Beardall, J., Young, E., Roberts, S. (2001 a). Approaches for determining phytoplankton nutrient limitation. *Aquat. Sci.* 63:44–69.
 19. Béchet, Q., Shilton, A., Guieysse, B. (2013). Modeling the effects of light and temperature on algae growth: state of the art and critical assessment for productivity prediction during outdoor cultivation. *Biotechnol. Adv.* 31:1648–1663.
 20. Becker, A, Meister A., Wilhelm C. (2002). Flow cytometric discrimination of various phycobilin-containing phytoplankton groups in a hypertrophic reservoir. *Cytometry* 48:45–57.
 21. Becker, A. (2000). Dissertation: Methoden und Modelle zur Phytoplanktonanalyse am Beispiel einer Restaurierungsmaßnahme an der Bleilochtsperre, Universität Mainz.
 22. Beeton, A.M., (2002). Large freshwater lakes: Present states, trends and future. *Environ. Conserv.* 29:21–38.
 23. Bender, M., Grande, K., Johnson, K., Marra, J., Williams, P.J.L., Sieburth, J., Pilson, M, Langdon, C., Hitchcock, G., Orchardo, J., Hunt, C., Donaghay, P., Heinemann, K. (1987). A Comparison of 4 Methods for Determining Planktonic Community Production. *Limnol. Oceanogr.* 32 (5):1085–1098.
 24. Bender, M., Orchardo, J., Dickson, M.L., Barber, R., Lindley, S. (1999). *In vitro* O₂ fluxes compared with ¹⁴C production and other rate terms during the JGOFS Equatorial Pacific experiment. *Deep Sea Res.* 46:637–654.
 25. Bergström, A.K. (2010). The use of TN:TP and DIN:TP ratios as indicators for phytoplankton nutrient limitation in oligotrophic lakes affected by N deposition. *Aquat. Sci.* 72:277–281.
 26. Bergström, A.K. and Jansson, M. (2006). Atmospheric nitrogen deposition has caused nitrogen enrichment and eutrophication of lakes in the northern Hemisphere. *Global Change Biol.* 12:63–643.
 27. Bertilsson, S., Berglund, O., Karl, D.M., Chisholm, S.W. (2003). Elemental composition of marine *Prochlorococcus* and *Synechococcus*: implications for the ecological stoichiometry of the sea. *Limnol. Oceanogr.* 48:1721–1731.
 28. Bouterfas, R., Belkoura, M., Dauta, A. (2002). Light and temperature effects on the growth rate of three freshwater [2pt] algae isolated from a eutrophic lake. *Hydrobiol.* 489:207–217.
 29. Bouvy, M., Nascimento, S.M., Molica, R.J.R., Ferreira, A., Huszar, V., Azevedo, S.M.F.O. (2003). Limnological features in Tapacurá reservoir (northeast Brazil) during a severe drought. *Hydrobiol.* 493:115–130.
 30. Boyer J. N., Kelble C. R., Ortner P. B., Rudnick D. T. (2009). Phytoplankton Bloom Status: Chlorophyll A Biomass as an Indicator of Water Quality Condition in the Southern Estuaries of Florida, USA, *Ecological Indicators* 9(6):56–57.
 31. Braun, B.Z. (1974). Light absorption, emission and photosynthesis. Botanical monographs.
 32. Briand, J.F., Leboulanger, C., Humbert, J.F., Bernard, C., and Dufour, P. (2004). *Cylindrospermopsis raciborskii* (Cyanobacteria) invasion at mid-latitudes: selection, wide physiological tolerance, or global warming? *J. Phycol.* 40:231–238.

33. Brock, T. D. (1973). Lower pH limit for the existence of blue- green algae: evolutionary and ecological implications. *Science* 179(4072):480–483.
34. Burkhardt, S., Zondervan, I., Riebesell, U. (1999). Effect of CO₂ concentration on the C:N:P ratio in marine phytoplankton: a species comparison. *Limnol. Oceanogr.* 44: 683–690.
35. Burnap, R.L., Hagemann, M., Kaplan, A. (2015). Regulation of CO₂ concentrating mechanism in cyanobacteria. *Life* 5:348–371.
36. Butterwick, C., Heaney, S., Talling, J. (2005). Diversity in the influence of temperature on the growth rates of freshwater algae, and its ecological relevance. *Freshw. Biol.* 50:291–300.
37. Camarero, L. and Catalan, J. (2012). Atmospheric phosphorus deposition may cause lakes to revert from phosphorus limitation back to nitrogen limitation. *Nat. Commun.* 3:1118.
38. Caperon, J. and Meyer, J. (1972). Nitrogen-limited growth of marine phytoplankton – I. Changes in population characteristics with steady-state growth rate. *Deep-Sea Res.* 19:601–618.
39. Capone, D.G., Ferrier M. D., Carpenter E. J. (1994). Amino acid cycling in colonies of the planktonic marine cyanobacterium *Trichodesmium thiebautii*. *Appl. Environ. Microbiol.* 60:3989–3995.
40. Caraco, N.F. and Miller, R. (1998). Effects of CO₂ on competition between a cyanobacterium and eukaryotic phytoplankton. *Can. J. Fish. Aquat. Sci.* 55:54–62.
41. Cardol, P., Forti, G., Finazzi, G. (2011). Regulation of electron transport in microalgae. *BBA* 1807:912–918.
42. Carey, C.C., Ibelings, B.W., Hoffmann, E.P., Hamilton, D.P., Brookes, J.D. (2012). Eco-physiological adaptations that favour freshwater cyanobacteria in a changing climate. *Water Res.* 46:1394–1407.
43. Cellamare, M., Rolland, A., Jacquet, S. (2010). Flow cytometry sorting of freshwater phytoplankton. *J. Appl. Phycol.* 22:87–100.
44. Chakraborty, P., Acharyya, T., Raghunadh Babu, P.V., Bandhyopadhyay, D. (2011). Impact of salinity and pH on phytoplankton community in a tropical freshwater system: an investigation with pigment analysis by HPLC. *J. Environ. Monit.* 13(3):614–620.
45. Chapman, D. (1996). *Water Quality Assessments: A guide to the use of biota, sediments and water in environmental monitoring*. Second edition, E&FN Spon, London, UK.
46. Chellappa, N.T., Câmara, F.R.A., Rocha, O. (2009). Phytoplankton community: indicator of water quality in the Armando Ribeiro Gonçalves Reservoir and Pataxó Channel, Rio Grande do Norte, Brazil. *Braz. J. Biol.* 69(2):241–251.
47. Chen C.Y. and Durbin E.G. (1994). Effects of pH on the growth and carbon uptake of marine phytoplankton. *Mar. Ecol. Prog. Ser.* 109: 83–94.
48. Chen, X.F., Yang, L.Y., Xiao, L., Miao, A.J., Xi. B.D. (2012). Nitrogen removal by denitrification during cyanobacterial bloom in Lake Taihu. *J. Freshw. Ecol.* 27:243–258.

49. Cho, S.H., Ji, S.C., Hur, S.B., Bae, J., Park, I.S., Song, Y.C. (2007). Optimum temperature and salinity conditions for growth of green algae *Chlorella ellipsoidea* and *Nannochloris oculata*. *Fish. Sci.* 73:1050–1056.
50. Choi, K.J., Nakhost, Z., Bárzana, E., Karel, M. (1987). Lipid content and fatty acid composition of green algae *Scenedesmus obliquus* grown in a constant cell density apparatus. *Food Biotechnol.* 1(1):117–128.
51. Cloern, J.E. (2001). Our evolving conceptual model of the coastal eutrophication 350 problem. *Mar. Ecol. Prog. Ser.* 210:223–253.
52. Coates, J. (2000). Interpretation of infrared spectra, a practical approach. *Enc. Anal. Chem.* 1–23.
53. Coloso, J.J., Cole, J.J., Pace, M.L. (2011). Short-term variation in thermal stratification complicates estimation of lake metabolism. *Aquat. Sci.* 73:305–315.
54. Comín, F.A. and Valiela, I. (1993). On the controls of phytoplankton abundance and production in coastal lagoons. *J. Coast. Res.* 9(4):895–906.
55. Converti, A., Casazza, A.A., Ortiz, E.Y., Perego, P., Del Borghi, M. (2009). Effect of temperature and nitrogen concentration on the growth and lipid content of *Nannochloropsis oculata* and *Chlorella vulgaris* for biodiesel production. *Chem. Eng. Process.* 48(6):1146–1151.
56. Cook, J.R. (1963) Adaptations in growth and division in *Euglena* effected by energy supply. *J. Protozool.* 10:436–444.
57. Cullen, J.J. (1982). The deep chlorophyll maximum: comparing vertical profiles of chlorophyll a. *Can. J. Fish. Aquat. Sci.* 39(5):791–803.
58. da Silva, T.L., Roseiro, J.C., Reis, A. (2012). Applications and perspectives of multi-parameter flow cytometry to microbial biofuels production processes. *Trends Biotechnol.* 30(4):225–232.
59. Dalu, T., Froneman, P.W., Richoux, N.B. (2014). Phytoplankton Community Diversity along a River-estuary Continuum. *Trans. R. Soc. S. Afr.* 69 (2):107–116.
60. Davidson, I.R. (1991). Environmental effects on algal photosynthesis: temperature. *J. Phycol.* 27:2–8.
61. Dean, A.P. and Sigeo, D.C. (2006). Molecular heterogeneity in *Aphanizomenon flos-aquae* and *Anabaena flos-aquae* (Cyanophyta): a synchrotron-based Fourier-transform infrared study of lake micro-populations. *Eur. J. Phycol.* 41:201–12.
62. Dean, A.P., Estrada, B., Nicholson, J.M., Sigeo, D.C. (2008 a). Molecular response of *Anabaena flos-aquae* to differing concentrations of phosphorus: A combined Fourier transform infrared and X-ray microanalytical study. *Phycol. Res.* 56:193–201.
63. Dean, A.P., Nicholson, J.M., Sigeo, D.C. (2008 b). Impact of phosphorus quota and growth phase on carbon allocation in *Chlamydomonas reinhardtii*: an FTIR microspectroscopy study. *Eur. J. Phycol.* 43:345–354.
64. Dean, A.P., Nicholson, J.M., Sigeo, D.C. (2012). Changing patterns of carbon allocation in lake phytoplankton: an FTIR analysis. *Hydrobiol.* 684:109–127.
65. Dean, A.P., Sigeo, D.C., Estrada, B., Pittman, J.K. (2010). Using FTIR spectroscopy for rapid determination of lipid accumulation in response to nitrogen limitation in freshwater microalgae. *Bioresour. Technol.* 101:4499–4507.

66. Demir N. (2007). Changes in the phytoplankton community of a coastal, hyposaline lake in western Anatolia, Turkey. *Limnol.* 8:337–342.
67. De-Montigny, C. and Prairie, Y. (1993). The relative importance of biological and chemical processes in the release of phosphorus from a highly organic sediment. *Hydrobiol.* 253:141–150.
68. Deneke, R. and Nixdorf, B. (1999). On the occurrence of clear-water phases in relation to shallowness and trophic state: a comparative study. *Hydrobiol.* 408–409:251–262.
69. Diaz, R.J. and Rosenberg, R. (2008). Spreading dead zones and consequences for marine ecosystems. *Science* 321 (5891):926–929.
70. Dillon, P.J. and Rigler, F.H. (1974). The phosphorus-chlorophyll relationship in lakes. *Limnol. Oceanogr.* 19:767–773.
71. DIN 38412-L16. (1985). German standard methods for the examination of water, waste water and sludge; test methods using water organisms (group L); determination of chlorophyll a in surface water (L 16). <https://dx.doi.org/10.31030/1210055>
72. Downing, J.A., Watson, S.B., McCauley, E. (2001). Predicting cyanobacteria dominance in lakes. *Can. J. Fish. Aquat. Sci.* 58:1905–1908.
73. Droop, M.R. (1973). Nutrient limitation in osmotrophic protista, *Am. Zool.*, 13:209–214.
74. Dugdale, R.C. and Goering J.J. (1967). Uptake of new and regenerated forms of nitrogen in primary productivity. *Limnol. Oceanogr.* 12:196–206.
75. Dunker, S., Nadrowski, K., Jakob, T., Kasprzak, P., Becker, A., Langner, U., Kunath, C., Harpole, S., Wilhelm, C. (2016). Assessing in situ dominance pattern of phytoplankton classes by dominance analysis as a proxy for realized niches. *Harmful Algae* 58:74–84.
76. Duygu, D.Y., Udoh, A.U., Ozer, T.B., Akbulut, A., Erkaya, I.A., Yildiz, K., Guler, D. (2012). Fourier transform infrared (FTIR) spectroscopy for identification of *Chlorella vulgaris* Beijerinck 1890 and *Scenedesmus obliquus* (Turpin) Kützing 1833. *Afr. J. Biotechnol.* 11:3817–3824.
77. Edwards, K.F., Thomas, M.K., Klausmeier, C.A., Litchman, E. (2016). Phytoplankton growth and the interaction of light and temperature: A synthesis at the species and community level. *Limnol. Oceanogr.* 61:1232–1244.
78. Edwards, K.F., Litchman, E., Klausmeier, C.A. (2013). Functional traits explain phytoplankton responses to environmental gradients across lakes of the United States. *Ecology* 94:1626–1635.
79. Elliott, J.A., Irish, A.E., Reynolds, C.S. (2001). The effects of vertical mixing on a phytoplankton community: a modelling approach to the intermediate disturbance hypothesis. *Fresh Water Biol.* 46:1291–1297.
80. Elmorjani, K. and Herdman, M. (1987). Metabolic control of phycocyanin degradation in the cyanobacterium *Synechocystis* PCC 6803: a glucose effect. *J. Gen. Microbiol.* 133:1685–1694.
81. Elser, J.J., Bracken, M.E.S., Cleland, E.E., Gruner, D.S., Harpole, W.S., Hillebrand, H., Ngai, J.T., Seabloom, E.W., Shurin, J.B., Smith, J.E. (2007). Global Analysis of Nitrogen and Phosphorus Limitation of Primary Producers in Freshwater, Marine and

- Terrestrial Ecosystems. *Ecol. Lett.* 10:1135–1142.
82. Elser, J.J., Marzolf, E.R., Goldman, C.R. (1990). Phosphorus and nitrogen limitation of phytoplankton growth in the freshwaters of North America: a review and critique of experimental enrichments. *Can. J. Fish. Aquat. Sci.* 47:1468–1477.
83. Ensminger I., Busch F., Huner N.P.A. (2006). Photostasis and cold acclimation: sensing low temperature through photosynthesis. *Physiol. Plant.* 126:28–44.
84. Escalera, L., Reguera, B., Moita, T., Pazos, Y., Cerejo, M., Cabanas, J.M., Ruiz-Villarreal, M. (2010). Bloom dynamics of *Dinophysis acuta* in an upwelling system: in situ growth versus transport. *Harmful Algae* 9:312–322.
85. Eschbach, E., Reckermann, M., John, U., Medlin, L. (2001). A simple and highly efficient fixation method for *Chrysochromulina polylepis* (Prymnesiophytes) for analytical flow cytometry. *Cytometry* 44:126–32.
86. European Environmental Agency. (2001). Eutrophication in Europe's Coastal Waters. Topic Report No. 7. Copenhagen, 86 p.
87. Falkowski, P.G. (2000). Rationalizing elemental ratios in unicellular algae. *J. Phycol.* 36:3–6.
88. Falkowski, P.G. and Raven J.A. (1997). Aquatic Photosynthesis. Blackwell Science, Malden, MA.
89. Falkowski, P.G., Wyman, K., Ley, A.C., Mauzerall, D.C. (1986). Relationship of steady state photosynthesis to fluorescence in eukaryotic algae. *Biochim. Biophys. Acta.* 849:183–192.
90. Fanesi, A., Wagner, H., Becker, A., Wilhelm, C. (2016). Temperature affects the partitioning of absorbed light energy in freshwater phytoplankton. *Freshw. Biol.* 61:1365–1378.
91. Fanesi, A., Wagner, H., Birarda, G., Vaccari, L., Wilhelm, C. (2019). Quantitative macromolecular patterns in phytoplankton communities resolved at the taxonomical level by single-cell Synchrotron FTIR-spectroscopy. *BMC Plant Biol.* 19:142.
92. Fanesi, A., Wagner, H., Wilhelm, C. (2017). Supplementary material from phytoplankton growth rate modelling: can spectroscopic cell chemotyping be superior to physiological predictors? *Proc. R. Soc. B.* 284:20161956.
93. Fang, Y.Y., Yang, X.E., Pu, P.M., Chang, H.Q., Ding, X.F. (2004). Water eutrophication in Li-Yang Reservoir and its ecological remediation countermeasures. *Journal of Soil and Water Conservation*;18(6):183–186. (in Chinese)
94. Fietz, S. and Nicklisch, A. (2002). Acclimation of the diatom *Staphanodiscus neoastraea* and the cyanobacterium *Planktothrix agardhii* to simulated natural light fluctuations. *Photosynth. Res.* 72:95–106.
95. Finkel, Z.V., Quigg, A., Raven, J.A., Reinfelder, J.R., Scholfield, O.E., Falkowski, P.G. (2006). Irradiance and the elemental stoichiometry of marine phytoplankton. *Limnol. Oceanogr.* 51:2690–2701.
96. Flöder, S., Jaschinski, S., Wells, G., Burns, C.W. (2010). Dominance and Compensatory Growth in Phytoplankton Communities under Salinity Stress. *J. Exp. Mar. Biol. Ecol.* 395(1-2):223–231.
97. Flynn, K.J., Raven, J.A., Rees, T.A.V., Finkel, Z., Quigg, A., Beardall, J. (2010). Is the

- growth rate hypothesis applicable to microalgae? *J. Phycol.* 46:1–12.
98. Fogg, G.E. (1969). The physiology of an algal nuisance. *Proc. R. Soc. London Ser. B* 173:175–189.
99. Fogg, G.E. (1975). *Algal Cultures and Phytoplankton Ecology*, 2nd edition. University of Wisconsin Press, Madison and Milwaukee.
100. Fogg, G.E. (1980). Phytoplanktonic primary production. In *fundamentals of aquatic ecosystems*, edited by R.S.K. Barnes and K.H. Mann. Oxford, Blackwell Scientific Publications, pp. 24–45.
101. Foulds, I.J. and Carr, N.G. (1977). A proteolytic enzyme degrading phycocyanin in the cyanobacterium *Anabaena cylindrica*. *FEMS Microbiol. Lett.* 2:117–119.
102. Foy, R.H. (1980). The influence of surface to volume ratio on the growth rates of planktonic blue-green algae. *Br. phycol. J.* 15(3): 279–289.
103. Foy, R.H. and Gibson, C. (1993). The influence of irradiance, photoperiod and temperature on the growth kinetics of three planktonic diatoms. *Eur. J. Phycol.* 28:203–212.
104. Foy, R.H., Gibson, C.E., Smith, R.V. (1976). The influence of daylength, light intensity and temperature on the growth rates of planktonic blue-green algae. *Br. phycol. J.* 11: 151–163.
105. Fujimoto, N., Sudo, R., Sugiura, N., Inamori, Y. (1997). Nutrient-limited growth of *Microcystis aeruginosa* and *Phormidium tenue* and competition under various N:P supply ratios and temperatures. *Limnol. Oceanogr.* 42:250–256.
106. Gaarder, T. and Gran, H.H. (1927). Investigation of the production of plankton in the Oslo Fjord. *Rapp. P.-v. Cons. int. Explor. Mer.* 42:1-48.
107. Ganf, G.G. and Oliver, R.L. (1982). Vertical separation of light and nutrients as a factor causing replacement of green algae by blue-green algae in the plankton of a stratified lake. *J. Ecol.* 70:829–844.
108. Garcia, N.S., Bonachela, J.A., Martiny, A.C. (2016). Interactions between growth-dependent cell size, nutrient availability and cellular elemental stoichiometry of marine *Synechococcus*. *ISME J.* 10:2715–2724.
109. Geider, R.J. (1987). Light and temperature dependence of the carbon to chlorophyll a ratio in microalgae and cyanobacteria: implication for physiology and growth of phytoplankton. *New Phytol.* 106:1–34.
110. Geider, R.J. and La Roche, J. (2002). Redfield revisited: variability of C:N:P in marine microalgae and its biochemical basis. *Eur. J. Phycol.* 37:1–17.
111. Geider, R.J. and Osborne, B.A. (1989). Respiration and microalgal growth: a review of the quantitative relationship between dark respiration and growth. *New Phytol.* 112:327–94.
112. Geider, R.J., MacIntyre, H.L., Kana, T.M. (1996). A dynamic model of photoadaptation in phytoplankton. *Limnol. Oceanogr.* 41:1–15.
113. Gharib, S.M., El-Sherif, A.Z.M., Abdel-Halim, M., Radwan, A.A. (2011). Phytoplankton and environmental variables as a water quality indicator for the beaches at Matrouh, South-Eastern Mediterranean Sea, Egypt: an assessment. *Oceanol.* 53(3):819–836.

114. Gilbert, M., Domin, A., Becker, A., Wilhelm, C. (2000). Estimation of Primary Productivity by Chlorophyll a in vivo Fluorescence in Freshwater Phytoplankton. *Photosynthetica* 38: 111–126.
115. Giordano, M. and Ratti, S. (2013). The biomass quality of algae used for CO₂ sequestration is highly species-specific and may vary over time. *J. Appl. Phycol.* 25:1431–1434.
116. Giordano, M., Beardall, J., Raven, J.A. (2005). CO₂ concentrating mechanisms in algae: mechanisms, environmental modulation, and evolution. *Annu. Rev. Plant. Biol.* 56:99–131.
117. Giordano, M., Kansiz, M., Heraud, P., Beardall, J., Wood, B., McNaughton, D. (2001). Fourier transform infrared spectroscopy as a novel tool to investigate changes in intracellular macromolecular pools in the marine microalga *Chaetoceros muellerii* (Bacillariophyceae). *J. Phycol.* 37:271–279.
118. Glibert, P.M., Allen, J.I., Bouwman, A., Brown, C.W., Flynn, K.J., Lewitus, A.J., Madden, C.J. (2010). Modeling of HABs and eutrophication: status, advances, challenges. *J. Mar. Systems.* 83:262–275.
119. Gokce, D. and Ozhan, D. (2011). Limno-ecological properties of deep reservoir, Karakaya HEPP, Turkey. *Gazi University J. Sci.* 24(4):663–669.
120. Goldman, C.R. and Byron, E.R. (1986). A technical summary of changing water quality in Lake Tahoe: The first five years of the Lake Tahoe Interagency Monitoring Program (Tahoe Research Group, Institute of Ecology, University of California).
121. Goldman, J.C. and Shapiro, M.R. (1973). Carbon dioxide and pH: effect on species succession of algae. *Limnol. Oceanogr.* 182:306–307.
122. Goldman, J.C., McCarthy, J.J., Peavey, D.G. (1979). Growth rate influence on the chemical composition of phytoplankton in oceanic waters. *Nature* 279:210–215.
123. Gophen, M., Smith, V.H., Nishri, A., Threlkeld, S.T. (1999). Nitrogen deficiency, phosphorus sufficiency, and the invasion of Lake Kinneret, Israel, by the N₂-fixing cyanobacterium *Aphanizomenon ovalisporum*. *Aquat. Sci.* 61:293–306.
124. Gordillo, F., Goutx, M., Figueroa, F., Niell, F. (1998). Effects of light intensity, CO₂ and nitrogen supply on lipid class composition of *Dunaliella viridis*. *J. Appl. Phycol.* 10:135–144.
125. Göröcs Z, Tamamitsu, M., Bianco, V., Wolf, P., Roy, S., Shindo, K., Yanny, K., Wu, Y., Koydemir, H.C., Rivenson, Y., Ozcan, A. (2018). A deep learning-enabled portable imaging flow cytometer for cost-effective, high-throughput, and label-free analysis of natural water samples. *Light Sci. Appl.* 7(1):66.
126. Gotham I.J. and Rhee F.Y. (1981). Comparative kinetic studies of nitrate-limited growth and nitrate uptake in phytoplankton in continuous culture. *J. Phycol.* 17:309–314.
127. Guildford, S.J. and Hecky, R.E. (2000). Total nitrogen, total phosphorus, and nutrient limitation in lakes and oceans: Is there a common relationship? *Limnol. Oceanogr.* 45: 1213–1223.
128. Gunkel, G. (1994). Bioindikatoren in aquatischen Ökosystemen - Bioindikatoren in limnischen und küstennahen Ökosystemen - Grundlagen, Verfahren und Methoden.

- Gustav Fischer Verlag Jena 540 S.
129. Hall, S.R., Smith, V.H., Lytle, D.A., Leibold, M.A. (2005). Constraints on primary producer N:P stoichiometry along N:P supply ratio gradients. *Ecology* 86:1894–1904.
 130. Halsey, K.H. and Jones, B.M. (2015). Phytoplankton strategies for photosynthetic energy allocation. *Annu. Rev. Mar. Sci.* 7:265–297.
 131. Hansen, P.J. (2002). Effect of high pH on the growth and survival of marine phytoplankton: implications for species succession. *Aquat. Microb. Ecol.* 28:279–288.
 132. Hao, J., Chen, Y., Wang, F., LIN., P. (2012). Seasonal thermocline in the China Seas and northwestern Pacific Ocean. *J. Geophys. Res.* 117:C02022
 133. Harris, G.P. (1986). Preamble. In *Phytoplankton Ecology*. Springer Netherlands, pp. 1–15.
 134. Haug, A., Mykkestad, S., Sakshaug, E. (1973). Studies on the phytoplankton ecology of the Trondheimsfjord. I. The chemical composition of phytoplankton populations. *J. Exp. Mar. Biol. Ecol.* 11:15–26.
 135. Havens, K.E., James, R.T., East, T.L., Smith, V.H. (2003). N:P ratios, light limitation, and cyanobacterial dominance in a subtropical lake impacted by non-point source nutrient pollution. *Environ. Pollut.* 122(3):379–390.
 136. Healey, F.P. (1975). Physiological indicators of nutrient deficiency in algae. *Fish. Mar. Serv. Res. Div. Tech. Rep.* 585:30.
 137. Hecky, R.E. and Kilham, P. (1988). Nutrient limitation of phytoplankton in freshwater and marine environments: A review of recent evidence on the effects of enrichment. *Limnol. Oceanogr.* 33:796–822.
 138. Heraud, P., Wood, B.R., Tobin, M.J., Beardall, J., McNaughton, D. (2005). Mapping of nutrient-induced biochemical changes in living algal cells using synchrotron infrared microspectroscopy. *FEMS Microbiol. Lett.* 249:219–225.
 139. Herczeg, A.L. and Fairbanks, R.G. (1987). Anomalous carbon isotope fractionation between atmospheric CO₂ and dissolved inorganic carbon induced by intense photosynthesis. *Geochim. Cosmochim. Acta.*, 51:895–899.
 140. Hillebrand, H., Steinert, G., Boersma, M., Malzahn, A., Meunier, C. L., Plum, C. Ptacnik, R. (2013). Goldman revisited: Faster growing phytoplankton has lower N:P and lower stoichiometric flexibility. *Limnol. Oceanogr.* 58:2076–2088.
 141. Hirschmugl, C.J., Bayarri, Z.E., Bunta, M., Holt, J.B., Giordano, M. (2006). Analysis of the nutritional status of algae by Fourier transform infrared chemical imaging. *Infrared Physics Technol.* 49:57–63.
 142. Hofstraat, J., Van Zeijl, W., De Vreeze, M., Peeters, J., Peperzak, L., Colijn, F., Rademaker, T. (1994). Phytoplankton monitoring by flow cytometry. *J. Plankton Res.* 16:1197–1224.
 143. Horne, A.J. and Goldman, C.R. (1994). *Limnology*. Mc Graw-Hill, Inc., New York, NY.
 144. Hou, D., He, J., Lu, C., Sun, Y., Zhang, F., Otgonbayar, K. (2013). Effects of Environmental Factors on Nutrients Release at Sediment-Water Interface and Assessment of Trophic Status for a Typical Shallow Lake, Northwest China. *Sci. World J.* 2013(3):716342.

145. Hsiu-Ping Li, Gwo-Ching Gong, Tung-Ming Hsiung. (2002). Phytoplankton pigment analysis by HPLC and its application in algal community investigations: Bot. Bull. Acad. Sin. 43:283–290.
146. Huisman, J. and Hulot, F.D. (2005). Population Dynamics of Harmful Cyanobacteria. Factors affecting species composition. In Harmful Cyanobacteria, Aquatic Ecology Series. eds. Huisman, J, Matthijs, HCP, and Visser, PM, Dordrecht, The Netherlands: Springer. 143–176.
147. Huisman, J., Jonker, R.R., Zonneveld, C., Weissing, F.J. (1999). Competition for light between phytoplankton species: experimental tests of mechanistic theory. Ecology 80:211–222.
148. Hutchinson, G.E. (1957). A Treatise on Limnology, vol. 1, New York, Wiley.
149. Hyenstrand, P., Blomqvist, P., Pettersson, A. (1998). Factors determining cyanobacterial success in aquatic systems: a literature review. Archiv für Hydrobiologie Special Issues. Advan. Limnol. 51:41–62.
150. Ignatiades, L. and Smayda, T.J. (1970). Autecological studies on the marine diatom *Rhizosolenia fragilissima* Bergon. I. The influence of light, temperature, and salinity. J. Phycol. 6:332–339.
151. IPCC (2007). Climate change 2007: synthesis report. IPCC, Geneva
152. Jakob, T., Wagner, H., Stehfest, K., Wilhelm, C. (2007). A complete energy balance from photons to new biomass reveals a light- and nutrient-dependent variability in the metabolic costs of carbon assimilation. J. Exp. Bot. 58:2101–2112.
153. Jebsen, C., Norici, A., Wagner, H., Palmucci, M., Giordano, M., Wilhelm, C. (2012). FTIR spectra of algal species can be used as physiological fingerprints to assess their actual growth potential. Physiol. Plant. 146(4):427–438.
154. Jeffrey, S.W., Mantoura, R.F.C., Wright, S.W. (Ed.) (1997). Phytoplankton pigments in oceanography: guidelines to modern methods. Monographs on Oceanographic Methodology, 10. UNESCO Publishing: Paris, France.
155. Jeppesen, E., Jensen J.P., Søndergaard M., Lauridsen T.L., Pedersen L.J., Jensen L. (1997). Top-down control in freshwater lakes: the role of nutrient state, submerged macrophytes and water depth. Hydrobiol. 342–343:151–164.
156. Jeppesen, E., Kronvang, B., Meerhoff, M., Søndergaard, M., Hansen, K.M., Andersen, H.E., Lauridsen, T.L., Liboriussen, L., Beklioglu, M., O' zen, A., Olesen, J.E. (2007). Climate change effects on runoff, catchment phosphorus loading and lake ecological state, and potential adaptations. J. Environ. Qual. 38:1930–1941.
157. Jöhnk, K.D., Huisman, J., Sharples, J., Sommeijer, B., Visser, P.M., Stroom, J.M. (2008). Summer heatwaves promote blooms of harmful cyanobacteria. Glob. Change Biol. 14:495–512.
158. Jungandreas, A., Wagner, H., Wilhelm, C. (2012). Simultaneous measurement of the silicon content and physiological parameters by FTIR spectroscopy in diatoms with siliceous cell walls. Plant Cell Physiol. 53:2153–2162.
159. Kalacheva, G.S., Zhila, N.O., Volova, T.G. (2002). Lipid and hydrocarbon compositions of a collection strain and a wild sample of the green microalga *Botryococcus*. Aquat. Ecol. 36:317–330.

160. Kana, T.M. (1992). Relationship between photosynthetic oxygen cycling and carbon assimilation in *Synechococcus* WH7803 (Cyanophyta). *J. Phycol.* 28:304–308.
161. Kansiz, M., Heraud, P., Wood, B., Burden, F., Beardall, J., McNaughton, D. (1999). Fourier transform infrared microspectroscopy and chemometrics as a tool for the discrimination of cyanobacterial strains. *Phytochemistry* 52:407–417.
162. Karacaoğlu D, Dalkiran N, Dere Ş. (2006). Factors affecting the phytoplankton diversity and richness in a shallow eutrophic lake in Turkey. *J. Freshw. Ecol.* 21(4):575–581.
163. Karentz, D. and Smayda, T.J. (1984). Temperature and seasonal occurrence patterns of 30 dominant phytoplankton species in Narragansett Bay over a 22-year period (1959–1980). *Mar. Ecol. Prog. Ser.* 18:277–293.
164. Kaushik, B.D. (1994). Algalization of rice in salt-affected soils. *Ann. Agri. Res.* 14:105–106.
165. Kenesi, G., Shafik, H.M., Kovacs, A.W., Herodek, S., Presling, M. (2009). Effect of nitrogen forms on growth, cell composition and N₂ fixation of *Cylindrospermopsis raciborskii* in phosphorus-limited chemostat cultures. *Hydrobiol.* 623:191–202.
166. Kenne, G. and Merwe D. (2013). Classification of Toxic Cyanobacterial Blooms by Fourier-Transform Infrared Technology (FTIR). *Adv. Microbiol.* 3:1–8.
167. Kim, D.I., Matsuyama, Y., Nagasoe S., Yamaguchi, M., Yoon, Y.H., Oshima, Y, Imada, N., Honjo, T. (2004). Effects of temperature, salinity and irradiance on the growth of the harmful red tide dinoflagellate *Cochlodinium polykrikoides* Margalef (Dinophyceae). *J. Plankton Res.* 26:61–66.
168. Klausmeier, C.A. and Litchman, E. (2004). Phytoplankton growth and stoichiometry under multiple nutrient limitation. *Limnol. Oceanogr.* 49:1463–1470.
169. Klausmeier, C.A., Litchman, E., Daufresne, T., Levin, S.A. (2004). Optimal nitrogen-to-phosphorus stoichiometry of phytoplankton. *Nature* 429:171–174.
170. Kohl, J.G. and Nicklisch, A. (1988). *Ökophysiologie der Algen*. Akademie Verlag. Stuttgart.
171. Kolber, Z. and Falkowski, P.G. (1993). Use of active fluorescence to estimate phytoplankton photosynthesis in situ. *Limnol. Oceanogr.* 38:1646–1665.
172. Konopka, A. and Brock, T.D. (1978). Effect of temperature on blue-green algae (cyanobacteria) in Lake Mendota. *Appl. Environ. Microbiol.* 36:572–576.
173. Kozerski, H.P. and Kleeberg, A. (1998). The sediments and benthic pelagic exchange in the shallow lake Muggelsee (Berlin, Germany). *Int. Rev. Hydrobiol.* 83:77–112.
174. Kromkamp, J. and Walsby, A.E. (1990). A computer model of buoyancy and vertical migration in cyanobacteria. *J. Plankton Res.* 12:161–183.
175. Kroon, B.M.A. and Thoms, S. (2006). From electron to biomass: A mechanistic model to describe phytoplankton photosynthesis and steady-state growth rates. *J. Phycol.* 42:593–609.
176. Kuhl, A. and Lorenzen, H. (1964). *Methods in cell physiology* Academic Press New York-London, D. M. Prescott (ed.).
177. Kwandrans J, Eloranta P, Kawecka B, Wojtan K. (1998). Use of benthic diatom communities to evaluate water quality in rivers of southern Poland. *J. Appl. Phycol.*

- 10:193–201.
178. Lampert, W., Fleckner, W., Rai, H., Taylor, B.E. (1986). Phytoplankton control by grazing zooplankton: a study on the spring clear-water phase. *Limnol. Oceanogr.* 31:478–490
179. Langdon, C. (1988). On the causes of interspecific differences in the growth-irradiance relationship for phytoplankton. II. A general review. *J. Plankton Res.* 10:1291–1312.
180. Langner, U., Jakob, T., Toepel, J., Wilhelm, C. (2004). Whole lake primary production assessment by bio-optical modelling. *Stud. Quat.* 21:45–49.
181. Larson, C.A. and Belovsky, G.E. (2013). Salinity and Nutrients Influence Species Richness and Evenness of Phytoplankton Communities in Microcosm Experiments from Great Salt Lake, Utah, USA. *J. Plankton Res.* 35(5):1154–1166.
182. Laurens, L.M. and Wolfrum, E.J. (2011). Feasibility of spectroscopic characterization of algal lipids: chemometric correlation of NIR and FTIR spectra with exogenous lipids in algal biomass. *BioEnergy Res.* 4:22–35.
183. Lavaud J., Strzepek R.F., Kroth P.G. (2007). Photoprotection capacities differ among plankton diatoms: possible consequence on their spatial distribution related to fluctuations in the underwater light climate. *Limnol. Oceanogr.* 52:1188–1194.
184. Laws, E.A. and Bannister, T.T. (1980). Nutrient- and light-limited growth of *Thalassiosira fluviatilis* in continuous culture, with implications for phytoplankton growth in the ocean. *Limnol. Oceanogr.* 25:457–473.
185. Lee, G.F. and Jones-Lee, A. (1998). Determination of nutrient limiting maximum algal biomass in waterbodies. G. Fred Lee & Associates, El macero, CA
186. Lehtiniemi, M., Engström-Öst, J., Viitasalo, M. (2005). Turbidity decreases anti-predator behavior in pike larvae, *Esox Lucius*. *Environ. Biol. Fish.* 73:1–8.
187. Leroux R., Gregori G., Leblanc K., Carlotti F., Thyssen M., Dugenne M., Pujo-Pay M., Conan P., Jouandet M.P., Bhairy N., Berline L. (2018) Combining laser diffraction, flow cytometry and optical microscopy to characterize a nanophytoplankton bloom in the Northwestern Mediterranean. Special issue of MERMEX project: Recent advances in the oceanography of the Mediterranean Sea. *Prog. Oceanogr.* 163:248–259.
188. Lewis, W.M.Jr. (1978). Dynamics and succession of the phytoplankton in a tropical lake: Lake Lanao, Philippines. *J. Ecol.* 66:849–880.
189. Li, J.X. and Liao, W.G., (2002). Discussion on the synthetic adjustive guidelines for the prevention and cure of eutrophication. *Protection of Water Resource* 2(5):4–5.
190. Linkens, G.F. (1972) Nutrients and eutrophication. *Am. Soc. Limnol. Oceanogr. Spec. Symp.* 1
191. Litchman, E. (2000). Growth rates of phytoplankton under fluctuating light. *Freshw. Biol.* 44:223–235.
192. Litchman, E. and Klausmeier, C.A. (2001). Competition of phytoplankton under fluctuating light. *Am. Nat.* 157:170–187.
193. Litchman, E., de Tezanos Pinto, P., Klausmeier, C.A., Thomas, M.K., Yoshiyama, K. (2010). Linking traits to species diversity and community structure in phytoplankton. *Hydrobiol.* 653:15–28.

194. Liu, H.B., Laws, E.A., Villareal, T.A., Buskey, E.J. (2001). Nutrient-limited growth of *Aureoumbra lagunensis* (Pelagophyceae), with implications for its capability to outgrow other phytoplankton species in phosphate-limited environments. *J. Phycol.* 37:500–508.
195. Locke, A. and Sprules, W.G. (2000) Effects of acidic pH and phytoplankton on survival and condition of *Bosmina longirostris* and *Daphnia pulex*. *Hydrobiol.* 437:187–196.
196. Lohrenz, S.E. and Taylor, C.D. (1987) Inorganic ^{14}C as a probe of growth rate-dependent variations in intracellular free amino-acid and protein composition of NH_4^+ -limited continuous cultures of *Nannochloris atomus* Butcher, *J. Exp. Mar. Biol. Ecol.* 106:31–55.
197. Lopez, J., Garcia, N.S., Talmy, D., Martiny, A.C. (2016). Diel variability in the elemental composition of the marine cyanobacterium *Synechococcus*. *J. Plankton Res.* 38:1052–1061.
198. López-Flores, R., Boix, D., Badosa, A., Brucet, S., Quintana, X. (2006). Pigment composition and size distribution of phytoplankton in a confined Mediterranean salt marsh ecosystem. *Mar. Biol.* 149:1313–1324.
199. López-Flores, R., Quintana, X.D., Romaní, A.M., Bañeras, L., Ruiz-Rueda, O., Compte, J., Green, A.J., Egozcue, J.J. (2014). A compositional analysis approach to phytoplankton composition in coastal Mediterranean wetlands: influence of salinity and nutrient availability. *Estuar. Coast Shelf Sci.* 136:72–81.
200. Low-Décarie, E., Bell, G., Fussmann, G.F. (2015). CO_2 alters community composition and response to nutrient enrichment of freshwater phytoplankton. *Oecologia* 177:875–883.
201. Low-Décarie, E., Fussmann, G.F., Bell, G. (2011). The effect of elevated CO_2 on growth and competition in experimental phytoplankton communities. *Glob. Change Biol.* 17:2525–2535.
202. Lynn, S.G., Kilham, S.S., Kreeger, D.A., Interlandi, S.J. (2000). Effect of nutrient availability on the biochemical and elemental stoichiometry in the freshwater diatom *Stephanodiscus minutulus* (Bacillariophyceae). *J. Phycol.* 36:510–522.
203. MacIntyre, H.L., Kana, T.M., Geider, R.J. (2000). The effect of water motion on short-term rates of photosynthesis by marine phytoplankton. *Trends Plant Sci.* 5:12–17.
204. Mainstone, C.P. and Parr, W. (2002). Phosphorus in rivers-ecology and management. *Sci. Total Environ.* 282–283:25–47.
205. Marie, D., Simon, N., Guillou, L. Partensky, F., Vaulot, D. (2001). DNA/RNA analysis of phytoplankton by flow cytometry. *Curr. Protoc. Cytom.* 11:Unit 11.12.
206. Marra J. (1978). Effect of short-term variations in intensity on photosynthesis of a marine phytoplankton: a laboratory simulation study. *Mar. Biol.* 46:191–202.
207. Marra, J. (2002). Approaches to the measurement of plankton production. In: Williams, P.J.I.B., Thomas, D.N. and Reynolds, C.S. (eds). *Phytoplankton productivity. Carbon assimilation in marine and freshwater ecosystems*. Oxford: Blackwell Science, pp. 78–108.

208. Matthews, R., Hilles, M., Pelletier, G. (2002). Determining trophic state in Lake Whatcom, Washington, a soft water lake exhibiting seasonal nitrogen limitation. *Hydrobiol.* 468:107–121.
209. Mayers, J.J., Flynn, K.J., Shields, R.J. (2013). Rapid determination of bulk microalgal biochemical composition by Fourier-Transform Infrared spectroscopy. *Bioresour. Technol.* 148:215–220.
210. McGinn, P.J., Dickinson, K.E., Bhatti, S., Frigon, J.C., Guiot, S.R., O’Leary, S.J. (2011). Integration of microalgae cultivation with industrial waste remediation for biofuel and bioenergy production: opportunities and limitations. *Photosyn Res.* 109:231–247.
211. Mevik, B. and Wehrens, R. (2007). The pls package: principal component and partial least squares regression in R. *J. Stat. Softw.* 18:1–24
212. Miglio, R., Palmery, S., Salvalaggio, M., Carnelli, L., Capuano, F., Borrelli, R. (2013). Microalgae triacylglycerols content by FT-IR spectroscopy. *J. Appl. Phycol.* 25:1621–1631.
213. Millie, D.F., Fahnenstiel, G.L., Carrick, H.J., Lohrenz, S.E, Schofield, O.M.E. (2002). Phytoplankton pigments in coastal Lake Michigan: Distributions during the spring isothermal period and relation with episodic sediment resuspension. *J. Phycol.* 38:639–648.
214. Minas, H.J. and Codispoti, L.A. (1993). Estimation of primary production by observation of changes in the mesoscale nitrate field. *ICES Mar. Sci. Symp.* 197:215–235.
215. Mitra, A., Castellani, C., Gentleman, W., Jónasdóttir, S.H., Flynn, K.J., Bode, A., Halsband, C., Kuhn, P., Licandro, P., Agersted M.D., Calbet, A., Lindeque, P.K., Koppelman, R., Møller, E.F., Gislason, A., Nielsen, T.G., St-John, M.A. (2014). Bridging the gap between marine biogeochemical and fisheries sciences; configuring the zooplankton link. *Prog. Oceanogr.*, 129:176–199.
216. Molot, L.A. (2017). The effectiveness of cyanobacteria nitrogen fixation: Review of bench top and pilot scale nitrogen removal studies and implications for nitrogen removal programs. *Environ. Rev.* 25(3):292–295.
217. Montagnes, D.J., Morgan, G., Bissinger, J.E., Atkinson, D., Weisse, T. (2008). Short-term temperature change may impact freshwater carbon flux: a microbial perspective. *Glob. Change Biol.* 14:2823–2838.
218. Montecchiario, F. and Giordano, M. (2010). Compositional homeostasis of the dinoflagellate *Protoceratium reticulatum* grown at three different pCO₂. *J. Plant Physiol.* 167:110–113.
219. Montecchiario, F., Hirschmugl, C.J., Raven, J.A., Giordano, M. (2006). Homeostasis of cell composition during prolonged darkness. *Plant Cell Environ.* 29:2198–2204.
220. Moore, P.A. Jr. and Reddy, K.R. (1994). Role of Eh and pH on phosphorus geochemistry in sediments of Lake Okeechobee, Florida. *J. Environ. Qual.* 23: 955–964.
221. Morris, D.P. and Lewis, W.M. (1988). Phytoplankton nutrient limitation in Colorado mountain lakes. *Freshw. Biol.* 20:315–327.
222. Moss, B., Jeppesen, E., Søndergaard, M., Lauridsen, T.L., Liu, Z. (2013). Nitrogen,

- macrophytes, shallow lakes and nutrient limitation: resolution of a current controversy? *Hydrobiol.* 710:3–21.
223. Moustaka-Gouni, M., Kormas, K.A., Polykarpou, P., Gkelis, S., Bobori, D.C., Vardaka, E. (2010). Polyphasic evaluation of *Aphanizomenon issatschenkoi* and *Raphidiopsis mediterranea* in a Mediterranean lake. *J. Plankton Res.* 32:927–936.
224. Müller, P., Li, X.P., Niyogi, K.K. (2001). Non-photochemical quenching. A response to excess light energy. *Plant Physiol.* 125:1558–1566.
225. Müller, S. and Nebe-von-Caron, G. (2010). Functional single-cell analyses—flow cytometry and cell sorting of microbial populations and communities. *FEMS Microbiol. Rev.* 34:554–587.
226. Murphy, K. J., Kennedy, M. P., McCarthy, V., Ó'Hare, M.T., Irvine K., Adams, C. (2002). A review of ecology based classification systems for standing freshwaters. SNIFFER Project Number: W (99)65, Environment Agency R&D Technical Report: E1-091/TR.
227. Mur, L., Gons, H.J., Van Liere, L. (1978). Competition of the green alga *Scenedesmus* and the blue-green *Oscillatoria*. *Mitteilungen der Internationale Vereinigung für Theoretisch und Angewandte Limnologie.* 21:473–479.
228. Nielsen, D.L., Brock, M.A., Rees, G.N., Baldwin, D.S. (2003). Effects of Increasing Salinity on Freshwater Ecosystems in Australia. *Aust. J. Bot.* 51:655–665.
229. Nikolai, S.J. and Dzialowski, A.R. (2014). Effects of internal phosphorus loading on nutrient limitation in a eutrophic reservoir. *Limnol.* 49:33–41.
230. Nürnberg, G.K. (1987). The comparison of internal phosphorus loads in lake with hypolimnetic anoxia: laboratory incubation in situ hypolimnetic phosphorus accumulation. *Limnol. Oceanogr.* 32 (5): 1160–1164.
231. O'Donnell, S., Demshemino, I., Yahaya, M., Nwadike, I., Okoro, L. (2013). A review on the spectroscopic analyses of biodiesel. *Eur. Int. J. Sci. Technol.* 2:137–146.
232. Ojala, A. (1993) Effects of light and temperature on the cell size and some biochemical components in two freshwater cryptophytes. *Nord. J. Bot.* 13(6):697–705.
233. Olson, R.J. and Sosik, H.M. (2007). A submersible imaging-in-flow instrument to analyze nano-and microplankton: imaging FlowCytobot. *Limnol. Oceanogr. Methods* 5:195–203.
234. Olsen, S., Chan, F., Li, W., Zhao, S., Søndergaard M., Jeppesen, E. (2015). Strong impact of nitrogen loading on submerged macrophytes and algae: a long-term mesocosm experiment in a shallow Chinese lake. *Freshw. Biol.* 60:1525–1536.
235. Osborne, B.A. and Raven, J.A. (1986). Growth light level and photon absorption by cells of *Chlamydomonas reinhardtii*, *Dunaliella tertiolecta* (Chlorophyceae, Volvocales), *Scenedesmus obliquus* (Chlorophyceae, Chlorococcales) and *Euglena viridis* (Euglenophyceae, Euglenales). *Br. Phycol. J.* 21:303–313.
236. Paerl, H.W. (1988). Nuisance phytoplankton blooms in coastal, estuarine, and inland waters. *Limnol. Oceanogr.* 33:823–847.
237. Paerl, H.W. and Huisman, J. (2009). Climate change: a catalyst for global expansion of harmful cyanobacterial blooms. *Environ. Microbiol. Rep.* 1:27–37.
238. Paerl, H.W. and Otten, T.G. (2013). Harmful Cyanobacterial Blooms: causes,

- consequences, and controls. *Microb. Ecol.* 65(4):995–1010.
239. Paerl, H.W. and Paul, V.J. (2012). Climate change: links to global expansion of harmful cyanobacteria. *Water Res.* 46:1349–1363.
240. Paerl, H.W., Fulton, R.S., Moisaner, P.H., Dyble, J. (2001). Harmful Freshwater Algal Blooms, with an Emphasis on Cyanobacteria. *Sci. World J.* 1:76–113.
241. Paerl, H.W., Hall, N.S., Calandrino, E.S. (2011). Controlling harmful cyanobacterial blooms in a world experiencing anthropogenic and climatic-induced change. *Sci. Total Environ.* 409:1739–1745.
242. Pal, M., Samal, N.R., Roy, P.K., Roy, M.B. (2015). Electrical conductivity of lake water as environmental monitoring—a case study of Rudrasagar Lake. *IOSR J. Environ. Sci. Toxicol. Food Technol.* 9:66–71.
243. Palmucci, M., Ratti, S., Giordano, M. (2011). Ecological and evolutionary implications of carbon allocation in marine phytoplankton as a function of nitrogen availability: a Fourier transform infrared spectroscopy approach (1). *J. Phycol.* 47:313–323.
244. Parry, M.L., Canziani, O.F., Paltikof, J.P., van der Linden, P.J., Hansen, C.E. (2007). Climate change 2007: impacts, adaptation and vulnerability. Contribution of working group II to the fourth assessment report of the intergovernmental panel on climate change. Cambridge University Press, Cambridge.
245. Passarge, J., Hol, S., Escher, M., Huisman, J. (2006). Competition for nutrients and light: stable coexistence, alternative stable states or competitive exclusion? *Ecol. Monogr.* 76:57–72.
246. Pearson, K. (1895). Note on regression and inheritance in the case of two parents. *Proceedings of the Royal Society of London* 58:240–242.
247. Penn, M.R., Auer, M.T., Doerr, S.M., Driscoll, C.T., Brooks, C.M. Effler, S.W. (2000). Seasonality in phosphorus release rates from the sediments of a hypereutrophic lake under a matrix of pH and redox conditions. *Can. J. Fish. Aquat. Sci.*, 57, 1033 – 1041
248. Philips, E.J. (2002). Algae and Eutrophication. In: Bitton G, editor. *Encyclopedia of Environmental Microbiology*. New York: John Wiley and Sons.
249. Phillips, G., Jackson, R., Bennet, C., Chilvers, A. (1994). The importance of sediment phosphorus release in the restoration of very shallow lakes (The Norfolk Broads, England) and implications for biomanipulation. *Hydrobiol.* 275-276(1):445–456.
250. Picot, J., Guerin, C.L., Kim, C.L.V., Boulanger, C.M. (2012). Flow cytometry: retrospective, fundamentals and recent instrumentation. *Cytotechnol.* 64(2):109–130.
251. Pikuta, E.V. and Hoover, R.B. (2007). Microbial extremophiles at the limits of life. *Crit Rev Microbiol.* 33(3):183–209.
252. Pistorius, A.M., DeGrip, W.J., Egorova-Zachernyuk, T.A. (2009). Monitoring of biomass composition from microbiological sources by means of FT-IR spectroscopy. *Biotechnol. Bioeng.* 103:123–129.
253. Poorter, H., Remkes, C., Lambers, H. (1990). Carbon and nitrogen economy of 24 wild species differing in relative growth rate. *Plant Physiol.* 94:621–627.
254. Pramanik, J. and Keasling, J.D. (1997). Stoichiometric model of *Escherichia coli*

- metabolism: incorporation of growth-rate dependent biomass composition and mechanistic energy requirements. *Biotechnol. Bioeng.* 56:398–421.
255. Prášil, O., Kolber, Z., Berry, J.A., Falkowski, P.G. (1996). Cyclic electron flow around photosystem II *in vivo*. *Photosynth. Res.* 48:395–410.
256. Price, G.D., Badger, M.R., Woodger, F.J., Long, B.M. (2008). Advances in understanding the cyanobacterial CO₂-concentrating-mechanism (CCM): functional components, Ci transporters, diversity, genetic regulation and prospects for engineering into plants. *J. Exp. Bot.* 59(7):1441–1461.
257. Ptacnik, R., Andersen, T., Tamminen, T. (2010). Performance of the Redfield Ratio and a family of nutrient limitation indicators as thresholds for phytoplankton N vs. P limitation. *Ecosystems* 13:1201–1214.
258. Quay, P.D., Emerson, S., Quay B.M., Devol, A.H. (1986). The carbon cycle for Lake Washington – a stable isotope study. *Limnol. Oceanogr.* 31:596–611.
259. Ramm, K. and Scheps, V. (1997). Phosphorus balance of a polytrophic shallow lake with the consideration of phosphorus release. *Hydrobiol.* 342:43–53.
260. Raven, J.A. (1993). Limits on growth rates. *Nature*, 361:209–210.
261. Raven J.A. and Beardall J. (2003) Carbohydrate Metabolism and Respiration in Algae. In: Larkum A.W.D., Douglas S.E., Raven J.A. (eds) *Photosynthesis in Algae. Advances in Photosynthesis and Respiration*, vol 14. Springer, Dordrecht
262. Raven, J.A. and Johnston, A.M. (1991). Mechanisms of inorganic carbon acquisition in marine phytoplankton and their implications for the use of other resources. *Limnol. Oceanogr.* 36:1701–1714.
263. Raven, J.A., Giordano, M., Beardall, J., Maberly, S.C. (2012). Algal evolution in relation to atmospheric CO₂: carboxylases, carbon-concentrating mechanisms and carbon oxidation cycles. *Philos. Trans. R. Soc. Lond. B Biol. Sci.* 367(1588):493–507.
264. Redden, A.M. and Rukminasari, N. (2008). Effects of increases in salinity on phytoplankton in the broadwater of the Myall Lakes, NSW, Australia - Springer. *Hydrobiol.* 608:87–97.
265. Redfield A.C. (1934). On the proportions of organic derivatives in sea water and their relation to the composition of plankton. In James Johnstone Memorial Volume (Daniel, R.J., editor). University of Liverpool Press, Liverpool, pp. 176–192.
266. Redfield, A.C. (1958). The biological control of chemical factors in the environment. *Am. Sci.*, 46:205-221.
267. Redshaw, C.J., Mason, C.F., Hayes, C.R., Roberts, R.D. (1990). Factors influencing phosphate exchange across the sediment-water interface of eutrophic reservoirs. *Hydrobiol.* 192:233–245.
268. Regaudie-de-Gioux, A., Lasternas, S., Agustí, S., Duarte, C.M. (2014). Comparing marine primary production estimates through different methods and development of conversion equations. *Front. Mar. Sci.* 1:19.
269. Renaud, S.M., Thinh, L.V., Lambrinidis, G., Parry, D.L. (2002). Effect of temperature on growth, chemical composition and fatty acid composition of tropical Australian microalgae grown in batch cultures. *Aquaculture* 211:195–214.

270. Reyes, I., Martín, G., Reina, M., Arechederra, A., Serrano, L., Casco, M.A., Toja, J. (2007). Phytoplankton from NE Doñana marshland ("El Cangrejo Grande", Doñana Natural Park, Spain). *Limnetica* 26(2):307–318.
271. Reynolds C.S. (2006). *Ecology of Phytoplankton*. Cambridge: Cambridge University Press. pp. 535.
272. Reynolds, C.S. (1984). *The Ecology of Freshwater Phytoplankton*. Cambridge: Cambridge University Press, pp. 384.
273. Reynolds, C.S. (1998). What factors influence the species composition of phytoplankton in lakes of different trophic status? *Hydrobiol.* 369:11–26.
274. Reynolds, C.S. and Walsby, A.E. (1975). Water blooms. *Biol. Rev.* 50:437–481.
275. Rhee, G.Y. (1974). Phosphate uptake under nitrate limitation by *Scenedesmus* sp. and its ecological implications. *J. Phycol.* 10:470–475.
276. Rhee, G.Y. (1978). Effects of N:P atomic ratios and nitrate limitation on algal growth, cell composition, and nitrate uptake. *Limnol. Oceanogr.* 23:10–25.
277. Rhee, G.Y. and Gotham, I.J. (1980). Optimum N:P ratios and coexistence of planktonic algae. *J. Phycol.* 16:486–489.
278. Rhee, G.Y. and Gotham, I.J. (1981). The effect of environmental factors on phytoplankton growth: temperature and the interactions of temperature with nutrient limitation. *Limnol. Oceanogr.* 26:635–648.
279. Richaud, C., Zabulon, G., Joder, A., Thomas, J.C. (2001). Nitrogen or sulfur starvation differentially affects phycobilisome degradation and expression of the *nblA* gene in *Synechocystis* strain PCC 6803. *J. Bacteriol.* 183:2989–2994.
280. Riebesell, U. (2004). Effects of CO₂ enrichment on marine phytoplankton. *J. Oceanogr.* 60:719–729.
281. Ritchie, R.J. (1991). Membrane potential and pH control in the cyanobacterium *Synechococcus* R-2 PCC7242. *J. Plant Physiol.* 137:409–418.
282. Robarts, R.D. and Zohary, T. (1987). Temperature effects on photosynthetic capacity, respiration, and growth rates of bloom-forming cyanobacteria. *New Zealand J. Mar. Freshwat. Res.* 21:391–399.
283. Robinson, C., Tilstone, G., Rees, A. P., Smyth, T., Fishwick, J.R., Tarran, G.A., Luz, B., Barkan, E., David, E. (2009). Comparison of *in vitro* and *in situ* plankton production determinations. *Aquat. Microb. Ecol.* 54:13–34.
284. Rodhe, W. (1969). Crystallization of eutrophication concepts in northern Europe. In: *Eutrophication, causes, consequences, correctives*. National Academy of Sciences, Washington D.C. pp. 50–64.
285. Romo, S. and Miracle, M.R. (1995). Diversity of the phytoplankton assemblages of a polymictic hypertrophic lake. *Arch. Hydrobiol.* 132(3): 363–384
286. Ross, O.N. and Geider, R.J. (2009). New cell-based model of photosynthesis and photo-acclimation: accumulation and mobilisation of energy reserves in phytoplankton. *Mar. Ecol. Prog. Ser.* 383:53–71.
287. Rutten, T.P., Sandee, B., Hofman, A.R. (2005). Phytoplankton monitoring by high performance flow cytometry: a successful approach? *Cytometry Part A* 64:16–26.
288. Sakamoto, M. (1966). Primary production by phytoplankton community in some

- Japanese lakes and its dependence on lake depth. Arch. Hydrobiol. 62:1–28.
289. Sallal A.K., Nimer N.A., Radwan S.S. (1990). Lipid and fatty acid composition of freshwater cyanobacteria. J. Gen. Microbiol. 136:2043–2048.
290. Sanz, A., Morena-Vivián, C., Maldonado, J.M., González-Fontes, A. (1995). Effect of a constant supply of different nitrogen sources on protein and carbohydrate content and enzyme activities of *Anabaena variabilis* cells. Physiol. Plant. 95:39–44.
291. Schindler, D.W. (1977). Evolution of phosphorus limitation in lakes: natural mechanisms compensate for deficiencies of nitrogen and carbon in eutrophied lakes. Science 195:260–262.
292. Schöl, A., Kirchesch, V., Bergfeld, T., Müller, D. (1999). Model-based analysis of oxygen budget and biological processes in the regulated rivers Mosel and Saar: modelling the influence of benthic filter feeders on phytoplankton. Hydrobiol. 410:167–176.
293. Shapiro J. (1997). The role of carbon dioxide in the initiation and maintenance of blue-green dominance in lakes. Freshw. Biol. 37:307–323.
294. Shapiro, J. (1990). Current beliefs regarding dominance of bluegreens: the case for the importance of CO₂ and pH. Verhandlungen der Internationalen Vereinigung für Theoretische und Angewandte Limnologie 24:38–54.
295. Shapiro, J. (1973). Blue-green algae: why they become dominant. Science 179:382–38.
296. Sharma, K.K., Schuhmann, H., Schenk, P.M. (2012). High lipid induction in microalgae for biodiesel production. Energies 5(5):1532–1553.
297. Shifrin, N.S. and Chisholm, S.W. (1981). Phytoplankton lipids: interspecific differences and effects of nitrate, silicate and light-dark cycles. J. Phycol. 17:374–384.
298. Shuter, B. (1979). A model of physiological adaptation in unicellular algae. J. Theor. Biol. 78:519–552.
299. Sigee, D.C., Bahrami, F., Estrada, B., Webster, R.E., Dean, A.P. (2007). The influence of phosphorus availability on carbon allocation and P quota in *Scenedesmus subspicatus*: a synchrotron-based FTIR analysis. Phycologia 46(5):583–592.
300. Sigee, D.C., Dean, A., Levado, E., Tobin, M.J. (2002). Fourier-transform infrared spectroscopy of *Pediastrum duplex*: Characterization of a micro-population isolated from a eutrophic lake. Eur. J. Phycol. 37(1):19–26.
301. Sigman, D.M. and Hain, M.P. (2012). The Biological Productivity of the Ocean: Section 1. Nature Education Knowledge 3(6):21.
302. Singh, P.K. (1974). Effect of pH on Growth and Nitrogen Fixation in Aphanothece (Cyanophyta). Oikos 25(1):114–116.
303. Singh, S.P. and Singh, P. (2015). Effect of temperature and light on the growth of algae species: a review. Renew. Sust. Energy Rev. 50:431–444.
304. Smith, R.L. (1986). Elements of Ecology. Second Edition. Harper & Row, Publishers, Inc., New York, NY. pp. 677.
305. Smith, V.H. (1983). Low nitrogen to phosphorus ratios favour dominance by blue-green algae in lake phytoplankton. Science 221:669–771.
306. Smith, V.H., V.J. Bierman, B.L. Jones, Havens, K.E. (1995). Historical trends in the

- Lake Okeechobee ecosystem. IV. Nitrogen:phosphorous ratios, cyanobacterial biomass, and nitrogen fixation potential. Arch. Hydrobiol. Monogr. Beitr. 107:69–86.
307. Sommer, U., Gliwicz, Z.M., Lampert, W., Duncan, A. (1986). The PEG-model of seasonal succession of planktonic events in fresh waters. Arch. Hydrobiol. 106:433–471.
308. Sosik, H.M. and Mitchell, B.G. (1994). Effects of temperature on growth, light absorption, and quantum yield in *Dunaliella tertiolecta* (Chlorophyceae). J. Phycol. 30:833–840.
309. Specchiulli, A., Focardi, S., Renzi, M., Scirocco, T., Cilenti, L., Breber, P., Bastianoni S. (2008). Environmental heterogeneity patterns and assessment of trophic levels in two Mediterranean lagoons: Orbetello and Varano, Italy. Sci. Total Environ. 402(2–3):285–298.
310. Srivastava, A.K, Poonam, B., Kumar, A., Rai, L., Neilan, B.A. (2009). Molecular Characterization and the Effect of Salinity on Cyanobacterial Diversity in the Rice Fields of Eastern Uttar Pradesh, India. Saline Syst. 5:4–9.
311. Steele, J.H. (1962). Environmental control of photosynthesis in the sea. Limnol. Oceanogr. 7(2):137–150.
312. Steeman-Nielsen, E. (1951). Measurement of production of organic matter in sea by means of carbon-14. Nature. 167 (4252):684–685.
313. Steeman-Nielsen, E. (1952). The use of radioactive carbon (C14) for measuring organic production in the sea. J. Cons. Int. Explor. Mer. 18:117–140.
314. Stehfest, K., Toepel, J., Wilhelm, C. (2005). The application of micro-FTIR spectroscopy to analyze nutrient stress-related changes in biomass composition of phytoplankton algae. Plant Physiol. Bioch. 43:717–726.
315. Sterner, R.W. and Elser, J.J. (2002). Ecological stoichiometry: the biology of elements from molecules to the biosphere (Princeton University Press).
316. Stevens, S.E., Balkwill, D.L., Paone, D.A.M. (1981). The effects of nitrogen limitation on the ultrastructure of the cyanobacterium *Agmenellum quadruplicatum*. Arch. Microbiol. 130:204–212.
317. Stigler, S.M. (1989). Francis Galton's account of the invention of correlation. Stat. Sci. (2):73–79.
318. Stock, C. and Dunne, J. (2010). Controls on the ration of mesozooplankton production to marine primary production in marine ecosystems. Deep-sea Res. I, 57:95–112.
319. Stock, C.A., Dunne, J.P., John, J.G. (2014). Global-scale carbon and energy flows through the marine planktonic food web: an analysis with a coupled physical-biological model. Prog. Oceanogr. 120:1–28.
320. Stumm, W. and Morgan, J.J. (1981). Aquatic Chemistry. 2nd ed. Wiley, New York.
321. Su, W., Jakob, T., Wilhelm, C. (2012). The Impact of Nonphotochemical Quenching of Fluorescence on the Photon Balance in Diatoms under Dynamic Light Conditions (1). J. Phycol. 48:336–346.
322. Talley, L. (2000). Properties of seawater (lecture 2). In SIO 210: Introduction to

- Physical Oceanography.
323. Talmy, D., Blackford, J., Hardman-Mountford, N.J., Dumbrell, A.J., Geider, R.J. (2013). An optimality model of photoadaptation in contrasting aquatic light regimes. *Limnol. Oceanogr.* 58:1802–1818.
324. Taraldsvik, M. and Myklestad, S. (2000). The effect of pH on growth rate, biochemical composition and extracellular carbohydrate production of the marine diatom *Skeletonema costatum*. *Eur. J. Phycol.* 35(2):189–194.
325. Tezuka, Y. (1989). The C:N:P ratio of *Microcystis* and *Anabaena* (bluegreen algae) and its importance for nutrient regeneration by aerobic decomposition. *Jpn. J. Limnol.* 50:149–155.
326. Thirupathaiiah, M., Samatha, Ch., Sammaiah, Ch. (2013). Diversity of fish fauna in lower Manair reservoir of Karimnagar district (A.P.) India Adv. In App. Sci. Res. 4(2):203–211.
327. Thyssen, M., Alvain, S., Lefèbvre, A., Dessailly, D., Rijkeboer, M., Guiselin, N., Creach, V., Artigas, L.F. (2015). High-resolution analysis of a North Sea phytoplankton community structure based on *in situ* flow cytometry observations and potential implication for remote sensing. *Biogeosciences* 12:4051–4066.
328. Toepel, J., Wilhelm, C., Meister, A., Becker, A., Martinez-Ballesta Mdel, C. (2004). Cytometry of freshwater phytoplankton. *Methods Cell Biol.* 75:375–407.
329. Tong, C.H., Yang, X.E., Pu, P.M. (2003). Degradation of aquatic ecosystem in the catchment of Mu-Ge Lake and its Remediation countermeasures. *JSWC* 17(1):72–88. (in Chinese)
330. Toseland, A., Daines, S.J., Clark, J.R., Kirkham, A., Strauss, J., Uhlig, C., Lenton, T.M., Valentin, K., Pearson, G.A., Moulton, V., Mock, T. (2013). The impact of temperature on marine phytoplankton resource allocation and metabolism. *Nature* 3:979–984.
331. Touloupakis, E., Cicchi, B., Benavides, A.M.S., Torzillo, G. (2016). Effect of high pH on growth of *Synechocystis* sp. PCC 6803 cultures and their contamination by golden algae (*Poteroiochromonas* sp.). *Appl. Microbiol. Biotechnol.* 100:1333–1341.
332. Urabe, J., Kyle, M., Makino, W., Yoshida, T., Andersen, T., Elser, J.J. (2002). Reduced light increases herbivore production due to stoichiometric effects of light/nutrient balance. *Ecology* 83:619–627.
333. US Geological Survey. (2013). Volatile Organic Compounds in the Nation's Ground Water and Drinking-Water Supply Wells: Supporting Information: Glossary.
334. US. EPA. (1980). Clean lakes program guidance manual. Report No. EPA-440/5-81-003. U.S. EPA, Washington, D.C.
335. Vargas, M.A., Rodriguez, H., Moreno, J., Olivares, H., Del Campo, J.A., Rivas, J., Guerrero, M.G. (1998). Biochemical composition and fatty acid content of filamentous nitrogen-fixing cyanobacteria. *J. Phycol.* 34: 812–817.
336. Vitousek, P. (1982). Nutrient cycling and nutrient use efficiency. *Am. Nat.* 119:553–572.
337. Vollenweider, R.A. and Kerekes, J.J. (1982). Eutrophication of waters: monitoring, assessment and control. OECD, Paris.

338. Vrede, T., Dobberfuhl, D.R., Kooijman, S., Elser, J.J. (2004). Fundamental connections among organism C:N:P stoichiometry, macromolecular composition, and growth. *Ecology* 85:1217–1229.
339. Wagner, H., Jungandreas, A., Fanesi, A., Wilhelm, C. (2014). Surveillance of C-allocation in microalgal cells. *Metabolites* 4:453–464.
340. Wagner, H., Dunker, S., Liu, Z., Wilhelm, C. (2013). Subcommunity FTIR-spectroscopy to determine physiological cell states. *Curr. Opin. Biotechnol.* 24:88–94.
341. Wagner, H., Fanesi, A., Wilhelm, C. (2016). Freshwater phytoplankton responses to global warming. *J. Plant Physiol.* 203:127–134.
342. Wagner, H., Jakob, T., Wilhelm, C. (2006). Balancing the energy flow from captured light to biomass under fluctuating light conditions. *New Phytol.* 169(1):95–108.
343. Wagner, H., Jebson, C., Wilhelm, C. (2019). Monitoring cellular C:n ratio in phytoplankton by means of FTIR-spectroscopy. *J. Phycol.*
344. Wagner, H., Liu, Z., Langner, U., Stehfest, K., Wilhelm, C. (2010). The use of FTIR spectroscopy to assess quantitative changes in the biochemical composition of microalgae. *J. Biophotonics* 3:557–566.
345. Walsby, A.E. (1982). Cell-water and cell-solute relations. In: N.G. Carr, and B.A. Whitton (Eds.), *The biology of cyanobacteria*. Blackwell Science Publications, Oxford, pp. 237–262.
346. Walsby, A.E. (1997). Numerical integration of phytoplankton photosynthesis through time and depth in a water column. *New Phytol.* 136:189–209.
347. Wang, S.R., Jin, X.C., Bu, Q.Y., Jiao, L.X., Wu, F.C. (2008). Effects of dissolved oxygen supply level on phosphorus release from lake sediments. *Colloid Surface A: Physicochemical and Engineering Aspects* 316, pp. 245–252.
348. Webb, B.W. and Nobilis, F. (2007). Long-term changes in river temperature and the influence of climatic and hydrological factors. *Hydrolog. Sci. J.* 52(1):74–85.
349. Weisse, T. and Stadler, P. (2006). Effect of pH on growth, cell volume, and production of freshwater ciliates, and implications for their distribution. *Limnol. Oceanogr.* 51(4):1708–1715.
350. Welch, E.B. and Cooke G.D. (1995). Internal phosphorus loading in shallow lakes: importance and control. *Lake Reservoir Manage.* 11:273–281.
351. Western D. (2001). Human-modified ecosystems and future evolution. *Proc. Natl. Acad. Sci. U. S. A.* 98(10):5458–5465.
352. Wetzel, R.G. (1975). *Limnology*. Saunders, Philadelphia, pp.743.
353. Wetzel, R.G. (2001). *Limnology: Lake and river ecosystems* (3rd ed.). San Diego, CA: Academic Press.
354. Widjaja, A., Chien, C.C., Ju, Y.H. (2009). Study of increasing lipid production from fresh water microalgae *Chlorella vulgaris*. *J. Taiwan Inst. Chem. Eng.* 40(1):13–20.
355. Wilhelm, C. and Jakob, T. (2011). From photons to biomass and biofuels: evaluation of different strategies for the improvement of algal biotechnology based on comparative energy balances. *Appl. Microbiol. Biotechnol.* 92:909–919.
356. Wilhelm, C. and Selmar, D. (2011). Energy dissipation is an essential mechanism to

- sustain the viability of plants: The physiological limits of improved photosynthesis. *J. Plant Physiol.* 168(2):79–87.
357. Wilhelm, C., Rudolph, I., Renner, W. (1991). A quantitative method based on HPLC-aided pigment analysis to monitor structure and dynamics of the phytoplankton assemblage-A study from Lake Meerfelder Maar (Eifel, Germany). *Arch. Hydrobiol.* 123(1):21–35.
358. Wilhelm, C., Volkmar, P., Lohmann, C., Becker, A., Meyer, M. (1995). The HPLC-aided pigment analysis of phytoplankton cells as a powerful tool in water quality control. *J. Water Supply Res. Technol.* 44:132–141.
359. Williams, P.J.L. (1993). Chemical and tracer methods of measuring plankton production. *ICES Mar. Sci. Symp.* 197:20–36.
360. Wood, N.B. and Haselkorn, R.H. (1980). Control of phycobiliprotein proteolysis and heterocyst differentiation in *Anabaena*. *J. Bacteriol.* 141:1375–1385.
361. Yacobi, Y.Z. and Zohary, T. (2010). Carbon:chlorophyll a ratio, assimilation numbers and turnover times of Lake Kinneret phytoplankton. *Hydrobiol.* 639:185–196.
362. Yang, Y., He, Z., Lin, Y., Philips, E.J., Yang, J., Chen, G., Stoffella, P.J., Powell, C.A. (2008). Temporal and spatial variations of nutrients in the Ten Mile Creek of South Florida, USA and effects on phytoplankton biomass. *J. Environ. Monitor.* 10:508–516.
363. Yu, Q., Wang, H.Z., Li, Y., Shao, J.C., Liang, X.M., Jeppesen E., Wang, H.J. (2015). Effects of high nitrogen concentrations on the growth of submersed macrophytes at moderate phosphorus concentrations. *Water Res.* 83:385–395.
364. Yvon-Durocher, G., Dossena, M., Trimmer, M., Woodward, G., Allen, A.P. (2015). Temperature and the biogeography of algal stoichiometry. *Global Ecol. Biogeogr.* 24:562–570.
365. Yvon-Durocher, G., Schaum, C.E., Trimmer, M. (2017). The temperature dependence of phytoplankton stoichiometry: investigating the roles of species sorting and local adaptation, *Front. Microbiol.* 8:1–14.
366. Zargar, S., Krishnamurthi, K., Saravana D.S., Ghosh, T.K., Chakrabarti, T. (2006). Temperature-induced stress on growth and expression of Hsp in freshwater alga *Scenedesmus quadricauda*. *Biomed. Environ. Sci.* 19(6):414–421.
367. Zhang, Y.L., Wu, Z.X., Liu, M.L., He, J.B. (2014). Thermal structure and response to long-term climatic changes in Lake Qiandaohu, a deep subtropical reservoir in China. *Limnol. Oceanogr.* 59(4):1193–1202.
368. Zhao, S.C. (2004). Mechanisms of Lake Eutrophication and technologies for controlling in China. *Adv. Earth Sci.* 19(1):138–140.

6 Acknowledgements

First of all, I want to thank my supervisor Prof. Dr. Christian Wilhelm for the possibility to work in his research group, for his continuous support and encouragement. I am especially grateful to Dr. Heiko Wagner for the patient introduction in the methods and concepts of FTIR-spectroscopy, for countless helpful discussion and for his invaluable advice and support in the preparation of presentations, posters and manuscripts. Special thanks go to Ms. Kerstin Flieger for HPLC analysis, as well as Dr. Susanne Dunker and Ms. Regina Sacher for the assistance in monitoring, sampling and analysis. I would also like to thank to all my colleagues in the research group Plant Physiology for the friendly atmosphere which made me enjoy my work.

I am exceedingly grateful to my parents, my husband and my son for their continuous and unlimited support during the study in Germany.

I am also thankful to the financial support by the City of Leipzig (Amt fuer Stadtgruen und Gewaesser) especially Andreas Kruspe. With regard to analysis of Lake Auensee, I acknowledge the Institute for Meteorology at the University Leipzig and the Synlab Services GmbH (Leipzig, Germany) for performing chemical analyses.

7 Curriculum vitae

Personal data

Name: Zhixin Liu
Address: Str. des 18. Oktober 23/609, 04103, Leipzig
Phone: 015229117431
E-Mail: zhixinliu@gmx.de
Place of birth: Shenyang, Liaoning, VR China
Nationality: Chinese

Education

Since 09/2009 University of Leipzig, Institute of Biology
PhD student at the research group Plant Physiology
Supervisor: Prof. Dr. Christian Wilhelm
10/2002 – 08/2009 University of Leipzig
Study of biology (Diploma, grade)
09/2001 – 07/2002 Studienkolleg of the University of Leipzig (M-Kurs)
03/2001 – 07/2001 DSH Kurs of the University of Leipzig
09/1999 – 02/2001 University of Shenyang (VR China), Study of biology

Scientific publications

Wagner, H., **Liu, Z.**, Langner, U., Stehfest, K., Wilhelm, C. (2010). The use of FTIR spectroscopy to assess quantitative changes in the biochemical composition of microalgae. *J. Biophotonics* 3:557–566.

Wagner, H., Dunker, S., **Liu, Z.**, Wilhelm, C. (2013). Subcommunity FTIR-spectroscopy to determine physiological cell states. *Curr. Opin. Biotechnol.* 24:88–94.

Conference contributions

Zhixin Liu, Heiko Wagner, Christian Wilhelm. (08/2011). Determination of macromolecular composition of phytoplankton algae from mixed cultures by FT-IR spectroscopy using Flow cytometry. 20. Photosynthese Workshop 2011–Poster presentation

Zhixin Liu, Heiko Wagner, Christian Wilhelm. (09/2011). Quantification of phytoplankton cell properties from mixed cultures and natural samples by FT-IR spectroscopy using Flow cytometry. Botanikertagung 2011–Poster presentation

Zhixin Liu, Heiko Wagner, Christian Wilhelm. (03/2010). Analysis of macromolecular composition from *Chlamydomonas reinhardtii* using infrared spectroscopy in comparison of biological methods. 13. Wissenschaft-liche Tagung der Sektion Phykologie–Poster presentation

Zhixin Liu, Heiko Wagner, Susanne Dunker, Chrisfield Kunath, Christian Wilhelm. (08/2010). Application of FT-IR spectroscopy combined with Flow cytometry to analyze the macromolecular composition from a mixture of phytoplankton algae. The 15th international congress of photosynthesis–Poster presentation

Zhixin Liu, Heiko Wagner, Christian Wilhelm. (10/2011). Quantification of phytoplankton cell properties from mixed cultures and natural samples by FT-IR spectroscopy using Flow cytometry. FTIR spectroscopy in microbiological and medical diagnostics–Poster presentation

Work experience

- | | |
|-----------------|---|
| 07/2013–02/2017 | Visiting scientist at the University of Munich, research group Molecular Plant |
| 10/2009–12/2011 | Supervision of practical courses of the research group Plant Physiology at the University of Leipzig |
| 04/2009–07/2009 | Student assistant at the Institute of Biology, University of Leipzig (Supervision of the practical course Plant identification) |

8 Declaration of authorship

I, Zhixin Liu, herewith declare that I have written the present thesis without improper aid and without the use of other resources than stated. I have marked any direct and indirect citations according to the guidelines of good scientific practice. No other persons provided support and contributed to this thesis. No PhD consultants were used, and no third party received direct or indirect financial benefits in goods and services for work related to the present thesis. This thesis was not submitted for dissertation or any other graduation at another academic institution. I made no previous attempts to obtain a doctoral degree.

Zhixin Liu

Leipzig, 19. June 2019

